기초과학연구

목 차

수학

J. Basic Sci. HUFS **62** (2026), pp. 1-30

CATEGORIFICATION OF QUANTUM GROUPS ASSOCIATED WITH QUIVER WITH LOOPS

Young Rock Kim

Abstract. We study a class of quantum groups U^- associated with quivers with possibly loops and provide a categorification by constructing their associated Khovanov-Lauda-Rouquier algebras R. We prove that the indecomposable projective module over R corresponds to the canonical basis of U^-. In the Jordan quiver case, we show that the cyclotomic algebras R^Λ categorify the irreducible highest weight U-module $V(\Lambda)$ for $\Lambda \in P^+$.

Introduction

Khovanov-Lauda-Rouquier algebras (also known as *quiver Hecke algebras, or KLR-algebras*) were independently introduced by Khovanov-Lauda [10, 11] and Rouquier [17]. In the Kac-Moody setting, the category of finitely generated graded projective modules over Khovanov-Lauda-Rouquier algebras categorifies the corresponding quantum groups. For symmetric Cartan datum, the indecomposable projective modules correspond to Lusztig's canonical basis [18, 22]. Moreover, the cyclotomic quotients of these algebras categorify the irreducible highest weight representations of quantum groups [6] and their crystals in the sense of Kashiwara [12].

In the Kac-Moody case, Varagnolo and Vasserot [22] showed that KLR-algebras admit a geometric realization as Steinberg-type convolution algebras associated with quiver flag varieties (without loops), generalizing classical Springer theory. For quivers with arbitrary loops, a presentation of these Steinberg-type algebras

Key words and phrases. Categorification, KLR-algebra, quiver with loops.

Major in Mathematics Education, Graduate School of Education, Hankuk University of Foreign Studies. This research was supported by the research fund of Hankuk University of Foreign Studies.

was given in [7]. Independently, Sauter [20] developed a generalized quiver-graded Springer theory, with [7] appearing as a special case for the type A Weyl group. In this context, it is natural to expect that these generalized KLR-algebras categorify a class of quantum groups associated with quivers that include loops and are related to Lusztig's canonical basis theory.

The authors in [7] established a partial connection under certain restrictions on the quiver that excluded the Jordan quiver case, since they considered a relatively small quantum group, namely the *quantum generalized Kac-Moody algebra* or *quantum Borcherds algebra*. The aim of this paper is to provide an appropriate quantum group framework for these Steinberg-type algebras, thereby filling the gap left in [7].

When quivers with loops are allowed, various generalizations of Kac-Moody quantum groups have been proposed. The most general case was introduced by T. Bozec [2] in his study of perverse sheaves on quiver representation varieties, possibly with loops. He showed that the Grothendieck group arising from Lusztig sheaves is generated by the elementary simple perverse sheaves, answering a question posed by Lusztig in [15]. In this setting, all partial flags are considered. The resulting Grothendieck groups are called *quantum Borcherds-Bozec algebras*, determined by a symmetric Borcherds-Cartan matrix $A = (a_{ij})_{i,j \in I}$, with diagonal entries can be ≤ 0. For an imaginary index i (i.e., $a_{ii} \leq 0$), there are infinitely many generators f_{in} ($n \in \mathbb{Z}_{>0}$) associated with it.

In this paper, we focus on the subalgebra U^- of the quantum Borcherds-Bozec algebras, derived from the complete flag varieties $\mathscr{F}_\nu$ for $\nu \in \mathbb{N}[I]$. This algebra has infinitely many generators f_{in} only when $a_{ii} = 0$. We first categorify U^- by constructing the corresponding KLR-algebras $R(\nu)$ ($\nu \in \mathbb{N}[I]$), using braid-like planar diagrams. We do not use the presentation of Steinberg algebras from geometry at the beginning since it is more complicated for expression. In particular, for $\nu = ni$ with $a_{ii} = 0$, the algebra $R(ni)$ is the wreath product $\mathbb{C}[x_1, \ldots, x_n] \rtimes \mathbb{C}[S_n]$, which coincides with the equivalent Borel-Moore homology ring $H_*^{GL_n}(\mathscr{Z})$ for the Steinberg variety $\mathscr{Z}$ of the complete flag variety GL_n/B_n.

Let $R = \oplus_{\nu \in \mathbb{N}[I]} R(\nu)$, and let $K_0(R)$ denote the Grothendieck group of the category of finitely generated graded projective R-modules. Using the framework developed in [10, 11] and a detailed treatment of the Jordan quiver case, we prove that there is a bialgebra isomorphism $\Gamma\colon {}_{\mathcal{A}}U^- \xrightarrow{\sim} K_0(R)$, where $\mathcal{A} = \mathbb{Z}[q, q^{-1}]$ and ${}_{\mathcal{A}}U^-$ is the $\mathcal{A}$-form of U^-. As mentioned above, the Steinberg-type variety

$\mathscr{Z}_\nu$ of the complete flag varieties $\mathscr{F}_\nu$ has been studied in [7] and [20]. We show that the algebra $R(\nu)$ is isomorphic to the Steinberg-type algebra $\widehat{R}_\nu$ of $\mathscr{Z}_\nu$. As a consequence, combining the results from classical Springer theory for GL_n and Varagnolo and Vasserot's work, we prove that the canonical basis elements in ${}_{\mathcal{A}}U^-$ correspond to the indecomposable projective modules of R under the isomorphism Γ.

Finally, in the Jordan quiver case, we show that the cyclotomic algebra R^Λ ($\Lambda \in P^+$) provides a categorification of the irreducible highest weight module $V(\Lambda)$. Essentially, we categorify the commutation relations of the generators $E_{i\ell}$ and f_{it} when $a_{ii} = 0$ in the entire quantum group. We further conjecture that this result could be extended to arbitrary Borcherds-Cartan data.

1. A quantum group of Borcherds-Cartan type

We introduce a class of quantum groups associated with quivers with arbitrary loops. These quantum groups are specific subalgebras of the *quantum Borcherds-Bozec algebras* introduced in [2], and they possess a geometric setting, arising from the complete flag varieties linked to quivers with loops.

1.1. Borcherds-Cartan matrices and the algebra U^-.

Let I be a finite index set. An integer-valued symmetric matrix $A = (a_{ij})_{i,j\in I}$ is called a *Borcherds-Cartan matrix* if

(i) $a_{ii} = 2, 0, -2, -4, \ldots,$
(ii) $a_{ij} = a_{ji} \in \mathbb{Z}_{\le 0}$ for $i \neq j$.

We set $I^+ = \{i \in I \mid a_{ii} = 2\}$, the set of *real indices*, $I^0 = \{i \in I \mid a_{ii} = 0\}$, the set of *isotropic indices*, $I^- = \{i \in I \mid a_{ii} < 0\}$, the set of *indefinite indices* and $I^{\le 0} = I^0 \sqcup I^-$, the set of *imaginary indices*.

Let $\mathbb{Z}[I]$ denote the set of $\mathbb{Z}$-linear combinations of I:

$$\mathbb{Z}[I] = \{\nu = \sum_{i\in I} \nu_i i \mid \nu_i \in \mathbb{Z}\}.$$

where $\mathbb{Z}$ is the ring of integers. Define a symmetric bilinear form $\nu, \nu' \mapsto \nu \cdot \nu'$ on $\mathbb{Z}[I]$ taking values in $\mathbb{Z}$, such that

$$i \cdot j = a_{ij} = a_{ji} \quad \text{for all } i, j \in I.$$

The triple $(I, A, \cdot)$ is called a *Borcherds-Cartan datum*.

Let q be an indeterminate. For $n \in \mathbb{N}$, we set

$$[n] = \frac{q^n - q^{-n}}{q - q^{-1}} \text{ and } [n]! = [n][n-1]\cdots[1].$$

Let $\mathbb{I} = I^+ \sqcup I^- \sqcup (I^0 \times \mathbb{Z}_{>0})$. We often write i for $(i,1)$ when $i \in I^0$.

Definition 1.1. The *quantum group* U^- associated to a given Borcherds-Cartan datum $(I, A, \cdot)$ is the associative algebra over $\mathbb{Q}(q)$ generated by f_{in} $((i,n) \in \mathbb{I})$ satisfying the following relations

$$\sum_{r+s=1-na_{ij}} (-1)^r f_i^{(r)} f_{jn} f_i^{(s)} = 0 \quad \text{for } i \in I^+, (j,n) \in \mathbb{I} \text{ and } i \neq (j,n),$$
$$f_{in} f_{jm} - f_{jm} f_{in} = 0 \quad \text{for } a_{ij} = 0.$$

Here we denote $f_i^{(n)} = f_i^n/[n]!$ for $i \in I^+$ and $n > 0$. The algebra U^- is $\mathbb{N}[I]$-graded by assigning $|f_{in}| = ni$.

Define a twisted multiplication on $U^- \otimes U^-$ by

$$(x_1 \otimes x_2)(y_1 \otimes y_2) = q^{-|x_2|\cdot|y_1|} x_1 y_1 \otimes x_2 y_2$$

for homogeneous x_1, x_2, y_1, y_2. Then we have an algebra homomorphism $\rho \colon U^- \to U^- \otimes U^-$ (with respect to the twisted multiplication on $U^- \otimes U^-$) given by

$$\rho(f_i) = f_i \otimes 1 + 1 \otimes f_i \ \text{ for } i \in I^\pm, \quad \rho(f_{in}) = \sum_{r+t=n} f_{ir} \otimes f_{it} \ \text{ for } i \in I^0, n > 0.$$

There is a nondegenerate symmetric bilinear form $\{\ ,\ \} \colon U^- \times U^- \to \mathbb{Q}(q)$ determined by

(i) $\{x, y\} = 0$ if $|x| \neq |y|$,
(ii) $\{1, 1\} = 1$,
(iii) $\{f_i, f_i\} = 1/(1-q^2)$ for $i \in I^\pm$,
$\{f_{in}, f_{in}\} = 1/\left((1-q^2)(1-q^4)\cdots(1-q^{2n})\right)$ for $i \in I^0, n > 0$,
(iv) $\{x, yz\} = \{\rho(x), y \otimes z\}$ for $x, y, z \in U^-$.

Let $\mathcal{A} = \mathbb{Z}[q, q^{-1}]$ be the ring of Laurent polynomials. The $\mathcal{A}$-form ${}_{\mathcal{A}}U^-$ is the $\mathcal{A}$-subalgebra of U^- generated by $f_i^{(n)}$ $(i \in I^+, n > 0)$, f_i $(i \in I^-)$ and f_{in} $(i \in I^0, n > 0)$.

Let $^-$ be the $\mathbb{Q}$-algebra involution of U^- given by $\overline{q} = q^{-1}$ and $\overline{f_{in}} = f_{in}$ for all $(i,n) \in \mathbb{I}$.

1.2. Geometric setting for U^-.

We briefly review the geometric construction for U^- given in [2, 13, 15]. Let (I, H) be a quiver with vertices set I and arrows set H. For each $h \in H$, let h' and h'' be the origin and the target vertices of h, respectively. We allow h' and h'' to be equal. Define

$$h_i = \#\{\text{loops on } i\} \ \text{ for } i \in I, \quad h_{ij} = \#\{i \to j\} \ \text{ for } i \neq j.$$

Fix $\nu = \sum_{i \in I} \nu_i i \in \mathbb{N}[I]$ with $\mathrm{ht}(\nu) := \sum_{i \in I} \nu_i = n$. We set

$$V_\nu = \bigoplus_{i \in I} \mathbb{C}^{\nu_i}, \ E_\nu = \bigoplus_{h \in H} \mathrm{Hom}(\mathbb{C}^{\nu_{h'}}, \mathbb{C}^{\nu_{h''}}) \text{ and } G_\nu = \prod_{i \in I} \mathrm{GL}_{\nu_i}(\mathbb{C}).$$

Then G_ν acts on E_ν by conjugation:

$$g \cdot (x_h) = (g_{h''} x_h g_{h'}^{-1}).$$

We denote by $D_{G_\nu}(E_\nu)$ the bounded G_ν-equivariant derived category of $\mathbb{C}$-constructible complexes on E_ν, and by $P_{G_\nu}(E_\nu)$ the abelian subcategory of G_ν-equivariant perverse sheaves on E_ν.

Let $\mathrm{Seq}(\nu)$ be the set of all sequences $\boldsymbol{i} = i_1 i_2 \dots i_n$ in I^n such that $\nu = i_1 + i_2 \cdots + i_n$. For $\boldsymbol{i} \in \mathrm{Seq}(\nu)$, define

$$\mathscr{F}_{\boldsymbol{i}} = \{W = (0 \subsetneq W_1 \subsetneq \cdots \subsetneq W_n = V_\nu) \mid \underline{\dim}(W_k / W_{k-1}) = i_k\},$$
$$\widetilde{\mathscr{F}_{\boldsymbol{i}}} = \{(x, W) \in E_\nu \times \mathscr{F}_{\boldsymbol{i}} \mid x(W_k) \subseteq W_{k-1}\}.$$

Let G_ν acts on $\widetilde{\mathscr{F}_{\boldsymbol{i}}}$ diagonally. The first projection $\pi_{\boldsymbol{i}} : \widetilde{\mathscr{F}_{\boldsymbol{i}}} \to E_\nu$ is a G_ν-equivariant proper map, which yields $\mathcal{L}_{\boldsymbol{i}} = (\pi_{\boldsymbol{i}})_!(\mathbb{C}_{\widetilde{\mathscr{F}_{\boldsymbol{i}}}}[\dim \widetilde{\mathscr{F}_{\boldsymbol{i}}}])$ a semisimple complex in $D_{G_\nu}(E_\nu)$. We denote

(i) $\mathbf{P}_\nu$ is the set of isomorphism classes of simple perverse sheaves appearing in $\mathcal{L}_{\boldsymbol{i}}$ as a summand with a possible shift for all $\boldsymbol{i} \in \mathrm{Seq}(\nu)$,

(ii) $\mathbf{Q}_\nu$ is the full subcategory of $D_{G_\nu}(E_\nu)$ whose objects are finite direct sums of shifts of the simple perverse sheaves coming from $\mathbf{P}_\nu$,

(iii) $\mathbf{K}_\nu$ is the Grothendieck group of $\mathbf{Q}_\nu$.

Form $\mathbf{K} = \bigoplus_{\nu \in \mathbb{N}[I]} \mathbf{K}_\nu$. By [2], the Grothendieck group $\mathbf{K}$ has a geometrically defined (twisted) $\mathcal{A}$-bialgebra structure that is isomorphic to the ${}_{\mathcal{A}}U^-$, associated with the Borcherds-Cartan matrix A given by

$$a_{ij} = \begin{cases} 2 - 2h_i & \text{for } i = j, \\ -h_{ij} - h_{ji} & \text{for } i \neq j. \end{cases} \tag{1.1}$$

This isomorphism is given explicitly as follows:

$$f_i^{(n)} \longleftrightarrow \mathbb{C}_{E_{ni}} \quad \text{for} \quad i \in I^+,$$
$$f_i \longleftrightarrow \mathbb{C}_{E_i} \quad \text{for } i \in I^-,$$
$$f_{in} \longleftrightarrow \mathbb{C}_{\{0\}\subseteq E_{ni}} \quad \text{for } i \in I^0,\ n > 0.$$

We identify $\mathbf{K}$ with ${}_{\mathcal{A}}U^-$ via the isomorphism and refer to $\mathbf{P}_\nu$ as the *canonical basis* of ${}_{\mathcal{A}}U^-_\nu$.

Remark 1.2. Let $i \in I^0, \nu = ni$. We denote by $\{\mathcal{O}_\lambda\}_{\lambda \vdash n}$ the nilpotent orbits (labelled by partitions of n) in E^{nil}_{ni} under the action of GL_{ni}. Then $f_{in} = IC(\mathcal{O}_{(1^n)})$ is the simple perverse sheaf associated with the closed orbit $\{0\}$ in E^{nil}_{ni}.

Let $i \in I^0$. We abbreviate $ii \cdots i \in \mathrm{Seq}(ni)$ by i^n and write f_i for $f_{(i,1)}$. The n-th power $f_i^n = \mathcal{L}_{i^n}$ is the Springer sheaf

$$\mathrm{Spr}_n = \pi_!(\mathbb{C}_{\widetilde{\mathscr{N}_n}}[\dim \widetilde{\mathscr{N}_n}]),$$

where $\mathscr{N}_n = E^{nil}_{ni}$, $\widetilde{\mathscr{N}_n} = \widetilde{\mathscr{F}}_{i^n}$, and $\pi = \pi_{i^n} : \widetilde{\mathscr{N}_n} \to \mathscr{N}_n$ is the Springer map. Therefore, we can write $f_i^n = \bigoplus_{\lambda \vdash n} IC(\mathcal{O}_\lambda) \otimes V_\lambda$ for some nonzero vector spaces V_λ, and f_i^n corresponding to the regular $\mathbb{C}[S_n]$-module under the Springer correspondence.

Recall that there is a geometric pairing

$$\mathbf{K} \times \mathbf{K} \longrightarrow \mathbb{Q}((q))$$

induced by the equivariant cohomology (see e.g. [16, 8.1.9]), which coincides with the bilinear form on ${}_{\mathcal{A}}U^-$ defined in Section 2.1.

In particular, when $i \in I^0$ and $n > 0$, we have

$$\{f_{in}, f_{in}\} = \sum_j \dim \left(H^j_{GL_n}(\mathrm{pt}) \right) q^j = \prod_{k=1}^{n} \frac{1}{1 - q^{2k}}.$$

2. Categorification of U^-

2.1. $\mathbb{Z}$-graded algebras and $\mathbb{Z}$-graded modules.

Let R be a $\mathbb{Z}$-graded $\mathbb{C}$-algebra. For a graded R-module $M = \bigoplus_{n\in\mathbb{Z}} M_n$, its graded dimension is defined to be

$$\mathbf{Dim}\, M = \sum_{n\in\mathbb{Z}} (\dim_{\mathbb{C}} M_n) q^n,$$

where q is a formal variable. For $m \in \mathbb{Z}$, we denote by $M\{m\}$ the graded R-module obtained from M by putting $(M\{m\})_n = M_{n-m}$. More generally, for $f(q) = \sum_{m\in\mathbb{Z}} a_m q^m \in \mathbb{N}[q, q^{-1}]$, we set $M^f = \bigoplus_{m\in\mathbb{Z}} (M\{m\})^{\oplus a_m}$.

Given two graded R-modules M and N, we denote by $\mathrm{Hom}_{R\text{-gr}}(M, N)$ the $\mathbb{C}$-vector space of degree-preserving homomorphisms and form the $\mathbb{Z}$-graded vector space

$$\mathrm{HOM}_R(M, N) = \bigoplus_{n\in\mathbb{Z}} \mathrm{Hom}_{R\text{-gr}}(M\{n\}, N) = \bigoplus_{n\in\mathbb{Z}} \mathrm{Hom}_{R\text{-gr}}(M, N\{-n\}).$$

2.2. **KLR-algebras** $R(\nu)$.

Let A be the Borcherds-Cartan matrix given by quiver as in (1.1). For $i \in I^{\leq 0}$, we define the polynomial

$$H_i(u, v) = (-1)^{a_{ii}/2}(u - v)^{-a_{ii}}.$$

For $i, j \in I$, we define

$$Q_{ij}(u, v) = (-1)^{h_{ij}}(u - v)^{-a_{ij}}.$$

Fix $\nu \in \mathbb{N}[I]$. The KLR-algebra $R(\nu)$ associated to A is defined to be the $\mathbb{C}$-algebra of the homogeneous generators given by diagrams (see [10] for a detailed explanation of the braid-like planar diagrams):

$1_{\boldsymbol{i}} =$ 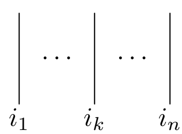 for $\boldsymbol{i} \in \mathrm{Seq}(\nu)$, $\deg(1_{\boldsymbol{i}}) = 0$,

$x_{k,\boldsymbol{i}} =$ 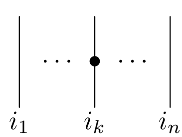 for $\boldsymbol{i} \in \mathrm{Seq}(\nu), 1 \leq k \leq n$, $\deg(x_{k,\boldsymbol{i}}) = 2$,

$\tau_{k,\boldsymbol{i}} =$ 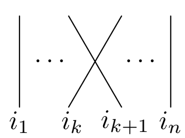 for $\boldsymbol{i} \in \mathrm{Seq}(\nu), 1 \leq k \leq n-1$, $\deg(\tau_{k,\boldsymbol{i}}) = -a_{i_k,i_{k+1}}$.

Subject to the following local relations:

(2.1)

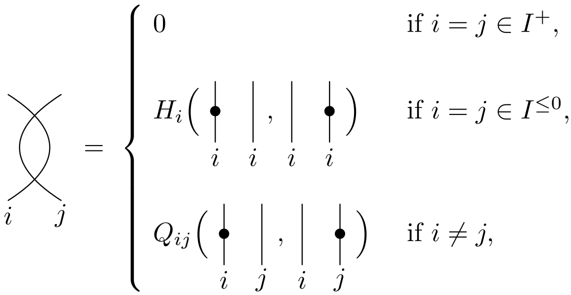

(2.2)

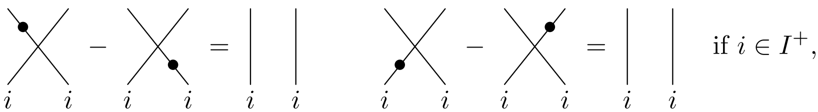

(2.3)

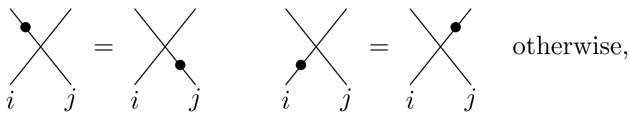

(2.4)

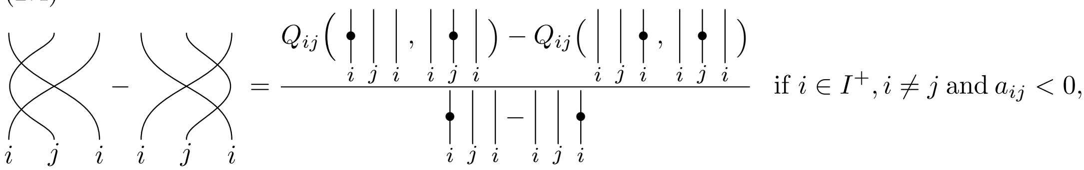

(2.5)

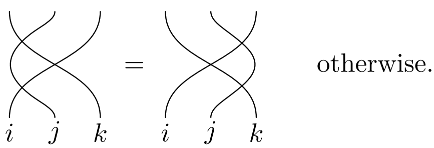

For $\boldsymbol{i}, \boldsymbol{j} \in \nu$, we set ${}_{\boldsymbol{j}}R(\nu)_{\boldsymbol{i}} = 1_{\boldsymbol{j}}R(\nu)1_{\boldsymbol{i}}$, then $R(\nu) = \bigoplus_{\boldsymbol{i},\boldsymbol{j}} {}_{\boldsymbol{j}}R(\nu)_{\boldsymbol{i}}$. Denote by $P_{\boldsymbol{i}} = R(\nu)1_{\boldsymbol{i}}$ (resp. ${}_{\boldsymbol{j}}P = 1_{\boldsymbol{j}}R(\nu)$) the gr-projective left (resp. right) $R(\nu)$-module.

For $\boldsymbol{i} \in \mathrm{Seq}(\nu)$, set $\mathscr{P}_{\boldsymbol{i}} = \mathbb{C}[x_1(\boldsymbol{i}), \ldots, x_n(\boldsymbol{i})]$ and form the $\mathbb{C}$-vector space $\mathscr{P}_\nu = \bigoplus_{\boldsymbol{i} \in \mathrm{Seq}(\nu)} \mathscr{P}_{\boldsymbol{i}}$. Each $\omega \in S_n$ acts on $\mathscr{P}_\nu$ by sending $x_a(\boldsymbol{i})$ to $x_{\omega(a)}(\omega(\boldsymbol{i}))$. We define an action of $R(\nu)$ on $\mathscr{P}_\nu$ as follows:

(i) If $\boldsymbol{i} \neq \boldsymbol{k}$, ${}_{\boldsymbol{j}}R(\nu)_{\boldsymbol{i}}$ acts on $\mathscr{P}_{\boldsymbol{k}}$ by 0.

(ii) For $f \in \mathscr{P}_{\boldsymbol{i}}$, $1_{\boldsymbol{i}} \cdot f = f$, $\;x_{k,\boldsymbol{i}} \cdot f = x_k(\boldsymbol{i}) f$.

(iii) If $\boldsymbol{i} = i_1 \dots i_n$ with $i_k = i,\ i_{k+1} = j$,

$$\tau_{k,\boldsymbol{i}} \cdot f = \begin{cases} \partial_k(f) = \frac{f - s_k f}{x_k(\boldsymbol{i}) - x_{k+1}(\boldsymbol{i})} & \text{if } i = j \in I^+, \\ (x_k(\boldsymbol{i}) - x_{k+1}(\boldsymbol{i}))^{-a_{ii}/2} s_k f & \text{if } i = j \in I^{\le 0}, \\ (x_k(s_k\boldsymbol{i}) - x_{k+1}(s_k\boldsymbol{i}))^{h_{ij}} s_k f & \text{if } i \neq j. \end{cases}$$

It is easy to check $\mathscr{P}_\nu$ is an $R(\nu)$-module with the action defined above.

2.3. **Algebras $R(ni)$ and their gr-irreducible modules.**

Let $\nu = ni$ for some $i \in I$. Note the unique sequence in $\mathrm{Seq}(ni)$ is i^n. The algebra $R(ni)$ is generated by $x_{1,i^n}, \dots, x_{n,i^n}$ of degree 2 and $\tau_{1,i^n}, \dots, \tau_{n-1,i^n}$ of degree $-a_{ii}$ subject to the following local relations:

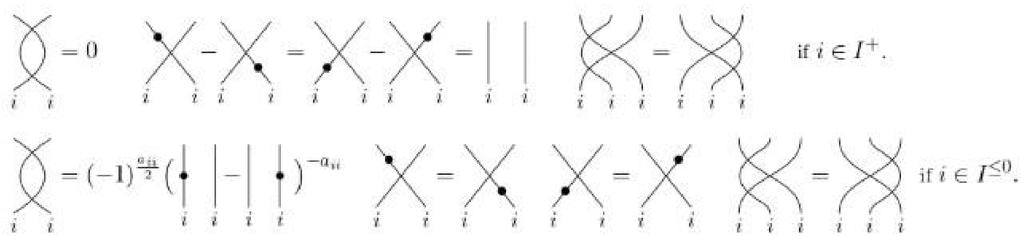

We will abbreviate x_{k,i^n} (resp. τ_{k,i^n}) for x_k (resp. τ_k). In all cases, $R(ni)$ has a basis

$$\{x_1^{r_1} \cdots x_n^{r_n} \tau_\omega \mid \omega \in S_n, r_1, \dots, r_n \ge 0\}.$$

Indeed, for example, if $i \in I^{\le 0}$, it suffices to consider the actions of these elements on $x_1^N x_2^N \cdots x_n^{nN}$ for $N \gg 0$.

Thus, we can identify the polynomial algebra $P_n = \mathbb{C}[x_1, \dots, x_n]$ with the subalgebra of $R(ni)$ generated by $x_1, \dots, x_n$. Consequently, the center of $R(ni)$ is identified with Z_n, the algebra of symmetric polynomials in $x_1, \dots, x_n$. We next consider the graded irreducible representations of $R(ni)$.

Case 1: $i \in I^+$.

By the representation theory of the nil-Hecke algebras, $R(ni)$ has a unique gr-irreducible module $V(i^n)$ of graded dimension $[n]!$, which is isomorphic to $R(ni) \otimes_{P_n} \mathbf{1}_n \left\{\frac{n(n-1)}{2}\right\}$. Here, $\mathbf{1}_n$ is the one-dimensional trivial module over P_n on which each x_k acts by 0.

Case 2: $i \in I^-$.

In this case, $R(ni)$ has only trivial idempotents. It has a unique gr-irreducible module $V(i^n)$, which is the one-dimensional trivial module with the gr-projective cover $R(ni)$.

Case 3: $i \in I^0$.

In the case, the degree zero part $R(ni)_0$ is the symmetric group algebra $\mathbb{C}S_n$.

Denote by $\mathcal{P}_n$ the set of partitions of n. It is well known that $\mathbb{C}S_n$ has $|\mathcal{P}_n|$ many irreducible modules.

Let V be an irreducible $\mathbb{C}S_n$-module (which is also an indecomposable projective module). Then, we define

$$\widetilde{V} := \frac{R(ni) \otimes_{R(ni)_0} V}{R(ni)_{>0} \otimes_{R(ni)_0} V}$$

as a gr-irreducible $R(ni)$-module. In other words, $\widetilde{V}$ is obtained from V by annihilating the actions of $x_1, \ldots, x_n$. Moreover, all gr-irreducible $R(ni)$-modules can be obtained in this way. When no confusion arises, we denote $\widetilde{V}$ simply by V. We have shown the following:

Proposition 2.1. *If $V_1, \ldots, V_{|\mathcal{P}_n|}$ is a complete set of non-isomorphic classes of irreducible $\mathbb{C}S_n$-modules, then $V_1, \ldots, V_{|\mathcal{P}_n|}$ is a complete set of non-isomorphic classes of gr-irreducible $R(ni)$-modules. In particular, the gr-Jacobson radical $J^{gr}(R(ni)) = R(ni)_{>0}$.*

Let $V_{i,n}$ be the one-dimensional trivial module over $\mathbb{C}[S_n]$. Note that

$$V_{i,n} = \mathbb{C}S_n \cdot e_{i,n} = \mathbb{C} \cdot e_{i,n},$$

where $e_{i,n}$ is defined by

$$e_{i,n} = \frac{1}{n!} \sum_{\omega \in S_n} \omega \in \mathbb{C}[S_n].$$

If $r + t = n$, then the restriction of $V_{i,n}$ to $\mathbb{C}[S_r] \otimes \mathbb{C}[S_t]$-modules gives

$$\mathrm{Res}^n_{r,t} V_{i,n} \cong V_{i,r} \otimes V_{i,t} = \mathbb{C}S_n \cdot e_{i,r} \otimes \mathbb{C}S_n \cdot e_{i,t}.$$

The gr-projective cover of $R(ni)$-module $V_{i,n}$ is $P_{i,n} = R(ni)e_{i,n}$, which has a basis

$$\{x_1^{r_1} \cdots x_n^{r_n} \cdot e_{i,n} \mid r_1, \ldots, r_n \geq 0\},$$

the restriction of $P_{i,n}$ to $R(ri) \otimes R(ti)$-modules gives

$$\mathrm{Res}^n_{r,t} P_{i,n} \cong P_{i,r} \otimes P_{i,t}. \tag{2.6}$$

Since $e_{i,n}R(ni)e_{i,n}$ is spanned by $\{f \cdot e_{i,n} \mid f \in Z_n\}$, we see that

$$(P_{i,n}, P_{i,n}) = \mathbf{Dim}(e_{i,n}R(ni)e_{i,n}) = \mathbf{Dim}\ Z_n \\ = 1/\left((1-q^2)(1-q^4)\cdots(1-q^{2n})\right). \tag{2.7}$$

Here (,) is the Khovanov-Lauda's form defined in (2.8).

2.4. **Grothendieck groups $K_0(R)$ and $G_0(R)$.**

Using the polynomial representation $\mathscr{P}_\nu$ of $R(\nu)$, one can obtain by a similar argument in [10, Theorem 2.5] that $\mathscr{P}_\nu$ is a faithful $R(\nu)$-module and ${}_{\boldsymbol{i}}R(\nu)_{\boldsymbol{j}}$ ($\boldsymbol{i}, \boldsymbol{j} \in \nu$) has a basis

$$\{x_{1,\boldsymbol{i}}^{r_1}\cdots x_{n,\boldsymbol{i}}^{r_n}\cdot \widehat{\omega}_{\boldsymbol{j}} \mid r_1, \dots, r_n \geq 0,\ \omega \in S_n \text{ such that } \omega(\boldsymbol{j}) = \boldsymbol{i}\},$$

where $\widehat{\omega}_{\boldsymbol{j}} \in {}_{\boldsymbol{i}}R(\nu)_{\boldsymbol{j}}$ is uniquely determined by a fixed reduced expression of ω.

Assume that there is a sequence ${i_1}^{m_1}\cdots {i_t}^{m_t} \in \mathrm{Seq}(\nu)$ such that $i_1, \dots, i_t$ are all distinct. Similar to [10, Theorem 2.9], the center $Z(R(\nu))$ of $R(\nu)$ can be described as

$$Z(R(\nu)) \cong \bigotimes_{k=1}^{t} \mathbb{C}[z_1, \dots, z_{m_k}]^{S_{m_k}},$$

where the latter is a tensor product of symmetric polynomial algebras such that the generators in $\mathbb{C}[z_1, \dots, z_{m_k}]$ are of degree 2. Moreover, $R(\nu)$ is a free $Z(R(\nu))$-module of rank $((m_1 + \cdots + m_t)!)^2$. It is also a gr-free $Z(R(\nu))$-module of finite rank. So we have

$$\mathbf{Dim} Z(R(\nu)) = \prod_{k=1}^{t}\left(\prod_{c=1}^{m_k}\frac{1}{1-q^{2c}}\right)$$

and

$$\mathbf{Dim} R(\nu) \in \mathbb{Z}[q, q^{-1}] \cdot \mathbf{Dim} Z(R(\nu)).$$

Denote by

$R(\nu)$-Mod: the category of finitely generated graded $R(\nu)$-modules,

$R(\nu)$-fMod: the category of finite-dimensional graded $R(\nu)$-modules,

$R(\nu)$-pMod: the category of projective objects in $R(\nu)$-Mod.

Up to isomorphism and degree shifts, each $R(\nu)$ has only finitely many gr-irreducible modules, all of which are finite-dimensional and are irreducible $R(\nu)$-modules by forgetting the grading.

Let $\mathbb{B}_\nu$ be the set of equivalence classes of gr-irreducible $R(\nu)$-modules. Choose one representative S_b from each equivalence class and denote by P_b the gr-projective cover of S_b. The Grothendieck group $G_0(R(\nu))$ (resp. $K_0(R(\nu))$) of $R(\nu)$-fMod (resp. $R(\nu)$-pMod) are free $\mathbb{Z}[q,q^{-1}]$-modules with $q[M]=[M\{1\}]$, and with a basis $\{[S_b]\}_{b\in\mathbb{B}_\nu}$ (resp. $\{[P_b]\}_{b\in\mathbb{B}_\nu}$).

Let $R=\bigoplus_{\nu\in\mathbb{N}[I]} R(\nu)$ and form

$$G_0(R)=\bigoplus_{\nu\in\mathbb{N}[I]} G_0(R(\nu)),\ K_0(R)=\bigoplus_{\nu\in\mathbb{N}[I]} K_0(R(\nu)).$$

The $\mathbb{Z}[q,q^{-1}]$-modules $K_0(R)$ and $G_0(R)$ are equipped with twisted bialgebras structure induced by the induction and restriction functors:

$$\mathrm{Ind}_{\nu,\nu'}^{\nu+\nu'}: R(\nu)\otimes R(\nu')\text{-Mod}\to R(\nu+\nu')\text{-Mod},\ M\mapsto R(\nu+\nu')1_{\nu,\nu'}\otimes_{R(\nu)\otimes R(\nu')} M,$$

$$\mathrm{Res}_{\nu,\nu'}^{\nu+\nu'}: R(\nu+\nu')\text{-Mod}\to R(\nu)\otimes R(\nu')\text{-Mod},\ N\mapsto 1_{\nu,\nu'}N,$$

where $1_{\nu,\nu'}=1_\nu\otimes 1_{\nu'}$. More precisely, we set $|x|=|\nu|\in\mathbb{N}[I]$ for $x\in R(\nu)$-Mod and equip $K_0(R)\otimes K_0(R)$ (resp. $G_0(R)\otimes G_0(R)$) with a twisted algebra structure via

$$(x_1\otimes x_2)(y_1\otimes y_2)=q^{-|x_2|\cdot|y_1|}x_1y_1\otimes x_2y_2,$$

then Res is a $\mathbb{Z}[q,q^{-1}]$-algebra homomorphism by Mackey's Theorem [10, Proposition 2.18].

The $K_0(R)$ and $G_0(R)$ are dual to each other with respect to the bilinear pairing $(\ ,\ )\colon K_0(R)\times G_0(R)\to\mathbb{Z}[q,q^{-1}]$ given by

$$([P],[M])=\mathbf{Dim}(P^\psi\otimes_{R(\nu)} M)=\mathbf{Dim}(\mathrm{HOM}_{R(\nu)}(\overline{P},M)), \tag{2.8}$$

where ψ is the anti-involution of $R(\nu)$ obtained by flipping diagrams about horizontal axis, which turns a left $R(\nu)$-module into a right one, and $\overline{P}=\mathrm{HOM}(P,R(\nu))^\psi$. There is also a symmetric bilinear form $(\ ,\ )\colon K_0(R)\times K_0(R)\to\mathbb{Z}(\!(q)\!)$ defined in the same way.

By (2.7) and [10, Proposition 3.3], we obtain the following proposition.

Proposition 2.2. *The symmetric bilinear form on $K_0(R)$ satisfies:*

1. $([M],[N])=0$ *if $M\in R(\nu)$-Mod, $N\in R(\mu)$-Mod with $\nu\neq\mu$,*
2. $(1,1)=1$, *where $1=\mathbb{C}$ as a module over $R(0)=\mathbb{C}$,*
3. $([P_i],[P_i])=1/(1-q^2)$ *for $i\in I^\pm$,*
   $([P_{i,n}],[P_{i,n}])=1/\big((1-q^2)(1-q^4)\cdots(1-q^{2n})\big)$ *for $i\in I^0, n>0$.*
4. $(x,yz)=(Res(x),y\otimes z)$ *for $x,y,z\in K_0(R)$.*

2.5. **Quantum Serre relations.**

Let $\boldsymbol{i}$ be a sequence with *divided powers* in ν:

$$\boldsymbol{i} = j_1 \dots j_{p_0} i_1^{(m_1)} k_1 \dots k_{p_1} i_2^{(m_2)} \ \dots \ i_t^{(m_t)} h_1 \dots h_{p_t},$$

where $i_1, \dots, i_t \in I^+$ and $\boldsymbol{i}$ is of the weight ν.

For such an $\boldsymbol{i}$, we assign the following idempotent of $R(\nu)$

$$1_{\boldsymbol{i}} = 1_{j_1 \dots j_{p_0}} \otimes e_{i_1,m_1} \otimes 1_{k_1 \dots k_{p_1}} \otimes e_{i_2,m_2} \otimes \ \cdots \ \otimes e_{i_t,m_t} \otimes 1_{h_1 \dots h_{p_t}},$$

where $e_{i,m} = x_1^{m-1} x_2^{m-2} \cdots x_{m-1} \tau_{w_0}$ with w_0 being the longest element in S_m.

We define the gr-projective modules for $\boldsymbol{i}$ by

$$_{\boldsymbol{i}}P = 1_{\boldsymbol{i}} R(\nu)\{-\langle \boldsymbol{i} \rangle\}, \quad P_{\boldsymbol{i}} = R(\nu)\psi(1_{\boldsymbol{i}})\{-\langle \boldsymbol{i} \rangle\},$$

where

$$\langle \boldsymbol{i} \rangle = \sum_{k=1}^{t} \frac{m_k(m_k-1)}{2}.$$

In particular, for $i \in I^+$ and $n \geq 0$,

$$P_{i^{(n)}} = R(ni)\psi(e_{i,n}) \left\{ -\frac{n(n-1)}{2} \right\} \cong R(ni) e_{i,n} \left\{ \frac{n(n-1)}{2} \right\}. \tag{2.9}$$

Proposition 2.3. *Suppose $i \in I^+$, $j \in I$, $i \neq j$. Let $n \in \mathbb{Z}_{>0}$ and $m = 1 - na_{ij}$. We have isomorphisms of graded left $R(\nu)$-modules*

$$\bigoplus_{c=0}^{\lfloor \frac{m}{2} \rfloor} P_{i^{(2c)} j^n i^{(m-2c)}} \cong \bigoplus_{c=0}^{\lfloor \frac{m-1}{2} \rfloor} P_{i^{(2c+1)} j^n i^{(m-2c-1)}} \quad \text{if } j \in I^{\pm},$$

$$\bigoplus_{c=0}^{\lfloor \frac{m}{2} \rfloor} R(i^m j^n) \psi(e_{i,2c} \otimes e_{j,n} \otimes e_{i,m-2c}) \{-\langle i^{(2c)} i^{(m-2c)} \rangle\}$$

$$\cong \bigoplus_{c=0}^{\lfloor \frac{m-1}{2} \rfloor} R(i^m j^n) \psi(e_{i,2c+1} \otimes e_{j,n} \otimes e_{i,m-2c-1}) \{-\langle i^{(2c+1)} i^{(m-2c-1)} \rangle\} \quad \text{if } j \in I^0.$$

Moreover, if $a_{ij} = 0$, then

$$P_{ij} \cong P_{ji} \quad \text{for } i, j \in I,$$

$$R(i^n j) \cdot e_{i,n} \otimes 1_j \cong R(i^n j) \cdot 1_j \otimes e_{i,n} \quad \text{for } i \in I^0, j \in I,$$

$$R(i^n j^m) \cdot e_{i,n} \otimes e_{j,m} \cong R(i^n j^m) \cdot e_{j,m} \otimes e_{i,n} \quad \text{for } i, j \in I^0.$$

Proof. The proof is the same as the 'Box' calculations in [11]. We only explain the last isomorphism. Let $i, j \in I^0$ with $a_{ij} = 0$. Note that

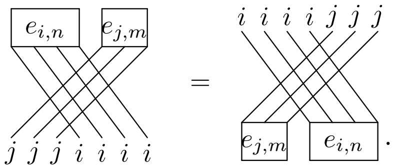

The right multiplication by

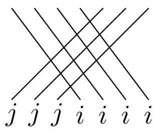

is a map from $R(i^n j^m) \cdot e_{i,n} \otimes e_{j,m}$ to $R(i^n j^m) \cdot e_{j,m} \otimes e_{i,n}$, which has the obvious inverse by flipping this diagram. $\square$

Let $K_0(R)_{\mathbb{Q}(q)} = \mathbb{Q}(q) \otimes_{\mathbb{Z}[q,q^{-1}]} K_0(R)$. By (2.6) and Proposition 2.3, we have a well-defined bialgebra homomorphism

$$\begin{aligned} \Gamma_{\mathbb{Q}(q)} \colon U^- &\to K_0(R)_{\mathbb{Q}(q)} \\ f_i &\mapsto [P_i] \qquad \text{for } i \in I^{\pm} \\ f_{in} &\mapsto [P_{i,n}] \qquad \text{for } i \in I^0, n > 0. \end{aligned}$$

By Proposition 2.2, the bilinear form $\{\ ,\ \}$ on U^- and the Khovanov-Lauda's form $(\ ,\ )$ on $K_0(R)_{\mathbb{Q}(q)}$ coincide under the map $\Gamma_{\mathbb{Q}(q)}$, that is

$$(\Gamma_{\mathbb{Q}(q)}(x), \Gamma_{\mathbb{Q}(q)}(y)) = \{x, y\} \quad \text{for } x, y \in U^-.$$

Thus, $\Gamma_{\mathbb{Q}(q)}$ is injective by the non-degeneracy of $\{\ ,\ \}$. We have

$$\Gamma_{\mathbb{Q}(q)}(\overline{x}) = \overline{\Gamma_{\mathbb{Q}(q)}(x)} \quad \text{for } x \in U^-.$$

Moreover, $\Gamma_{\mathbb{Q}(q)}$ induces an injective $\mathcal{A}$-bialgebra homomorphism $\Gamma \colon {}_{\mathcal{A}}U^- \to K_0(R)$.

2.6. **Surjectivity of $\Gamma_{\mathbb{Q}(q)}$ and Γ.**

Let $\nu \in \mathbb{N}[I]$. Define $\underline{\nu}$ to be the set of sequences $\boldsymbol{i}$ of type ν with 'parameters' in $i \in I^0$. Such a sequence is of the form

$$\boldsymbol{i} = j_1 \dots j_{p_0} (\boldsymbol{i_1}, \boldsymbol{n_1}) k_1 \dots k_{p_1} (\boldsymbol{i_2}, \boldsymbol{n_2}) \ \dots \ (\boldsymbol{i_t}, \boldsymbol{n_t}) h_1 \dots h_{p_t},$$

with $(i_1,n_1),\dots,(i_t,n_t)\in I^0\times\mathbb{Z}_{>0}$ and such that the expended sequence

$$j_1\dots j_{p_0}\underbrace{i_1\dots i_1}_{n_1}k_1\dots k_{p_1}\underbrace{i_2\dots i_2}_{n_2}\;\cdots\;\underbrace{i_t\dots i_t}_{n_t}h_1\dots h_{p_t}$$

belongs to ν. For each $\boldsymbol{i}\in\underline{\nu}$, we assign the following idempotent of $R(\nu)$

$$1_{\boldsymbol{i}}=1_{j_1\dots j_{p_0}}\otimes e_{i_1,n_1}\otimes 1_{k_1\dots k_{p_1}}\otimes e_{i_2,n_2}\otimes\;\cdots\;\otimes e_{i_t,n_t}\otimes 1_{h_1\dots h_{p_t}}.$$

We define the character of $M\in R(\nu)$-fMod as

$$\mathrm{Ch}M=\sum_{\boldsymbol{i}\in\underline{\nu}}\mathbf{Dim}(1_{\boldsymbol{i}}M)\boldsymbol{i}\;\in\mathbb{Z}[q,q^{-1}]\underline{\nu}.$$

Each $\boldsymbol{i}\in\underline{\nu}$ determines a monomial $\Theta_{\boldsymbol{i}}$ in U^- under the correspondence

$$i\mapsto f_i\;\text{ for } i\in I^{\pm},\quad (i,n)\mapsto f_{in}\;\text{ for } i\in I^0, n>0.$$

Let U^-_ν be the $\mathbb{Q}(q)$-subspace of U^- spanned by $\Theta_{\boldsymbol{i}}$ for all $\boldsymbol{i}\in\underline{\nu}$. Combining with $\Gamma_{\mathbb{Q}(q)}$, we obtain a $\mathbb{Q}(q)$-linear map

$$\mathbb{Q}(q)\underline{\nu}\longrightarrow U^-_\nu\xrightarrow{\Gamma_{\mathbb{Q}(q)}}K_0(R(\nu))_{\mathbb{Q}(q)},$$

which has the dual map

$$G_0(R(\nu))_{\mathbb{Q}(q)}\xrightarrow{\mathrm{Ch}}\mathbb{Q}(q)\underline{\nu}.$$

We next show that the character map Ch is injective.

Let $i\in I^0,\nu=ni$. Then

$$\underline{\nu}=\{(i,n_1)\dots(i,n_t)\mid n_1+\cdots+n_t=n\}.$$

Since $\Gamma_{\mathbb{Q}(q)}\colon U^-_{ni}\to K_0(R(\nu))_{\mathbb{Q}(q)}$ is injective and they have the same dimension $|\mathcal{P}_n|$, we see that $\Gamma_{\mathbb{Q}(q)}$ is an isomorphism in this case and so $\mathrm{Ch}\colon G_0(R(ni))_{\mathbb{Q}(q)}\to\mathbb{Q}(q)\underline{\nu}$ is injective.

Lemma 2.4. *Let $i\in I^0$. The characters of all non-isomorphic gr-irreducible $R(ni)$-modules are $\mathbb{Q}(q)$-linearly independent.*

Example 2.5. Recall that the irreducible $\mathbb{C}[S_n]$-modules are *Specht modules* parametrized by the partitions λ of n (see, for example, [3]).

In this example, we consider the case when $n = 3$. Then the irreducible $\mathbb{C}S_3$-modules and their characters are given by

$$S^{(3)} = P_{i,3} = \mathbb{C}S_3 \cdot e_{i,3}, \quad \mathrm{Ch}\ S^{(3)} = e_{i,3} + e_{i,1} \otimes e_{i,2} + e_{i,2} \otimes e_{i,1} + e_{i,1} \otimes e_{i,1} \otimes e_{i,1}$$
$$S^{(21)} = \mathbb{C}S_3 \cdot 1/3(1 + s_1 - s_2s_1 - s_1s_2s_1), \quad \mathrm{Ch}\ S^{(21)} = e_{i,1} \otimes e_{i,2} + e_{i,2} \otimes e_{i,1} + 2e_{i,1} \otimes e_{i,1} \otimes e_{i,1}.$$
$$S^{(111)} = \mathbb{C}S_3 \cdot 1/6(1 - s_1 - s_2 + s_1s_2 + s_2s_1 - s_1s_2s_1), \quad \mathrm{Ch}\ S^{(111)} = e_{i,1} \otimes e_{i,1} \otimes e_{i,1}$$

Here, $S^{(3)}, S^{(21)}, S^{(111)}$ are the Specht modules.

Let $i \in I$ and $n \geq 0$. Define a functor

$$\Delta_{i^n} \colon R(\nu)\text{-Mod} \to R(\nu - ni) \otimes R(ni)\text{-Mod}$$
$$M \mapsto (1_{\nu - ni} \otimes 1_{ni})M.$$

For each $M \in R(\nu)$-fMod, we define

$$\varepsilon_i M = \max\{n \geq 0 \mid \Delta_{i^n} M \neq 0\}.$$

The following lemma can be proved by the same manner in [10, Section 3.2].

Lemma 2.6. *Let $i \in I$ and $M \in R(\nu)$-fMod be a gr-irreducible module with $\varepsilon_i M = n$. Then $\Delta_{i^n} M$ is isomorphic to $K \otimes V$ for some gr-irreducible $K \in R(\nu - ni)$-fMod with $\varepsilon_i K = 0$ and some gr-irreducible $V \in R(ni)$-fMod. Moreover, we have*

$$M \cong hd\ Ind_{\nu - ni, ni} K \otimes V.$$

Recall that a gr-irreducible $R(ni)$-module V has one of the following forms:

(i) if $i \in I^+$, then $V = V(i^n)$, the unique gr-irreducible module of the nil-Hecke algebra,
(ii) if $i \in I^-$, then $V = V(i^n)$ is the one-dimensional trivial module,
(iii) if $i \in I^0$, then V has $|\mathcal{P}_n|$ many choices.

Theorem 2.7. *The map Ch: $G_0(R(\nu))_{\mathbb{Q}(q)} \to \mathbb{Q}(q)\underline{\nu}$ is injective.*

Proof. We show that the characters of elements in $\mathbb{B}_\nu$ are linearly independent over $\mathbb{Q}(q)$ by induction on $\ell(\nu)$. The case of $\ell(\nu) = 0$ is trivial. Assume for $\ell(\nu) < n$, our assertion is true. Now, suppose $\ell(\nu) = n$ and we are given a non-trivial linear combination

$$\sum_M c_M \mathrm{Ch} M = 0 \tag{2.10}$$

for some $M \in \mathbb{B}_\nu$ and some $c_M \in \mathbb{Q}(q)$. Choose $i \in I$. We prove by a downward induction on $k = n, \dots, 1$ that $c_M = 0$ for all M with $\varepsilon_i M = k$.

If $k = n$ and $M \in \mathbb{B}_\nu$ with $\varepsilon_i M = n$, then $\nu = ni$ and M is a gr-irreducible $R(ni)$-module. When $i \in I^+ \sqcup I^-$, our assertion is trivial. When $i \in I^0$, it follows from Lemma 2.4.

Assume for $1 \leq k < n$, we have $c_L = 0$ for all L with $\varepsilon_i L > k$. Taking out the terms with i^k-tail in the rest of (2.10), we obtain

$$\sum_{M:\, \varepsilon_i M = k} c_M \mathrm{Ch}(\Delta_{i^k} M) = 0. \tag{2.11}$$

By Lemma 2.6, we can assume $\Delta_{i^k} M \cong K_M \otimes V_M$ for gr-irreducible $K_M \in R(\nu - ki)$-fMod with $\varepsilon_i K_M = 0$ and gr-irreducible $V \in R(ki)$-fMod. Then (2.11) becomes

$$\sum_{M:\, \varepsilon_i M = k} c_M \mathrm{Ch} K_M \otimes \mathrm{Ch} V_M = 0.$$

Note that if $[M] \neq [M']$ in $\mathbb{B}_\nu$, then we have $[K_M] \neq [K_{M'}]$ or $[V_M] \neq [V_{M'}]$.

By the induction hypothesis, $\mathrm{Ch}K$ $(K \in \mathbb{B}_{\nu - ki})$ are linearly independent, and by Lemma 2.4, if $i \in I^0$, $\mathrm{Ch}V$ $(V \in \mathbb{B}_{ki})$ are linearly independent. It follows that $c_M = 0$ for all M with $\varepsilon_i M = k$. Since each gr-irreducible $R(\nu)$-modules M has $\varepsilon_i M > 0$ for at least one $i \in I$, the theorem has been proved. $\square$

Remark 2.8. We see from the proof that the map $\mathrm{Ch}\colon G_0(R(\nu)) \to \mathbb{Z}[q, q^{-1}]\underline{\nu}$ is also injective. If we set $\mathrm{ch} = \mathrm{Ch}|_{q=1}$, then by a similar argument, the ungraded characters of elements in $\mathbb{B}_\nu$ are linearly independent over $\mathbb{Z}$.

Corollary 2.9. $\Gamma_{\mathbb{Q}(q)}\colon U^- \to K_0(R)_{\mathbb{Q}(q)}$ *is an isomorphism.*

We next consider the surjectivity of $\Gamma\colon {}_{\mathcal{A}}U^- \to K_0(R)$.

For $\lambda \vdash n$, let S^λ denote the Specht module corresponding to λ (or the Young diagram of shape λ). Let $\prec$ be the dominance ordering on $\mathcal{P}_n$. For $\mu \prec \lambda$, we denote by $S^{\lambda/\mu}$ the shew representation of $\mathbb{C}S_n$ corresponding to the skew diagram λ/μ.

Lemma 2.10. [3, Proposition 3.5.5] *Let $\lambda \vdash n$ be a partition and $(b_1, \dots, b_\ell) \vDash n$ be a composition of n. Then*

$$Res^n_{b_1,\dots,b_\ell} S^\lambda = \bigoplus (S^{\lambda^{(1)}} \otimes S^{\lambda^{(2)}/\lambda^{(1)}} \otimes \cdots \otimes S^{\lambda/\lambda^{(\ell-1)}}),$$

where the sum runs over all sequences $\lambda^{(1)} \prec \lambda^{(2)} \prec \cdots \prec \lambda^{(\ell)} = \lambda$ *such that* $|\lambda^{(j)}/\lambda^{(j-1)}| = b_j$ *for all* $j = 1, \ldots, \ell$.

Lemma 2.11. [3, Proposition 3.5.12] *Assume* $|\lambda/\mu| = k$. *The multiplicity of the trivial representation* $S^{(k)}$ *in* $S^{\lambda/\mu}$ *is* 1 *if* λ/μ *is totally disconnected, and* 0 *otherwise.*

Proposition 2.12. *Let* $\lambda \vdash n$. *Let* $\mathbf{c} \vDash n$ *be a composition of* n, *which determines a partition* $\lambda_{\mathbf{c}} \vdash n$. *Then*

$$\dim_{\mathbb{C}}(e_{i,\mathbf{c}} \cdot S^{\lambda}) = \begin{cases} 1 & \text{if } \lambda_{\mathbf{c}} = \lambda, \\ 0 & \text{if } \lambda_{\mathbf{c}} > \lambda, \end{cases}$$

where $>$ *is the lexicographical order of partitions.*

Proof. The proposition follows from Lemma 2.10 and Lemma 2.11, using the fact that the Kostka number

$$K_{\lambda,\mathbf{c}} = K_{\lambda,\lambda_{\mathbf{c}}} = \begin{cases} 1 & \text{if } \lambda_{\mathbf{c}} = \lambda, \\ 0 & \text{if } \lambda_{\mathbf{c}} > \lambda. \end{cases}$$

□

Note that Lemma 2.4 can be derived directly from the proposition above.

For $i \in I^0, \lambda = (c_1, \ldots, c_r) \vdash n$, we set

$$P_{i,\lambda} = P_{i,c_1} \cdots P_{i,c_r} = R(ni) \cdot e_{i,\lambda}.$$

Then $(P_{i,\lambda}, S^{\mu}) = \dim_{\mathbb{C}}(e_{i,\lambda} \cdot S^{\mu})$ and according to Proposition 2.12, the matrix

$$\{(P_{i,\lambda}, S^{\mu})\}_{\lambda,\mu \vdash n}$$

unitriangular. It follows that each $[P] \in K_0(R(ni))$ can be written as a $\mathbb{Z}[q, q^{-1}]$-linear combination of $[P_{i,\lambda}]$ for $\lambda \vdash n$.

More generally, we write the set I as

$$I = \{i_1, i_2, \ldots, i_k, \ldots\}.$$

For a gr-irreducible $R(\nu)$-module M, we let $c_1 = \varepsilon_{i_1} M$ and assume $\Delta_{i_1^{c_1}} M = M_1 \otimes V_M$ for gr-irreducible M_1 with $\varepsilon_{i_1} M_1 = 0$ and gr-irreducible $V_M \in R(c_1 i_1)$-Mod.

If $i_1 \in I^0$, then $V_M = S^{\lambda^{(1)}}$ for some $\lambda^{(1)} \vdash c_1$. So we get a pair $(c_1, \lambda^{(1)})$, where we set $\lambda^{(1)} = 0$ when $i_1 \notin I^0$. Inductively, $c_k = \varepsilon_{i_k} M_{k-1}$ and $\Delta_{i_k{}^{c_k}} M_{k-1} =$

$M_k \otimes V_{M_{k-1}}$, and we obtain $(c_k, \lambda^{(k)})$. If we do not get $M_k = 0$ after I exhausted, we can continue the above process from i_1. Therefore, each $b \in \mathbb{B}_\nu$ is assigned by a sequence

$$W_b = (c_1, \lambda^{(1)})(c_2, \lambda^{(2)}) \cdots (c_k, \lambda^{(k)}) \cdots ,$$

and we see from Lemma 2.6 that b is uniquely determined by W_b.

Set

$$P_{(c_k,\lambda^{(k)})} = \begin{cases} P_{i_k^{(c_k)}} & \text{if } i_k \in I^+, \\ P_{i_k{}^{c_k}} & \text{if } i_k \in I^-, \\ P_{i_k,\lambda^{(k)}} & \text{if } i_k \in I^0, \end{cases}$$

and

$$P_{W_b} = \cdots P_{(c_k,\lambda^{(k)})} \cdots P_{(c_2,\lambda^{(2)})} P_{(c_1,\lambda^{(1)})}.$$

Let $b, b' \in \mathbb{B}_\nu$ with $W_b = (c_1, \lambda^{(1)})(c_2, \lambda^{(2)}) \cdots$ and $W_{b'} = (d_1, \mu^{(1)})(d_2, \mu^{(2)}) \cdots$. We denote $W_b > W_{b'}$ if for some t,

$$(c_1, \lambda^{(1)}) = (d_1, \mu^{(1)}), \ldots, (c_{t-1}, \lambda^{(t-1)}) = (d_{t-1}, \mu^{(t-1)})$$

but

$$c_t > d_t \text{ or } c_t = d_t, \lambda^{(t)} > \mu^{(t)}.$$

Proposition 2.13. *$HOM(P_{W_b}, S_{b'}) = 0$ if $b > b'$ and $HOM(P_{W_b}, S_b) \cong \mathbb{C}$.*

Proof. For $i \in I^+$, we have $\mathrm{HOM}(P_{i^{(n)}}, V(i^n)) \cong \mathbb{C}$ since $P_{i^{(n)}}$ is the graded projective cover of $V(i^n)$. For $i \in I^-$, $R(ni) = P_{i^n}$ is the graded projective cover of $V(i^n)$. The results follows immediately from the Frobenius reciprocity and Proposition 2.12, which deals with the case when $i \in I^0$. $\square$

By proposition above, each $[P] \in K_0(R(\nu))$ can be written as a $\mathbb{Z}[q, q^{-1}]$-linear combination of $[P_{W_b}]$ for $b \in \mathbb{B}_\nu$. Therefore, Γ is surjective.

Theorem 2.14. *$\Gamma : {}_{\mathcal{A}}U^- \to K_0(R)$ is an isomorphism.*

For $M \in R(\nu)$-fMod, let $M^* = \mathrm{HOM}_{\mathbb{C}}(M, \mathbb{C})^\psi$ be the dual module in $R(\nu)$-fMod with the action given by

$$(zf)(m) := f(\psi(z)m) \text{ for } z \in R(\nu), f \in \mathrm{HOM}_{\mathbb{C}}(M, \mathbb{C}), m \in M.$$

As proved in [10, Section 3.2], for each gr-irreducible $R(\nu)$-module L, there is a unique $r \in \mathbb{Z}$ such that $(L\{r\})^* \cong L\{r\}$, and the graded projective cover of $L\{r\}$ is stable under the bar-involution $^-$.

3. **Geometric realization of R**

In this chapter, we prove the following theorem:

Theorem 3.1. *Under Γ, the canonical bases in $\bigsqcup_{\nu\in\mathbb{N}[I]}\mathbf{P}_\nu$ of $\mathbf{K} = {}_{\mathcal{A}}U^-$ are mapped to the self-dual indecomposable projective modules in $K_0(R)$.*

Let's consider the Jordan quiver first.

3.1. **Jordan quiver case.**

Assume $I = I^0 = \{i\}$ and ${}_{\mathcal{A}}U^-$ be the associated quantum group. Following the notations in Remark 1.2, it is already known that the canonical basis of ${}_{\mathcal{A}}U^-_{ni}$ is the $\{IC(\mathcal{O}_\lambda)\}_{\lambda\vdash n}$. In the following lemma, we denote by $K_0(S_n)$ the Grothendieck group of the finite dimensional $\mathbb{C}[S_n]$-modules, then $\bigoplus_n K_0(S_n)$ is a $\mathbb{Z}$-algebra with the multiplication induced by the induction of modules.

Lemma 3.2. *If we have an isomorphism $\Phi : \mathcal{A}\otimes_{\mathbb{Z}} (\bigoplus_n K_0(S_n)) \to {}_{\mathcal{A}}U^-$ of $\mathcal{A}$-algebras, which sends the trivial representation $S^{(n)}$ to $f_{in} = IC(\mathcal{O}_{(1^n)})$ or $IC(\mathcal{O}_{(n)})$, then it maps the irreducible $\mathbb{C}[S_n]$-modules to the canonical bases of ${}_{\mathcal{A}}U^-$. More precisely:*

(i) *If $\Phi(S^{(n)}) = IC(\mathcal{O}_{(1^n)})$, then $\Phi(S^\lambda) = IC(\mathcal{O}_{\widetilde{\lambda}})$ for all $\lambda\vdash n$, where $\widetilde{\lambda}$ is the transpose of λ.*

(ii) *If $\Phi(S^{(n)}) = IC(\mathcal{O}_{(n)})$, then $\Phi(S^\lambda) = IC(\mathcal{O}_\lambda)$ for all $\lambda\vdash n$.*

Proof. Let Λ be the ring of symmetric functions. By [14] (see also [21, Example 3.10]), there is an $\mathcal{A}$-algebra isomorphism

$$\mathcal{A}\otimes_{\mathbb{Z}}\Lambda \xrightarrow{\sim} {}_{\mathcal{A}}U^-,$$

which sends the Schur functions s_λ to $IC(\mathcal{O}_\lambda)$ for all λ. By the classical representation theory of the symmetric group, there is an $\mathcal{A}$-algebra isomorphism

$$\mathcal{A}\otimes_{\mathbb{Z}} (\bigoplus_n K_0(S_n)) \xrightarrow{\sim} \mathcal{A}\otimes_{\mathbb{Z}}\Lambda,$$

which sends the Specht module S^λ to s_λ. Furthermore, we have an $\mathcal{A}$-algebra involution ω of $\mathcal{A}\otimes_{\mathbb{Z}} (\bigoplus_n K_0(S_n))$ sending S^λ to $S^{\widetilde{\lambda}}$. □

Since $I = I^0 = \{i\}$, we have $K_0(R) = \bigoplus_n K_0(R(ni))$. There is an obvious $\mathcal{A}$-algebra isomorphism

$$\Omega : \mathcal{A}\otimes_{\mathbb{Z}} (\bigoplus_n K_0(S_n)) \xrightarrow{\sim} K_0(R),$$

which sends the irreducible modules to their gr-projective covers. We thus obtain an $\mathcal{A}$-algebra isomorphism $\Omega' = \Gamma^{-1}\Omega : \mathcal{A} \otimes_{\mathbb{Z}} (\bigoplus_n K_0(S_n)) \to {}_{\mathcal{A}}U^-$ with $\Omega'(S^{(n)}) = f_{in}$. By Lemma 3.2, we conclude that $\Omega'(S^{\lambda}) = IC(\mathcal{O}_{\widetilde{\lambda}})$ for all $\lambda \vdash n$. Therefore, Γ^{-1} maps the self-dual indecomposable projective modules to the canonical bases.

3.2. **Springer functor.**

For each n, we have the Springer functor (see e.g. [1, Chapter 8])

$$\mathrm{Hom}(\mathrm{Spr}_n, -) : P_{GL_{ni}}(E_{ni}^{nil}) \to \mathbb{C}[S_n]\text{-mod},$$

which is an equivalence of categories, mapping $\{IC(\mathcal{O}_\lambda)\}_{\lambda \vdash n}$ to irreducible modules. In particular,

$$\mathrm{Hom}(\mathrm{Spr}_n, IC(\mathcal{O}_{(1^n)})) = S^{(n)}, \quad \mathrm{Hom}(\mathrm{Spr}_n, \mathrm{Spr}_n) = \mathbb{C}[S_n], \tag{3.1}$$

It has a quasi-inverse

$$\mathrm{Spr}_n \otimes_{S_n} - : \mathbb{C}[S_n]\text{-mod} \to P_{GL_{ni}}(E_{ni}^{nil}),$$

According to [4, Theorem 1.3], this functor induces an algebra isomorphism

$$\bigoplus_n \mathrm{Spr}_n \otimes_{S_n} - : \mathcal{A} \otimes_{\mathbb{Z}} (\bigoplus_n K_0(S_n)) \xrightarrow{\sim} {}_{\mathcal{A}}U^-,$$

with the inverse $\bigoplus_n \mathrm{Hom}(\mathrm{Spr}_n, -)$. Thus, by Lemma 3.2, we obtain $\mathrm{Hom}(\mathrm{Spr}_n, IC(\mathcal{O}_\lambda)) = S^{\widetilde{\lambda}}$ for all $\lambda \vdash n$.

3.3. **Proof of Theorem 3.1.**

Assume we are given an arbitrary quiver (I, H). Let $\nu \in \mathbb{N}[I]$. For $\boldsymbol{i}, \boldsymbol{j} \in \mathrm{Seq}(\nu)$, we define the Steinberg-type varieties

$$\mathscr{Z}_{\boldsymbol{i},\boldsymbol{j}} = \widetilde{\mathscr{F}_{\boldsymbol{i}}} \times_{E_\nu} \widetilde{\mathscr{F}_{\boldsymbol{j}}}, \quad \mathscr{Z}_\nu = \bigsqcup_{\boldsymbol{i},\boldsymbol{j}} \mathscr{Z}_{\boldsymbol{i},\boldsymbol{j}},$$

where the fiber product is taken with respect to the projections $\pi_{\boldsymbol{i}}$ and $\pi_{\boldsymbol{j}}$.

Define the G_ν-equivariant (Borel-Moore) homology spaces as

$$\widehat{R}_{\boldsymbol{i},\boldsymbol{j}} = H_*^{G_\nu}(\mathscr{Z}_{\boldsymbol{i},\boldsymbol{j}}), \quad \widehat{R}_\nu = \bigoplus_{\boldsymbol{i},\boldsymbol{j}} \widehat{R}_{\boldsymbol{i},\boldsymbol{j}}.$$

Then $\widehat{R}_\nu$ has a $\mathcal{A}$-algebra algebra structure defined by the convolution product (see [22] for details). Let $\mathcal{L}_\nu = \bigoplus_{\boldsymbol{i} \in \mathrm{Seq}(\nu)} \mathcal{L}_{\boldsymbol{i}}$. It is known that

$$\widehat{R}_\nu \cong \mathrm{Ext}^*_{G_\nu}(\mathcal{L}_\nu, \mathcal{L}_\nu).$$

For each $i \in I$, we set $P_i(u,v) = (u-v)^{h_i}$ and

$$P_i(u,v,w) = -\frac{P_i(v,u)P_i(u,w)}{(u-v)(u-w)} - \frac{P_i(u,w)P_i(v,w)}{(u-w)(v-w)} + \frac{P_i(u,v)P_i(v,w)}{(u-v)(v-w)}.$$
$$P_i'(u,v,w) = \frac{P_i(u,v)P_i(u,w)}{(u-v)(u-w)} + \frac{P_i(u,w)P_i(w,v)}{(u-w)(v-w)} - \frac{P_i(u,v)P_i(v,w)}{(u-v)(v-w)}.$$

The following result was proved in [7], and a more general treatment can be found in [20].

Proposition 3.3. [7] *$\widehat{R}_\nu$ is generated by $1_{\boldsymbol{i}}$, $x_{k,\boldsymbol{i}}$ $(1 \le k \le n)$, $\sigma_{k,\boldsymbol{i}}$ $(1 \le k \le n-1)$ for $\boldsymbol{i} \in Seq(\nu)$, such that $\widehat{R}_{\boldsymbol{i},\boldsymbol{j}} = 1_{\boldsymbol{i}}\widehat{R}_\nu 1_{\boldsymbol{j}}$, subject to the following defining relations: (we set $x_k = \sum_{\boldsymbol{i}} x_{k,\boldsymbol{i}}, \sigma_k = \sum_{\boldsymbol{i}} \sigma_{k,\boldsymbol{i}}$)*

$$1_{\boldsymbol{i}}1_{\boldsymbol{j}} = \delta_{\boldsymbol{i},\boldsymbol{j}}1_{\boldsymbol{i}}, \quad 1 = \sum_{\boldsymbol{i}\in \mathrm{Seq}(\nu)} 1_{\mathbf{i}}, \quad x_{k,\boldsymbol{i}} = 1_{\boldsymbol{i}}x_k = x_k 1_{\boldsymbol{i}}, \quad x_k x_\ell = x_\ell x_k,$$

$$\sigma_{k,\boldsymbol{i}} = 1_{s_k\boldsymbol{i}}\sigma_k = \sigma_k 1_{\boldsymbol{i}}, \quad \sigma_k\sigma_\ell = \sigma_\ell\sigma_k \ \text{ if } |k-\ell|>1,$$

$$\sigma_k^2 1_{\boldsymbol{i}} = \begin{cases} -\partial_k\left(P_{i_k}(x_k,x_{k+1})\right)\cdot \sigma_{k,\boldsymbol{i}} & \text{if } i_k = i_{k+1}, \\ Q_{i_k,i_{k+1}}(x_k,x_{k+1})1_{\boldsymbol{i}} & \text{if } i_k \ne i_{k+1}, \end{cases}$$

$$(x_{s_k(\ell)}\sigma_k - \sigma_k x_\ell)1_{\boldsymbol{i}} = \begin{cases} P_{i_k}(x_k,x_{k+1})1_{\boldsymbol{i}} & \text{if } \ell = k \text{ and } i_k = i_{k+1}, \\ -P_{i_k}(x_k,x_{k+1})1_{\boldsymbol{i}} & \text{if } \ell = k+1 \text{ and } i_k = i_{k+1}, \\ 0 & \text{otherwise,} \end{cases}$$

$$(\sigma_k\sigma_{k+1}\sigma_k - \sigma_{k+1}\sigma_k\sigma_{k+1})1_{\boldsymbol{i}}$$
$$= \begin{cases} P_{i_k}(x_k,x_{k+1},x_{k+2})\sigma_{k,\boldsymbol{i}} + P'_{i_k}(x_k,x_{k+1},x_{k+2})\sigma_{k+1,\boldsymbol{i}} & \text{if } i_k = i_{k+1} = i_{k+2}, \\ -P_{i_k}(x_k,x_{k+2})\frac{Q_{i_k,i_{k+1}}(x_k,x_{k+1}) - Q_{i_k,i_{k+1}}(x_{k+2},x_{k+1})}{x_k - x_{k+2}}1_{\boldsymbol{i}} & \text{if } i_k = i_{k+2} \ne i_{k+1}, \\ 0 & \text{otherwise.} \end{cases}$$

By direct calculation, we obtain the following proposition:

Proposition 3.4. *For each $\nu \in \mathbb{N}[I]$, there is an isomorphism $R(\nu) \xrightarrow{\sim} \widehat{R}_\nu$ of graded algebras, given by*

$$1_{\boldsymbol{i}} \mapsto 1_{\boldsymbol{i}}, \quad x_{k,\boldsymbol{i}} \mapsto x_{k,\boldsymbol{i}}, \quad \tau_{k,\boldsymbol{i}} \mapsto \begin{cases} \sigma_{k,\boldsymbol{i}} + (x_{k,\boldsymbol{i}} - x_{k+1,\boldsymbol{i}})^{-a_{i_k i_k}/2} & \text{if } i_k = i_{k+1} \in I^{\le 0}, \\ -\sigma_{k,\boldsymbol{i}} & \text{if } i_k = i_{k+1} \in I^+, \\ \sigma_{k,\boldsymbol{i}} & \text{if } i_k \ne i_{k+1}. \end{cases}$$

By a similar argument in [22, Section 4.6], we have an additive functor

$$Y_\nu : \mathbf{Q}_\nu \to \widehat{R}_\nu\text{-pMod}$$

given by

$$\mathcal{L} \mapsto \operatorname{Ext}^*_{G_\nu}(\mathcal{L}_\nu, \mathcal{L}),$$

which is an equivalence of semisimple categories. It has a quasi-inverse given by

$$\mathcal{P} \mapsto \mathcal{L}_\nu \otimes_{\widehat{R}_\nu} \mathcal{P}.$$

Similar to [4, Theorem 1.3], the functors Y_ν ($\nu \in \mathbb{N}[I]$) induces a $\mathcal{A}$-algebra isomorphism

$$\Gamma' : ({}_{\mathcal{A}}U^- \cong)\ \mathbf{K} \xrightarrow{\sim} \bigoplus_{\nu \in \mathbb{N}[I]} K_0(\widehat{R}_\nu)\ (\cong K_0(R)),$$

where the second isomorphism follows from Proposition 3.4. Moreover, we have

$$\Gamma'(f_i^{(n)}) = [P_{i^{(n)}}] \text{ for } i \in I^+, n > 0, \quad \Gamma'(f_i) = [P_i] \text{ for } i \in I^{\leq 0}. \tag{3.2}$$

Let $i \in I^0, n > 0$. Note that $\mathcal{L}_{ni}$ coincides with the Springer sheaf Spr_n. Thus,

$$(\widehat{R}_{ni})_0 = \operatorname{Ext}^0_{GL_{ni}}(\mathcal{L}_{ni}, \mathcal{L}_{ni}) \cong \mathbb{C}[S_n], \text{ and } \operatorname{Ext}^0_{GL_{ni}}(\mathcal{L}_{ni}, -) = \operatorname{Hom}(\operatorname{Spr}_n, -).$$

By (3.1), the degree zero part of $Y_{ni}(IC(\mathcal{O}_{(1^n)}))$ is the trivial $\mathbb{C}[S_n]$-module. Since $Y_{ni}(IC(\mathcal{O}_{(1^n)}))$ is its graded projective cover, we have

$$\Gamma'(f_{in}) = [P_{i,n}] \text{ for } i \in I^0, n > 0. \tag{3.3}$$

Combining (3.2) and (3.3), we conclude that $\Gamma' = \Gamma$, which proves Theorem 3.1.

4. Categorification of irreducible highest weight module in Jordan quiver case

We show in Jordan quiver case that the cyclotomic KLR-algebras provide a categorification of the irreducible highest weight U-modules.

4.1. The algebra U.

Given a Borcherds-Cartan matrix $A = (a_{ij})_{i,j \in I}$, we set

(a) $P^\vee = (\bigoplus_{i \in I} \mathbb{Z}h_i) \oplus (\bigoplus_{i \in I} \mathbb{Z}d_i)$, a free abelian group, the *dual weight lattice*,
(b) $\mathfrak{h} = \mathbb{Q} \otimes_{\mathbb{Z}} P^\vee$, the *Cartan subalgebra*,
(c) $P = \{\lambda \in \mathfrak{h}^* \mid \lambda(P^\vee) \subseteq \mathbb{Z}\}$, the *weight lattice*,
(d) $\Pi^\vee = \{h_i \in P^\vee \mid i \in I\}$, the set of *simple coroots*,

(e) $\Pi = \{\alpha_i \in P \mid i \in I\}$, the set of *simple roots*, which is linearly independent over $\mathbb{Q}$ and satisfies

$$\alpha_j(h_i) = a_{ij},\ \alpha_j(d_i) = \delta_{ij} \text{ for all } i, j \in I.$$

Let $P^+ = \{\Lambda \in P \mid \Lambda(h_i) \geq 0 \text{ for all } i \in I\}$ be the set of dominant integral weights. The free abelian group $Q = \bigoplus_{i \in I} \mathbb{Z}\alpha_i$ is called the root lattice. We identify Π with I, and identify the positive root lattice $Q_+ = \bigoplus_{i \in I} \mathbb{N}\alpha_i$ with $\mathbb{N}[I]$.

Definition 4.1. We define $\widehat{U}$ to be the $\mathbb{Q}(q)$-algebra generated by the elements q^h $(h \in P^\vee)$ and E_{in}, f_{in} $((i,n) \in \mathbb{I})$, satisfying

$$\begin{aligned}
&q^0 = 1, \quad q^h q^{h'} = q^{h+h'} \text{ for } h, h' \in P^\vee \\
&q^h E_{jn} q^{-h} = q^{n\alpha_j(h)} E_{jn}, \quad q^h f_{jn} q^{-h} = q^{-n\alpha_j(h)} f_{jn} \text{ for } h \in P^\vee, (j,n) \in \mathbb{I}, \\
&\sum_{r+s=1-na_{ij}} (-1)^r E_i^{(r)} E_{jn} E_i^{(s)} = 0 \text{ for } i \in I^+,\ (j,n) \in \mathbb{I} \text{ and } i \neq (j,n), \\
&\sum_{r+s=1-na_{ij}} (-1)^r f_i^{(r)} f_{jn} f_i^{(s)} = 0 \text{ for } i \in I^+, (j,n) \in \mathbb{I} \text{ and } i \neq (j,n), \\
&E_{in}E_{jm} - E_{jm}E_{in} = f_{in}f_{jm} - f_{jm}f_{in} = 0 \text{ for } a_{ij} = 0.
\end{aligned}$$

We assign $|q^h| = 0, |E_{in}| = n\alpha_i$ and $|f_{in}| = -n\alpha_i$ so that $\widehat{U}$ is Q-graded.

The algebra $\widehat{U}$ is endowed with a co-multiplication $\Delta\colon \widehat{U} \to \widehat{U} \otimes \widehat{U}$ given by

$$\begin{aligned}
&\Delta(E_i) = E_i \otimes 1 + K_i \otimes E_i \text{ for } i \in I^\pm, \quad \Delta(E_{in}) = \sum_{r+t=n} E_{ir}K_i^t \otimes E_{it} \text{ for } i \in I^0, n > 0, \\
&\Delta(f_i) = f_i \otimes K_i^{-1} + 1 \otimes f_i \text{ for } i \in I^\pm, \quad \Delta(f_{in}) = \sum_{r+t=n} f_{ir} \otimes K_i^{-r} f_{it}, \text{ for } i \in I^0, n > 0,
\end{aligned}$$

and $\Delta(q^h) = q^h \otimes q^h$. Here $K_i = q^{h_i}$ $(i \in I)$.

Let $\omega\colon \widehat{U} \to \widehat{U}$ be the $\mathbb{Q}(q)$-algebra involution given by

$$\omega(q^h) = q^{-h},\ \omega(E_{in}) = f_{in},\ \omega(f_{in}) = E_{in} \text{ for } h \in P^\vee,\ (i,n) \in \mathbb{I}.$$

Let $\widehat{U}^+$ (resp. $\widehat{U}^-$, resp. $\widehat{U}^{\geq 0}$) be the subalgebra of $\widehat{U}$ generated by E_{in} $((i,n) \in \mathbb{I})$ (resp. f_{in} $((i,n) \in \mathbb{I})$, resp. E_{in} $((i,n) \in \mathbb{I})$ and q^h $(h \in P^\vee)$). We identify $\widehat{U}^-$ with the U^- in Definition 1.1, and define a symmetric bilinear form $\{\ ,\ \}$ on $\widehat{U}^{\geq 0}$

by setting

$$\{x, y\} = \{\omega(x), \omega(y)\} \quad \text{for } x, y \in \widehat{U}^+,$$
$$\{q^h, 1\} = 1, \ \{q^h, E_{in}\} = 0, \quad \{q^h, K_j\} = q^{\alpha_j(h)}.$$

Definition 4.2. By the Drinfeld double process, we define the algebra U as the quotient of $\widehat{U}$ by the relations

$$\sum \{a_{(1)}, b_{(2)}\}\omega(b_{(1)})a_{(2)} = \sum \{a_{(2)}, b_{(1)}\}a_{(1)}\omega(b_{(2)}) \quad \text{for all } a, b \in \widehat{U}^{\geq 0}. \tag{4.1}$$

Here we use the Sweedler's notation and write $\Delta(x) = \sum x_{(1)} \otimes x_{(2)}$.

The subalgebra U^- of U generated by f_{in} $((i, n) \in \mathbb{I})$ coincides with Definition 1.1.

4.2. **Irreducible highest weight module in Jordan quiver case.**

Throughout this section, we assume that $I = I^0 = \{i\}$ and U be the associated algebra.

Let $\Lambda \in P^+$. The irreducible highest weight U-module $V(\Lambda)$ is given by

$$\begin{aligned} V(\Lambda) &\cong U \Big/ \Big(UE_i + \sum_{h \in P^\vee} U(q^h - q^{\Lambda(h)}) + \sum_{n>0} Uf_{in} \Big) \quad \text{if } \Lambda(h_i) = 0, \\ V(\Lambda) &\cong U \Big/ \Big(UE_i + \sum_{h \in P^\vee} U(q^h - q^{\Lambda(h)}) \Big) \quad \text{if } \Lambda(h_i) > 0. \end{aligned} \tag{4.2}$$

By [5, Appendix], if we define $\{\alpha_p\}_{p \geq 1}$ inductively:

$$\alpha_p = \varsigma_p(K_i^{-p} - K_i^p) - \varsigma_1 K_i \alpha_{p-1} - \varsigma_2 K_i^2 \alpha_{p-2} - \cdots - \varsigma_{p-1} K_i^{p-1} \alpha_1,$$

where

$$\varsigma_k = \prod_{s=1}^{k} \frac{1}{1 - q^{2s}}, \quad \alpha_1 = \varsigma_1(K_i^{-1} - K_i).$$

Then for any $\ell, t \geq 1$, the equation (4.1) yields

$$[E_{i\ell}, f_{it}] = \sum_{p=1}^{\min\{\ell, t\}} \alpha_p f_{i,t-p} E_{i,\ell-p}. \tag{4.3}$$

Define the functors

$\mathcal{F}_{i\ell}\colon R(ni)\text{-Mod} \to R((n+\ell)i)\text{-Mod}, \ M \mapsto (R((n+\ell)i)1_{ni} \otimes e_{i,\ell}) \otimes_{R(ni)} M,$

$\mathcal{E}_{i\ell}\colon R(ni)\text{-Mod} \to R((n-\ell)i)\text{-Mod}, \ M \mapsto 1_{(n-\ell)i} \otimes e_{i,\ell} M.$

Lemma 4.3. *Let $\ell, t \geq 1$. We have the following natural isomorphisms*

$$\mathcal{E}_{i\ell}\mathcal{F}_{it} \simeq \bigoplus_{p=0}^{\min\{\ell,t\}} \mathcal{F}_{i,t-p}\mathcal{E}_{i,\ell-p} \otimes Z_p,$$

where Z_p is the algebra of symmetric polynomials in p indeterminates, each of degree 2.

Proof. We prove the case where $t = \ell$ only. The other cases are similar. For simplicity, we omit the symbol "i". Assume first that $n \geq \ell$ and denote by $D_{n,\ell}$ (resp. $D_{n,\ell}^{-1}$) the set of minimal length left (resp. right) $S_n \times S_\ell$-coset representatives in $S_{n+\ell}$. Then $D_{n,\ell} \cap D_{n,\ell}^{-1} = \{v_0, \ldots, v_\ell\}$ is the set of minimal length $S_n \times S_\ell$-double coset representatives, where v_k can be expressed graphically

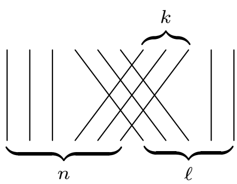

Note that

$$1_n \otimes e_\ell \cdot R(n+\ell) \cdot 1_n \otimes e_\ell = \sum_{u \in D_{n,\ell}} 1_n \otimes e_\ell \cdot u \cdot R(n) \otimes R(\ell) \cdot 1_n \otimes e_\ell. \tag{4.4}$$

Any $u \in D_{n,\ell}$ can be decomposed into $u = v \otimes v' \cdot v_k$ for some $0 \leq k \leq \ell$, $v \in D_{n-k,k}$ and $v' \in D_{k,\ell-k}$. Since $e_\ell \cdot v' = e_\ell$, we have
(4.5)

$$\begin{aligned} 1_n \otimes e_\ell \cdot R(n+\ell) \cdot 1_n \otimes e_\ell &= \sum_{k=0}^{\ell} \sum_{v \in D_{n-k,k}} 1_n \otimes e_\ell \cdot v \cdot v_k \cdot R(n) \otimes R(\ell) \cdot 1_n \otimes e_\ell \\ &= \bigoplus_{k=0}^{\ell} \bigoplus_{v \in D_{n-k,k}} v \otimes e_\ell \cdot v_k \cdot R(n) \otimes R(k) \otimes R(\ell-k) \cdot 1_n \otimes e_\ell \end{aligned}$$

On the other hand,

$$(R(n) \cdot 1_{n-k} \otimes e_k) \otimes_{R(n-k)} (1_{n-k} \otimes e_k \cdot R(n)) = \bigoplus_{v \in D_{n-k,k}} v \cdot (1_{n-k} \otimes R(k) e_k) \otimes_{R(n-k)} (1_{n-k} \otimes e_k \cdot R(n)).$$

Since $(1_{n-k} \otimes R(k)e_k) \cdot v_k = v_k \cdot (1_n \otimes R(k)e_k)$ and $v_k \cdot 1_{n-k} \otimes e_k \cdot R(n) = 1_n \otimes e_k \cdot v_k \cdot R(n)$, we see that

$1_n \otimes e_\ell \cdot \Big(v \cdot (1_{n-k} \otimes R(k)e_k)\Big) \cdot v_k \cdot 1_{n+k} \otimes e_{\ell-k}R(\ell-k)e_{\ell-k} \cdot \Big((1_{n-k} \otimes e_k \cdot R(n))\Big) \cdot 1_n \otimes e_\ell$
$= 1_n \otimes e_\ell \cdot \Big(v \otimes e_k \otimes e_{\ell-k} \cdot v_k \cdot R(n) \otimes R(k)e_k \otimes R(\ell-k)e_{\ell-k}\Big) \cdot 1_n \otimes e_\ell.$
$= v \otimes e_\ell \cdot v_k \cdot R(n) \otimes R(k) \otimes R(\ell-k) \cdot 1_n \otimes e_\ell.$

Hence for each $z \in e_{\ell-k}R(\ell-k)e_{\ell-k}$, the map

$$(R(n) \cdot 1_{n-k} \otimes e_k) \otimes_{R(n-k)} (1_{n-k} \otimes e_k \cdot R(n)) \to 1_n \otimes e_\ell \cdot R(n+\ell) \cdot 1_n \otimes e_\ell$$

$$x \otimes y \mapsto 1_n \otimes e_\ell \cdot x \cdot (v_k \cdot 1_{n+k} \otimes z) \cdot y \cdot 1_n \otimes e_\ell$$

is an injective $(R(n), R(n))$-bimodule homomorphism. Since $e_{\ell-k}R(\ell-k)e_{\ell-k} \cong Z_{\ell-k}$, we have proved that

$$\mathcal{E}_\ell \mathcal{F}_\ell \simeq \bigoplus_{k=0}^{\ell} \mathcal{F}_k \mathcal{E}_k \otimes Z_{\ell-k} \tag{4.6}$$

on $R(n)$. If $n < \ell$, then the direct sum in (4.5) ranges from $k=0$ to n, while the right hand side of (4.6) only makes sense for $k \leq n$. □

Choose $\Lambda \in P^+$ and set $a = \Lambda(h_i) \geq 0$. We define the cyclotomic algebra $R^\Lambda(n)$ to be the quotient of $R(n)$ by the two sided ideal generated by x_1^a, and form

$$R^\Lambda = \bigoplus_{n \geq 0} R^\Lambda(n), \quad K_0(R^\Lambda) = \bigoplus_{n \geq 0} K_0(R^\Lambda(n)).$$

If $a = 0$, then $R^\Lambda = R^\Lambda(0) = \mathbb{C}$ and $V(\Lambda)$ is the one dimensional trivial module by (4.2). So we assume that $a > 0$ in the following. Note that $R^\Lambda(n)$ has a basis

$$\{x_1^{r_1} \cdots x_n^{r_n} \tau_\omega \mid \omega \in S_n, 0 \leq r_1, \ldots, r_n < a\}.$$

Define the functors

$\mathcal{F}_{i\ell}^\Lambda \colon R^\Lambda(n)\text{-Mod} \to R^\Lambda(n+\ell)\text{-Mod}, \quad M \mapsto (R^\Lambda(n+\ell)1_n \otimes e_\ell) \otimes_{R^\Lambda(n)} M,$
$\mathcal{E}_{i\ell}^\Lambda \colon R^\Lambda(n)\text{-Mod} \to R^\Lambda(n-\ell)\text{-Mod}, \quad M \mapsto 1_{n-\ell} \otimes e_\ell M.$

Similar to Lemma 4.3, for $\ell, t \geq 1$, we have the following natural isomorphisms

$$\mathcal{E}_{i\ell}^\Lambda \mathcal{F}_{it}^\Lambda \simeq \bigoplus_{p=0}^{\min\{\ell,t\}} \mathcal{F}_{i,t-p}^\Lambda \mathcal{E}_{i,\ell-p}^\Lambda \otimes Z_p^\Lambda, \tag{4.7}$$

where $Z_p^\Lambda = \big(\mathbb{C}[x_1,\ldots,x_p]/(x_1^a,\ldots,x_p^a)\big)^{S_p}$, i.e., the symmetric polynomials in $x_1,\ldots,x_p$ such that no x_k^m $(m \geq a)$ appears. Thus Z_p^Λ is determined by all partitions λ with $\ell(\lambda) \leq p$ and $\lambda_1 \leq a-1$. We know that the generating function for such partitions is

$$\begin{bmatrix} a+p-1 \\ p \end{bmatrix} = \frac{(1-q^a)(1-q^{a+1})\cdots(1-q^{a+p-1})}{(1-q)(1-q^2)\cdots(1-q^p)},$$

and therefore

$$\mathbf{Dim}\, Z_p^\Lambda = \frac{(1-q^{2a})(1-q^{2(a+1)})\cdots(1-q^{2(a+p-1)})}{(1-q^2)(1-q^4)\cdots(1-q^{2p})} := \beta_p.$$

Lemma 4.4. *For any $p \geq 1$,*

$$\beta_p = \varsigma_p(1-q^{2pa}) - \varsigma_1 q^{2a}\beta_{p-1} - \varsigma_2 q^{4a}\beta_{p-2} - \cdots - \varsigma_{p-1}q^{2(p-1)a}\beta_1. \tag{4.8}$$

Proof. Using the notations

$$\begin{bmatrix} n \\ m \end{bmatrix} = \frac{(1-q^n)(1-q^{n-1})\cdots(1-q^{n-m+1})}{(1-q)(1-q^2)\cdots(1-q^m)}$$

for $n \geq m \geq 1$ and $(x;q)_n = (1-x)(1-xq)\cdots(1-xq^{n-1})$ for $n \geq 1$. We have

$$\begin{bmatrix} n+1 \\ m \end{bmatrix} = q^m \begin{bmatrix} n \\ m \end{bmatrix} + \begin{bmatrix} n \\ m-1 \end{bmatrix}, \quad (xq^m;q)_{n-m} = \frac{(x;q)_n}{(x;q)_m}. \tag{4.9}$$

To show the identity in the lemma, it is enough to show the following

$$(1-q^{pa}) = \sum_{k=0}^{p-1} q^{ka} \begin{bmatrix} p \\ k \end{bmatrix} (q^a;q)_{p-k},$$

which can be proved easily by an induction on p and using (4.9). $\square$

Let $\alpha_k = q^{-ka}\beta_k$ for all $k \geq 1$. By (4.8), for $p \geq 1$, we have

$$q^{-pa}\beta_p = \varsigma_p(q^{-pa} - q^{pa}) - \sum_{k=1}^{p-1} q^{-(p-k)a}\varsigma_k q^{ka}\beta_{p-k}.$$

Thus,

$$\alpha_p = \varsigma_p(q^{-pa} - q^{pa}) - \sum_{k=1}^{p-1} \varsigma_k q^{ka}\alpha_{p-k}.$$

Define the functors $E_{i\ell}^\Lambda, F_{i\ell}^\Lambda, K_i$ on $K_0(R^\Lambda)$ by

$$E_{i\ell}^\Lambda = \mathcal{E}_{i\ell}^\Lambda, \quad F_{i\ell}^\Lambda = q^{-\ell a}\mathcal{F}_{i\ell}^\Lambda, \quad K_i = q^a.$$

Then (4.7) gives

$$E_{i\ell}^{\Lambda}F_{it}^{\Lambda} = \sum_{p=0}^{\min\{\ell,t\}} q^{-pa}\beta_p F_{i,t-p}^{\Lambda}E_{i,\ell-p}^{\Lambda} = \sum_{p=0}^{\min\{\ell,t\}} \alpha_p F_{i,t-p}^{\Lambda}E_{i,\ell-p}^{\Lambda},$$

where

$$\alpha_p = \varsigma_p(K_i^{-p} - K_i^{p}) - \sum_{k=1}^{p-1} \varsigma_k K_i^k \alpha_{p-k}.$$

Let $K_0(R^{\Lambda})_{\mathbb{Q}(q)} = \mathbb{Q}(q) \otimes_{\mathbb{Z}[q,q^{-1}]} K_0(R^{\Lambda})$. Then by (4.3), the $K_0(R^{\Lambda})_{\mathbb{Q}(q)}$ is a weight U-modules (the weight spaces are $K_0(R^{\Lambda})_{\Lambda-ni} = K_0(R^{\Lambda}(n)))$ with the action of $E_{i\ell}$ (resp. $f_{i\ell}$) by $E_{i\ell}^{\Lambda}$ (resp. $F_{i\ell}^{\Lambda}$). The $\mathbb{Z}[q,q^{-1}]$-linear map

$$\varphi\colon K_0(R) \to K_0(R^{\Lambda}), \quad [P] \mapsto R^{\Lambda}(n) \otimes_{R(n)} [P]$$

is an isomorphism. For $[P] \in K_0(R(n))$, we have

$$\begin{aligned}
\varphi(f_{i\ell}[P]) &= \varphi(\mathrm{Ind}_{n,\ell}^{n+\ell} P \otimes R(\ell)e_{\ell}) \\
&= R^{\Lambda}(n+\ell) \otimes_{R(n+\ell)} R(n+\ell) \otimes_{R(n)\otimes R(\ell)} P \otimes R(\ell)e_{\ell} \\
&= R^{\Lambda}(n+\ell) \otimes_{R(n)\otimes R(\ell)} P \otimes R(\ell)e_{\ell} \\
&= (R^{\Lambda}(n+\ell)1_n \otimes e_{\ell}) \otimes_{R(n)} P \\
&= \mathcal{F}_{i\ell}^{\Lambda}\varphi([P]).
\end{aligned}$$

It follows that φ is U^--linear and $K_0(R^{\Lambda})$ is generated by 1_{Λ}, the trivial module over $R^{\Lambda}(0)$. Hence $K_0(R^{\Lambda})_{\mathbb{Q}(q)}$ is isomorphic to the irreducible highest weight module $V(\Lambda)$ given in (4.2), which can be identified with U^- as U^--modules.

Theorem 4.5. *If $I = I^0 = \{i\}$, then $K_0(R^{\Lambda})_{\mathbb{Q}(q)}$ is isomorphic to the irreducible highest weight module $V(\Lambda)$ for each $\Lambda \in P^+$.*

References

1. P. Achar, *Perverse sheaves and applications to representation theory*, Mathematical Surveys and Monographs, no. 258, Amer. Math. Soc., Providence, RI, 2021.
2. T. Bozec, *Quivers with loops and perverse sheaves*, Math. Ann. **362** (2015), 773-797.
3. T. Ceccherini-Silberstein, F. Scarabotti and F. Tolli, *Representation theory of the symmetric groups. The Okounkov-Vershik approach, character formulas, and partition algebras*, Cambridge University Press, 2010.
4. D. Clausen, *The Springer correspondence*, Harvard University, Cambidge USA, Diss., 2008.

5. Z. Fan, S.-J. Kang, Y. R. Kim and B. Tong, *Classical limit of quantum Borcherds-Bozec algebras*, J. Pure Appl. Algebra **225** (2021), 106502.
6. S.-J. Kang and M. Kashiwara, *Categorification of highest weight modules via Khovanov-Lauda-Rouquier algebras*, Invent. Math. **190**(3) (2012) 699-742.
7. S.-J. Kang, M. Kashiwara and E. Park, *Geometric realization of Khovanov-Lauda-Rouquier algebras associated with borcherds-cartan data*, Proc. Lond. Math. Soc. **107** (2013), 907-931.
8. S.-J. Kang and O. Schiffmann, *Canonical bases for quantum generalized Kac-Moody algebras*, Adv. Math. **200** (2006), 455-478.
9. S.-J. Kang, S.-j. Oh, E. Park, *Categorification of Quantum Generalized Kac-Moody Algebras and Crystal Bases*, Internat. J. Math., **23**(11) (2012) 13-88.
10. M. Khovanov and A. Lauda, *A diagrammatic approach to categorification of quantum groups* I, Represent. Theory **13**(14) (2009) 309-347.
11. M. Khovanov and A. Lauda, *A diagrammatic approach to categorification of quantum groups* II, Trans. Amer. Math. Soc. **363**(5) (2011) 2685-2700.
12. A. Lauda and M. Vazirani, *Crystals from categorified quantum groups*, Adv. Math. **228**(2) (2011) 803-861.
13. Y. Li and Z. Lin, *Canonical bases of Borcherds-Cartan type*, Nagoya Math. J. **194** (2009), 169-193.
14. G. Lusztig, *Green polynomials and singularities of unipotent classes*, Adv. Math. **42** (1981), 169-178.
15. G. Lusztig, *Tight monomials in quantized enveloping algebras*, Quantum deformations of algebras and their representations, ed. A.Joseph et al., Isr. Math. Conf. Proc. **7**, Amer. Math. Soc. 1993, 117-132.
16. G. Lusztig, *Introduction to quantum groups*, Springer, New York, 2010.
17. R. Rouquier, 2-*Kac-Moody algebras*, arXiv:0812.5023.
18. R. Rouquier, *Quiver Hecke algebras and* 2-*Lie algebras*, Algebra Colloq. **19**(2) (2012) 359-410.
19. B. Sagan, *T*he Symmetric Group: Representations, Combinatorial Algorithms, and Symmetric Functions, Grad. Texts in Math. **203**, 2001.
20. J.A.Sauter, *Generalized Quiver Hecke Algebras*, arXiv:1306.3892.
21. O. Schiffmann, *Lectures on canonical and crystal bases of Hall algebras* (2009), arXiv:0910.4460.
22. M. Varagnolo and E. Vasserot, *Canonical bases and KLR-algebras*, J. Reine Angew. Math. **659** (2011) 67-100.

J. Basic Sci. HUFS **62** (2026), pp. 31–50

LATEX-AWARE EMBEDDINGS FOR REVIEWER RECOMMENDATION ON EQUATION-DENSE STEM MANUSCRIPTS

Young Rock Kim

Abstract. The rapid growth of publications in Science, Technology, Engineering, and Mathematics (STEM) fields has increased the burden on editors to assign appropriate peer reviewers. Existing text-based recommendation approaches, however, often struggle with equation-dense manuscripts because they fail to capture the semantic and structural information encoded in mathematical expressions. To address this limitation, we propose a LaTeX-aware, domain-adaptive embedding method tailored for STEM literature, along with a fine-tuning strategy that can be adapted for journal-specific domains. We construct a large-scale corpus of raw LaTeX source files from arXiv Mathematics, apply LaTeX-aware processing and then evaluate our method on these domain-representative dataset. Experimental results show that our approach significantly outperforms classical embeddings and vanilla BERT particularly on equation-dense manuscripts with high equation density. Finally, we illustrate how the proposed embedding method can be seamlessly integrated into existing reviewer recommendation pipelines to enhance expertise matching in STEM submission workflows.

1. Introduction

Peer review is a cornerstone of scholarly publishing, ensuring the quality and integrity of academic manuscripts. However, the rapid growth in submission volume

Key words and phrases. LaTeX-Aware Embeddings, Latex language processing, Equation-Dense STEM Manuscripts, Large Language Model, Domain-adaptive finetuning, Reviewer Recommendation.

Major in Mathematics Education, Graduate School of Education, Hankuk University of Foreign Studies. This research was supported by the research fund of Hankuk University of Foreign Studies.

has substantially increased the burden on journal editors, who must carefully match manuscript topics with the expertise of reviewer candidates (RCs). Inappropriate reviewer assignments often lead to delayed reviews and degraded review quality, motivating the development of intelligent reviewer recommendation algorithms that automate and optimize the selection process [3, 2, 4, 1].

Reviewer recommendation research has increasingly focused on accurately estimating RC expertise. Early methods embedded manuscripts and reviewer publications into a shared semantic space using techniques such as LSA [5] or LDA [?], but these text-based approaches struggle with semantic alignment due to vocabulary mismatches—including synonyms, abbreviations, and mathematical notation. Later studies addressed some of these limitations by incorporating fairness mechanisms such as COI detection and reviewer bias mitigation [6, 9].

Recent advances in deep learning have significantly improved semantic representations, and LLMs trained on large corpora have enabled prompting-based reviewer recommendation [16]. Beyond assignment, LLMs have also been explored for improving review quality itself [65]. However, LLM-based approaches remain sensitive to prompt design and lack explicit fairness and COI mechanisms, limiting real-world reliability. To address these issues, hybrid frameworks integrating LLM semantics with algorithmic components for robustness have been proposed [17]. In parallel, substantial work has focused on enhanced embedding methods [66, 67], including domain-adaptive learning and fine-tuning strategies [70, 68, 69, 71]. (see Appendix **??** for a detailed review)

Parallel efforts in large-scale peer review systems show that reviewer assignment remains a critical open problem. Optimization-based frameworks have improved matching quality and workload balance [58], and NeurIPS 2024 introduced refinements to enhance stability and accuracy [59]. Yet text-matching approaches remain vulnerable to coordinated collusion attacks [60]. To address semantic limitations, recent studies have explored multi-factor models incorporating semantic, topical, and citation signals [61], as well as end-to-end ML systems and panel-level group recommendation methods [62, 63]. Meanwhile, increasing reviewer overload and declining review quality have prompted concerns about a peer review crisis [64], highlighting the need for domain-adaptive and semantically reliable recommendation systems. Motivated by this, we focus on a defining aspect of STEM manuscripts: most are written in LaTeX and convey core ideas through equations and symbolic expressions. General-purpose LLMs struggle with such content, as

BERT- and GPT-family models are not optimized for domain-specific vocabulary or equation structure, limiting their ability to embed STEM semantics.

We therefore propose a LaTeX-aware Fine-tuned embedding method, explicitly designed to embed equation-dense manuscripts. Our approach directly processes LaTeX inputs to improve embedding quality for structurally rich scientific documents. Furthermore, we introduce journal-specific fine-tuning to further adapt representations to individual editorial domains, yielding a more accurate and reliable reviewer recommendation framework.

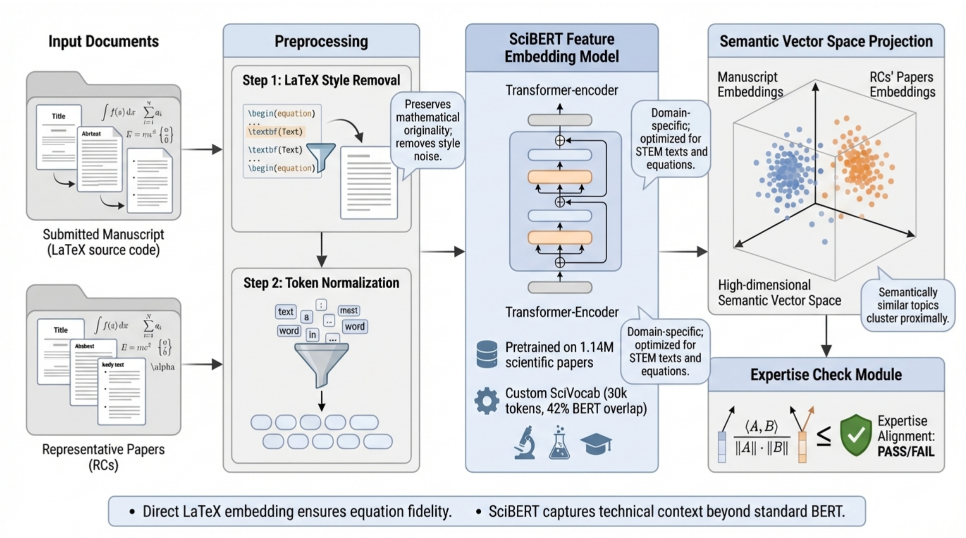

FIGURE 1. Feature embedding pipeline with LLMs, including how LaTeX manuscripts and reviewer papers are preprocessed, encoded by SciBERT, and mapped into a semantic vector space for similarity calculation of expertise check.

2. METHODOLOGY

The primary approach lies in performing equation-aware LaTeX preprocessing tailored to STEM manuscripts, and then embed the processed context using SciBERT, a domain specific language model for scientific text. To accurately reflect reviewer expertise, we further introduce a customized similarity metric designed to capture fine-grained topical relevance between manuscripts and reviewer candidates. By integrating these components, reviewer recommendation framework goes beyond conventional text matching approaches and enables reviewer recommendations that more faithfully reflect domain specific expertise. In addition, we incorporate domain-adaptive fine-tuning to support continual performance improvement across heterogeneous STEM disciplines.

2.1. **LaTeX-Aware Embeddings with LLMs for Equation-Dense STEM Manuscripts.** The feature embedding module transforms document data into embedding vectors for expertise check module. It encodes key textual features including titles, author information, abstracts, and introductions extracted from the submitted manuscript and RCs' representative papers into a high dimensional semantic vector space. This embedding preserves topical, keyword, and contextual signals, enabling related documents to be clustered proximally in the vector space. The resulting representations are subsequently used in the expertise check module to quantitatively measure semantic alignment between the manuscript and RCs, serving as a proxy for domain expertise. Unlike conventional approaches that rely on PDF or plain text, we use LaTeX source to better reflect the structural characteristics of STEM manuscripts. Such documents contain complex mathematical notation and symbolic expressions that are difficult for general language models to process. In particular, formulas often appear as unique instances in the corpus, and LaTeX commands (e.g., \alpha', \frac') differ substantially from natural language syntax, making it challenging for standard embedding methods to capture their semantic content. These properties necessitate a domain specific embedding strategy for LaTeX based text. To address this challenge, we apply a two stage preprocessing pipeline: (1) removal of non-essential LaTeX styling and formatting commands, and (2) token normalization to preserve formula structure. This procedure retains the core semantic structure of mathematical expressions while improving embedding efficiency.

Although general purpose LLMs such as GPT could be considered for feature embedding, prior studies indicate that they are less effective at capturing fine grained domain specific semantics compared to specialized models [27]. We therefore adopt SciBERT, a BERT-family Transformer encoder pretrained on scientific literature, as our embedding backbone. SciBERT is trained exclusively on scientific text, enabling more accurate contextual representations of mathematical formulas and technical expressions. As illustrated in Figure 1, we use SciBERT to embed both manuscripts and RCs' representative papers, allowing equation heavy STEM documents to be stably mapped into a semantically meaningful vector space.

2.2. **Domain-Adaptive Fine-Tuned Embeddings.** We further propose a fine-tuning strategy that enables domain-adaptive embedding learning tailored for the peer reviewer recommendation. Although the baseline SciBERT model is pretrained on large scale scientific corpora and provides high quality embeddings across broad scientific and technical domains, individual journals typically curate unique literature collections focused on specific subfields. As a result, a generic scientific embedding model alone may fail to capture fine grained, journal specific scholarly characteristics. To address this limitation, we introduce a journal adaptive fine-tuning strategy that aligns the embedding space with each journal's publication history and evolving research trends. This strategy is implemented via an internal embedding model management system integrated into the recommendation framework, whose conceptual architecture is illustrated in Figure 2. We construct a journal specific manuscript corpus and perform lightweight domain-adaptive fine-tuning of the pretrained SciBERT model on this corpus. Fully retraining the model is computationally expensive and prone to overfitting, particularly for small scale journals. We therefore adopt a LoRA (Low Rank Adaptation) [72] based approach, updating only a small subset of parameters via adapter modules. This design also enables a self-improving system: as new manuscripts are accepted and published, they are added to the journal corpus and incorporated into subsequent fine-tuning cycles. Consequently, the system progressively refines journal adapted embeddings over time, yielding increasingly accurate and context aware reviewer recommendations.

2.3. **LaTeX-Aware Embeddings for Peer Reviewer Recommendation.** Figure 3 illustrates the overall workflow of the hybrid peer reviewer recommendation framework with proposed LaTeX-aware embedding method. The process begins when an author submits a manuscript, after which the system aggregates reviewer candidates (RCs) through five distinct channels. The collected RCs, together with the submitted manuscript, serve as inputs to the recommendation framework. In the feature extraction module, key textual features are extracted from the LaTeX source files of both the submitted manuscript and the RCs' representative papers. Next, the affinity check module automatically excludes RCs who share

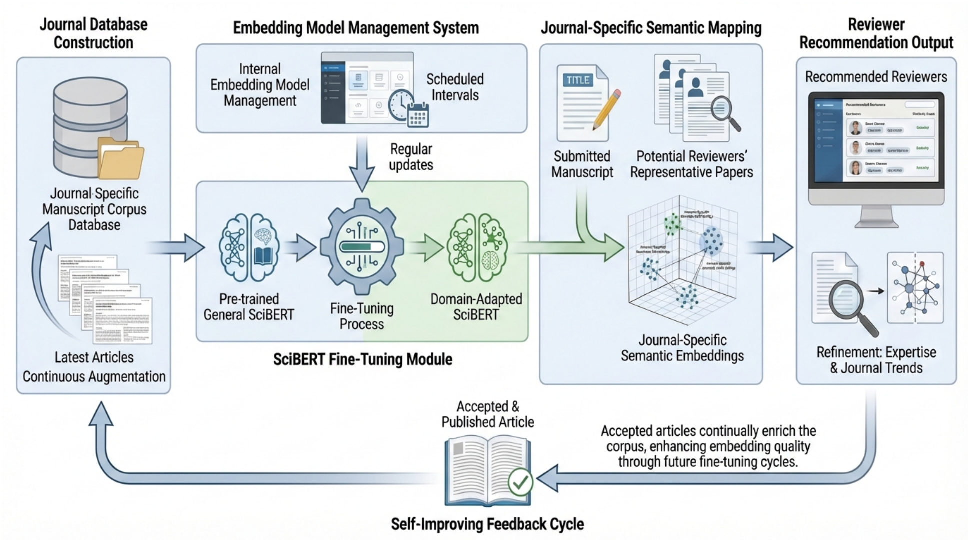

FIGURE 2. Journal-adaptive fine-tuning that fine-tunes SciBERT-based framework using journal-specific corpus, enabling tailored semantic representations.

coauthorship relations or institutional affiliations with the manuscript authors, thereby mitigating potential conflicts of interest (COIs). Subsequently, in the feature embedding module, SciBERT converts the extracted key textual features into embedding vectors. In the expertise check module, semantic similarity is computed between the embedding vectors of the submitted manuscript and those of the RCs' papers. Through topic clustering and similarity analysis, the system quantitatively estimates each RC's domain expertise and ranks candidates in descending order of relevance. Finally, the fair allocation and recommendation module applies fairness criteria to prevent excessive review workload for individual RCs and generates the final ranking, following the procedure described in [31]. In addition, accumulated journal specific papers are used to fine-tune the embedding model, enabling adaptation to journal specific scopes and editorial policies.

3. Experimental Results

In this section, we present three experiments to quantitatively evaluate the performance of the proposed embedding methodology for equation-dense STEM Manuscripts. The experiments are designed to address the following key research questions: (1) *Impact of Embedding Models on Reviewer Ranking Accuracy*: To what extent does the semantic representation ranking RCs' expertise? (2) *Robustness to Equation Density*: Given the characteristics of mathematical manuscripts, how do BERT and SciBERT differ in performance between high equation density papers and equation light papers? (3) *Effectiveness of Domain-Adaptive Journal Specific Fine-Tuning*: Does fine-tuning the pretrained SciBERT model on journal specific corpora yield statistically meaningful improvements in Expertise check?

3.1. **Datasets.** We construct our dataset from arXiv, a large scale open-access repository containing approximately 2.4M STEM preprints as of 2025 [19]. We focus on Mathematics, where tightly coupled natural language and equations provide a challenging testbed for domain specific language models and fine grained expertise matching [43]. Mathematics comprises 32 categories, which we use as target labels. Categories with insufficient samples (e.g., math.IT, math.MP) are excluded, while math.GM, math.HO, and math.LO are merged into Group1 (G1), and math.GN with math.KT into Group2 (G2). Category names are abbreviated (e.g., math.CO $\rightarrow$ CO), and the final distribution and abbreviations are summarized in Table 1. Category abbreviations and distributions are summarized in Table 1. To mitigate class imbalance in experiments, we randomly sample 2,000 papers per category, with proportional sampling for aggregated groups.

3.2. **Performance Evaluations. Evaluation Procedure** (1) Test Dataset and Comparison targets Construction: For each mathematics category, representative test papers are selected and the remaining papers for each experiment are used as comparison targets. Then, Key textual features are extracted from the raw LaTeX sources, and irrelevant LaTeX formatting elements are removed to construct the final evaluation inputs. (2) Similarity Calculation via Embedding: The preprocessed test papers and comparison papers are encoded into embedding vectors by each embedding model, and similarities are computed. (3) Ranking-Based Performance Measurement: For each test paper, similarity scores with all comparison papers are

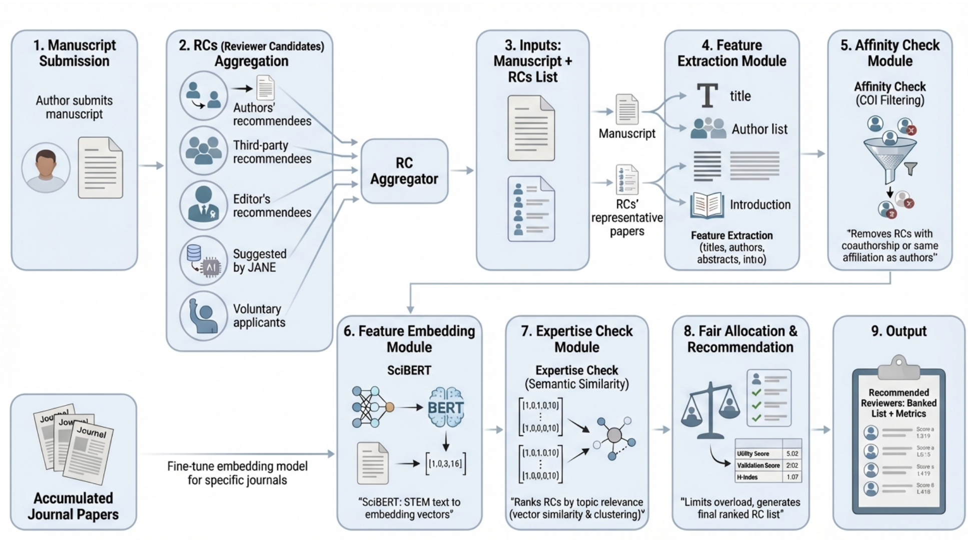

FIGURE 3. Overview of a hybrid peer reviewer recommendation framework applied with proposed embedding method, illustrating the end-to-end workflow from manuscript submission to final reviewer selection.

sorted in descending order to generate a ranking. The recommendation performance of each model is then evaluated by computing quantitative metrics.

Similarity Metrics

To quantify relevance between submitted manuscripts and reviewer candidates (RCs), we propose a customized similarity measure termed Scaled MaxSim:

$$\text{Scaled MaxSim}(\mathbf{C}, \mathbf{J}) = \frac{1}{2}\big(\sigma(\mathbf{C}_{\text{scaled}}) + \sigma(\mathbf{J}_{\text{scaled}})\big) \tag{1}$$

where $\mathbf{C}$ and $\mathbf{J}$ denote cosine similarity and Jaccard similarity score vectors, respectively. Cosine similarity captures semantic proximity in embedding space, while Jaccard similarity reflects keyword-level overlap. To balance these components, both vectors are first min–max normalized over all RC manuscripts, yielding $\mathbf{C}_{\text{scaled}}$ and $\mathbf{J}_{\text{scaled}}$. Softmax is then applied to emphasize highly relevant RCs, and the final score is defined as the arithmetic mean of the two transformed similarities, enhancing ranking discrimination.

TABLE 1. The category notation used in this study and the corresponding number of papers available on arXiv.

Category (Notation)	Entry	**Category (Notation)**	Entry	**Category (Notation)**	Entry
Commutative Algebra (AC)	4,651	Algebraic Geometry (AG)	16,029	Analysis of PDEs (AP)	14,098
Algebraic Topology (AT)	6,957	Classical Analysis and ODEs (CA)	7,309	Combinatorics (CO)	21,722
Category Theory (CT)	4,674	Complex Variables (CV)	6,752	Differential Geometry (DG)	13,055
Dynamical Systems (DS)	14,550	Functional Analysis (FA)	11,427	Group Theory (GR)	8,332
Geometric Topology (GT)	7,480	Mathematical Geometry (MG)	5,253	Numerical Analysis (NA)	10,666
Number Theory (NT)	10,049	Operator Algebras (OA)	4,683	Optimization and Control (OC)	18,004
Probability (PR)	18,005	Quantum Algebra (QA)	9,042	Rings and Algebras (RA)	6,766
Representation Theory (RT)	11,332	Symplectic Geometry (SG)	4,348	Spectral Theory (SP)	5,149
Statistics Theory (ST)	8,837	Group1 (G1)	4,829	Group2 (G2)	5,478

Evaluation metrics

We assess ranking quality using standard information retrieval metrics: Precision, MAP, nDCG, and Pairwise-F1 [30].

3.3. **Main Results.** This subsection presents the experimental results designed to evaluate both the embdding performance and practical viability of the proposed embedding method.

Experiment1: Impact of Embedding Models on Relevant Reviewer Ranking Accuracy

The objective of the first experiment is to establish a performance baseline by identifying which model in the feature embedding module yields the best ranking quality. We compare classical Word2Vec based embeddings (Gensim [33] and Gensim initialized with GoogleNews vectors [34]) against LLM based encoders (BERT [29] and SciBERT). For simplicity, we denote the Word2Vec models as Gensim and GoogleNews in subsequent tables. To ensure a fair comparison, the affinity check module is disabled to avoid filtering highly similar papers as COIs, allowing us to isolate embedding quality. Test data for this experiment are constructed by randomly selecting eight papers per category, and evaluation is performed over the full reviewer pool.

As shown in Table 2, LLM-based models (BERT and SciBERT) consistently outperform classical Word2Vec-based embeddings (Gensim and GoogleNews) across all categories and evaluation metrics (Precision, nDCG, MAP/AP, and Pairwise-F1). For example, on the OC category, SciBERT and BERT achieve nDCG@50 scores of 0.8594 and 0.8430, respectively, whereas Gensim and GoogleNews reach only 0.6959 and 0.4822. This result indicates that distributional semantics alone is insufficient for accurate matching in high domain complexity settings such as mathematics. Moreover, SciBERT generally surpasses BERT across most categories and metrics, demonstrating that domain specific pretraining on scientific literature is more effective than general purpose LLMs for capturing complex mathematical terminology and context.

Experiment 2: Robustness to Equation Density

In Experiment 1, we observed that SciBERT generally outperforms BERT when embedding LaTeX source data. The objective of this experiment is to investigate the factors underlying this performance gap, with a particular focus on the impact of equation density on embedding quality and ranking accuracy. To this end, we partition test papers into high equation density and low equation density groups based on the proportion of equations relative to text. Specifically, for each mathematics category, we first identify papers whose counts of equation tokens (defined as LaTeX commands beginning with "\") fall within the top 75% or bottom 25% relative to the overall average across all collected papers. From these subsets, we select one representative test paper per category for each density group through expertise validation, and compare the performance of SciBERT and BERT across these settings. Since this experiment uses one test paper per category, we report Average Precision (AP) instead of MAP.

The experimental results are shown in Figure 4. Overall, SciBERT outperforms BERT in both groups, but the magnitude of the performance gap differs substantially. In the low equation density group, SciBERT exceeds BERT on most metrics except for a few categories such as GT, although the gains are relatively modest. In contrast, in the high equation density group, SciBERT achieves substantially higher performance and widens the gap with BERT. Notably, SciBERT consistently dominates BERT on ranking quality metrics (AP, nDCG, and Pairwise-F1), while differences in Precision@50 and Precision@100 remain comparatively small. This indicates that SciBERT excels not merely at retrieving relevant documents, but at producing semantically coherent and stable top heavy rankings by better modeling relative ordering and semantic consistency. These findings demonstrate that SciBERT is particularly well suited to LaTeX-based STEM documents with dense equations and complex structure, beyond general natural language processing. Consequently, SciBERT based approaches are especially advantageous for expertise checking in reviewer recommendation scenarios involving equation heavy scholarly literature.

TABLE 2. Comparison of ranking performance across embedding models adapted in the embedding method.

Category	CO ($K = 50$)				CO ($K = 100$)			
metrics / model	Precision	nDCG	MAP	Pairwise F1	Precision	nDCG	MAP	Pairwise F1
w/ Gensim	0.4575	0.4676	0.4855	0.4541	0.4700	0.4735	0.4768	0.4684
w/ GoogleNews	0.2475	0.2726	0.2944	0.2398	0.2250	0.3116	0.2757	0.2210
w/ BERT	0.5775	0.5987	0.6279	0.5714	0.5788	0.6258	0.6023	0.5758
w/ SciBERT	**0.6725**	**0.7065**	**0.7326**	**0.6658**	**0.6438**	**0.7098**	**0.7049**	**0.6402**
Category	CV ($K = 50$)				CV ($K = 100$)			
metrics / model	Precision	nDCG	MAP	Pairwise F1	Precision	nDCG	MAP	Pairwise F1
w/ Gensim	0.3150	0.3452	0.3873	0.3061	0.3025	0.3962	0.3550	0.2980
w/ GoogleNews	0.2350	0.2601	0.3061	0.2296	0.2038	0.2742	0.2720	0.2008
w/ BERT	0.4250	0.4519	0.4864	0.4184	0.3725	0.4552	0.4490	0.3687
w/ SciBERT	**0.4700**	**0.5106**	**0.5714**	**0.4617**	**0.4425**	**0.5222**	**0.5210**	**0.4381**
Category	OC ($K = 50$)				OC ($K = 100$)			
metrics / model	Precision	nDCG	MAP	Pairwise F1	Precision	nDCG	MAP	Pairwise F1
w/ Gensim	0.6750	0.6959	0.7296	0.6684	0.6425	0.6722	0.7002	0.6389
w/ GoogleNews	0.4600	0.4822	0.5258	0.4515	0.4575	0.4973	0.4971	0.4533
w/ BERT	0.8125	0.8430	0.8852	0.8087	0.7638	0.7948	0.8406	0.7614
w/ SciBERT	**0.8400**	**0.8594**	**0.8922**	**0.8367**	**0.7900**	**0.8135**	**0.8551**	**0.7879**

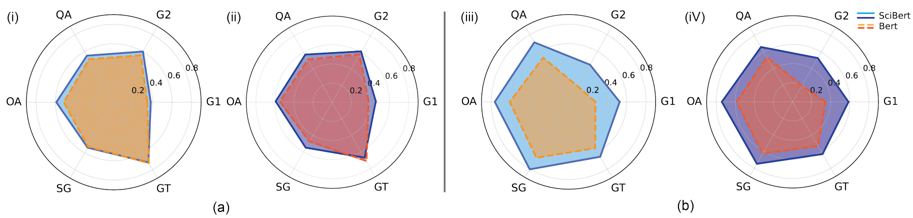

FIGURE 4. Performance gap between SciBERT and BERT under different equation density conditions. (a) The left radar plot reports AP@100 and the right radar plot presents nDCG@100 for the low equation-density group. (b) The left radar plot reports AP@100 and the right radar plot presents nDCG@100 for the high equation-density group.

Experiment 3: Effectiveness of Domain-Adaptive Journal Specific Fine-Tuning

Our domain-adaptive fine-tuning is performed with the SciBERT backbone fully frozen, using a LoRA based parameter efficient adaptation strategy. Rank-8 adapters are inserted into the Query (Q) and Value (V) projection layers, resulting in updates to only approximately 0.2% of the total model parameters. Fine-tuning is conducted for 1-2 epochs using a masked language modeling (MLM) objective with AdamW (learning rate 2×10^{-5}, weight decay 0.01) and batch size 16. The trained adapters are deployed as independent plug in modules. For fine-tuning, we assume a practical deployment scenario in which the proposed fine-tuning strategy is applied to a mathematics-specific academic journal. Accordingly, we use the full set of mathematical papers collected in our dataset as a proxy for the journal's publication history and employ them as the fine-tuning corpus. For evaluation, one representative test paper per category is selected through expert validation to ensure that each test paper accurately reflects the characteristics of its field. To clearly isolate the impact of fine-tuning, we report only @100 metrics in this experiment.

The effects of fine-tuning can be summarized as follows. First, as shown in Table 3, the largest performance gains are observed in pure and theory-oriented mathematics categories such as AG, AP, CA, CT, and DG. This indicates that domain specific terminology and structural patterns substantially benefit domain-adaptive learning, and that even minor fields consistently gain from fine-tuning. Second, the most pronounced improvements appear in the Pairwise-F1 metric, suggesting that fine-tuning strengthens clustering structure in the embedding space and more accurately captures semantic proximity among papers within the same field.

3.4. **Ablations.** In this subsection, we conduct a series of ablation studies to analyze how each proposed component contributes to the overall performance of the reviewer recommendation algorithm.

Importance of construction of Key Textual Feature

In this work, we extract textual content directly from the raw LaTeX sources of arXiv papers for embedding. Since embedding the full manuscript is computationally expensive and introduces redundant information that is irrelevant to reviewer recommendation, it is necessary to select contextual components that best capture a

TABLE 3. Changes in reviewer recommendation performance before and after fine-tuning (@100 metrics)

Category	Precision@100	AP@100	nDCG@100	Pairwise F1@100
AC	$0.170 \rightarrow 0.380$ ($\uparrow$)	$0.312 \rightarrow 0.357$ ($\uparrow$)	$0.471 \rightarrow 0.504$ ($\uparrow$)	$0.373 \rightarrow 0.414$ ($\uparrow$)
AG	$0.500 \rightarrow 0.670$ ($\uparrow$)	$0.707 \rightarrow 0.727$ ($\uparrow$)	$0.631 \rightarrow 0.699$ ($\uparrow$)	$0.667 \rightarrow 0.818$ ($\uparrow$)
AP	$0.670 \rightarrow 0.680$ ($\uparrow$)	$0.734 \rightarrow 0.764$ ($\uparrow$)	$0.703 \rightarrow 0.717$ ($\uparrow$)	$0.676 \rightarrow 0.737$ ($\uparrow$)
CA	$0.590 \rightarrow 0.740$ ($\uparrow$)	$0.756 \rightarrow 0.785$ ($\uparrow$)	$0.648 \rightarrow 0.766$ ($\uparrow$)	$0.646 \rightarrow 0.657$ ($\uparrow$)
CO	$0.940 \rightarrow 0.950$ ($\uparrow$)	$0.985 \rightarrow 0.961$ ($\downarrow$)	$0.954 \rightarrow 0.956$ ($\uparrow$)	$0.707 \rightarrow 0.768$ ($\uparrow$)
CT	$0.900 \rightarrow 0.920$ ($\uparrow$)	$0.926 \rightarrow 0.932$ ($\uparrow$)	$0.912 \rightarrow 0.926$ ($\uparrow$)	$0.879 \rightarrow 0.901$ ($\uparrow$)
CV	$0.790 \rightarrow 0.870$ ($\uparrow$)	$0.952 \rightarrow 0.955$ ($\uparrow$)	$0.838 \rightarrow 0.898$ ($\uparrow$)	$0.859 \rightarrow 0.899$ ($\uparrow$)
DS	$0.530 \rightarrow 0.420$ ($\downarrow$)	$0.688 \rightarrow 0.699$ ($\uparrow$)	$0.602 \rightarrow 0.644$ ($\uparrow$)	$0.686 \rightarrow 0.768$ ($\uparrow$)
DG	$0.460 \rightarrow 0.460$ ($\rightarrow$)	$0.559 \rightarrow 0.570$ ($\uparrow$)	$0.525 \rightarrow 0.492$ ($\downarrow$)	$0.459 \rightarrow 0.570$ ($\uparrow$)

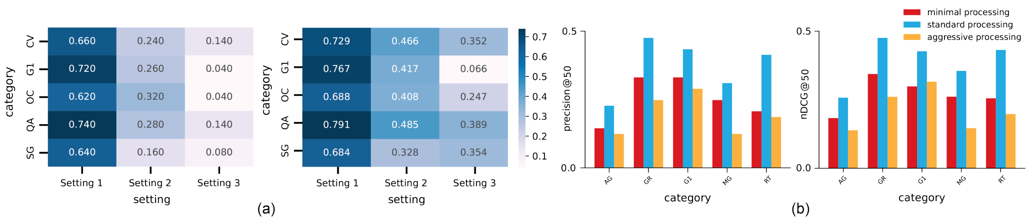

FIGURE 5. (a) Performance comparison across different contents composition settings. The left heatmap reports Precision@50, and the right heatmap presents nDCG@50. (b) Performance comparison across different LaTeX processing levels. The left bar chart shows Precision@50, and the right bar chart illustrates nDCG@50.

paper's core semantics. Titles and abstracts provide concise summaries of the main contributions, while introductions offer broader research context and background, which are critical for assessing reviewer expertise. We did not consider methodology sections, because it contain highly specific techniques and novel formulations that may introduce noise in topic similarity estimation. In this ablation, we evaluate how different constructions of key textual features affect embedding quality and recommendation performance under three settings: Setting 1: Title + Abstract + Introduction; Setting 2: Title + Abstract; Setting 3: Title only.

From the full results, we draw the following conclusions. Setting 1 consistently achieves the most stable and highest performance across all categories and metrics. As shown in Figure 5(a), the inclusion of the Introduction emerges as a key determinant of performance, since background information, problem formulation, and prior research context substantially contribute to semantic similarity estimation. Both Setting 2 and Setting 3 exhibit notable performance degradation relative to Setting 1 across most fields. In particular, Setting 2 shows pronounced drops in complex domains such as OC and CV, while Setting 3 suffers overall from insufficient contextual information. Collectively, this ablation demonstrates that Setting 1 (Title + Abstract + Introduction) provides the most faithful semantic representation of STEM manuscripts.

Importance of proper LaTeX Processing
Since we operate on raw LaTeX sources, we evaluate three preprocessing levels: minimal (comment removal only), standard (removing syntactic artifacts while preserving semantic symbols), and aggressive (retaining mostly natural language). As shown in Figure 5(b), standard processing consistently achieves the best performance across all metrics. Minimal processing leaves excessive LaTeX noise, while aggressive processing removes equation based semantics critical to STEM documents. Both issues degrade embedding quality, especially in equation heavy categories (e.g., RT). Overall, standard processing provides the optimal balance between noise reduction and information preservation.

4. Conclusion

In this work, we presented a LaTeX-aware embedding method for reviewer recommendation which is designed to address the limitations of general-purpose LLM-based approaches when applied to STEM manuscripts written in LaTeX. STEM documents convey core scientific meaning through equations and symbolic structures, which conventional textual embeddings fail to capture. To overcome this challenge, we introduced a LaTeX-aware preprocessing pipeline and adopted SciBERT as a domain-specialized encoder for accurately embedding equation-dense manuscripts.

Extensive experiments on large-scale arXiv Mathematics data demonstrate that the proposed approach substantially outperforms BERT-based and LLM-based baselines, with the performance gap most pronounced for high equation-density categories. Additionally, journal-specific domain-adaptive fine-tuning yields consistent improvements, highlighting the practical adaptability of our method to evolving editorial requirements.

Overall, this work illustrates that reviewer recommendation for STEM domains requires embedding method that explicitly account for the structural and semantic characteristics of LaTeX manuscripts. We expect our findings to facilitate the development of more accurate, transparent, and equitable reviewer assignment systems, and to motivate future efforts toward integrating symbolic reasoning, broader domain generalization, and real-world deployment in academic publishing workflows.

References

[1] Fu, Yongfan, Luo, Jian, Nan, Guofang, and Li, Dahui, Peer review expert group recommendation: A multi-subject coverage-based approach, Expert Systems with Applications **264** 125971, (2025), Elsevier.

[2] Lin, Jialiang, Song, Jiaxin, Zhou, Zhangping, Chen, Yidong, and Shi, Xiaodong, Automated scholarly paper review: Concepts, technologies, and challenges, Information fusion **98** 101830, (2023), Elsevier.

[3] Liu, Xiang, Suel, Torsten, and Memon, Nasir, A robust model for paper reviewer assignment, Proceedings of the 8th ACM Conference on Recommender systems 25–32, (2014).

[4] Aksoy, Meltem, Yanik, Seda, and Amasyali, Mehmet Fatih, A data-driven optimization approach for automated reviewer assignment using natural language processing, Intelligent Systems with Applications 200587, (2025), Elsevier.

[5] S. T. Dumais and J. Nielsen, Automating the assignment of submitted manuscripts to reviewers, Proceedings of the 15th ACM SIGIR Conference on Research and Development in Information Retrieval 233–244, (1992).

[6] M. A. Rodriguez and J. Bollen, Expertise modeling for matching papers with reviewers, Proceedings of the 13th ACM SIGKDD International Conference on Knowledge Discovery and Data Mining (KDD) 500–509, (2007).

[7] N. M. Kou, L. H. U, N. Mamoulis, and Z. Gong, Weighted coverage based reviewer assignment, Proceedings of the 2015 ACM SIGMOD International Conference on Management of Data 2031–2046, (2015).

[8] B. Li and Y. T. Hou, The new automated IEEE INFOCOM review assignment system, IEEE Network **30** 5 18–24, (2016).

[9] A. Kobren, B. Saha, and A. McCallum, Paper matching with local fairness constraints, Proceedings of the 25th ACM SIGKDD International Conference on Knowledge Discovery & Data Mining 1247–1257, (2019).

[10] Liu, Ou, Wang, Jun, Ma, Jian, and Sun, Yonghong, An intelligent decision support approach for reviewer assignment in R&D project selection, Computers in Industry **78** 1–10, (2016), Elsevier.

[11] J. Jin, B. Niu, P. Ji, and Q. Geng, An integer linear programming model of reviewer assignment with research interest considerations, Annals of Operations Research **291** 1 409–433, (2020).

[12] Y. Kalmukov, An algorithm for automatic assignment of reviewers to papers, Scientometrics **124** 3 1811–1850, (2020).

[13] S. Zhao, D. Zhang, Z. Duan, J. Chen, Y. Zhang, and J. Tang, A novel classification method for paper-reviewer recommendation, Scientometrics **115** 3 1293–1313, (2018).

[14] Z. Duan, S. Tan, S. Zhao, Q. Wang, J. Chen, and Y. Zhang, Reviewer assignment based on sentence pair modeling, Neurocomputing **366** 97–108, (2019).

[15] O. Anjum, H. Gong, S. Bhat, W.-M. Hwu, and J. Xiong, PaRe: A paper-reviewer matching approach using a common topic space, Proceedings of EMNLP-IJCNLP 2019 518–528, (2019).

[16] V. M. Karan, S. McQuistin, R. Yanagida, C. Perkins, G. Tyson, I. Castro, P. Healey, and M. Purver, A dataset for expert reviewer recommendation with large language models as zero-shot rankers, Proceedings of the 31st International Conference on Computational Linguistics (COLING) 11422–11427, (2025).

[17] I. Stelmakh, J. Wieting, G. Neubig, and N. B. Shah, A gold standard dataset for the reviewer assignment problem, arXiv:2303.16750, (2023).

[18] Y. Hou, J. Zhang, Z. Lin, H. Lu, R. Xie, J. McAuley, and W. X. Zhao, Large language models are zero-shot rankers for recommender systems, arXiv:2305.08845, (2023).

[19] arXiv, arXiv submission statistics, https://arxiv.org/stats/monthly_submissions, Accessed: April 2025, (2025).

[20] arXiv, arXiv category taxonomy, https://arxiv.org/category_taxonomy, Accessed: April 2025, (2025).

[21] Ginsparg, Paul, arXiv at 20, Nature **476** 7359 145–147, (2011).

[22] arXiv, arXiv Mathematics Subject Classification, https://arxiv.org/archive/math, Accessed: April 2025, (2025).

[23] Curry, Carolann Lee, Journal/Author Name Estimator (JANE), Journal of the Medical Library Association: JMLA **107** 1, 122, (2019).

[24] Laurel L. Haak, Martin Fenner, Laura Paglione, Ed Pentz, and Howard Ratner, ORCID: a system to uniquely identify researchers, Learned Publishing **25** 4, 259–264, (2012).

[25] Huh, Myung-Hoe, Introduction to social network analysis using R, Freedom Academy, Seoul, (2010).

[26] Krstovski, Kriste and Blei, David M, Equation embeddings, arXiv:1803.09123, (2018).

[27] Hallee, Logan, Kapur, Rohan, Patel, Arjun, Gleghorn, Jason P, and Khomtchouk, Bohdan, Contrastive learning and mixture of experts enables precise vector embeddings, arXiv:2401.15713, (2024).

[28] Beltagy, Iz, Lo, Kyle, and Cohan, Arman, SciBERT: A pretrained language model for scientific text, arXiv:1903.10676, (2019).

[29] Jacob Devlin, Ming-Wei Chang, Kenton Lee, Kristina Toutanova, BERT: Pre-training of Deep Bidirectional Transformers for Language Understanding, https://arxiv.org/abs/1810.04805, (2019).

[30] Ebrahimi, Sajad, Salamat, Sara, Arabzadeh, Negar, Bashari, Mahdi, and Bagheri, Ebrahim, exHarmony: Authorship and Citations for Benchmarking the Reviewer Assignment Problem, European Conference on Information Retrieval 1–16, (2025), Springer.

[31] Choi, Dong-Hoon, Hyun, Jin Woo, and Kim, Young Rock, An algorithm for peer reviewer recommendation based on scholarly activity assessment, IEEE Access **11**, 39609–39620, (2023).

[32] Herbert Voß, TeX Mathmode, `https://latex-tutorial.com/wp-content/uploads/2021/05/Mathmode.pdf`, (2014).

[33] Radim Rehurek, Gensim, `https://pypi.org/project/gensim/`, (2025).

[34] Mikolov, Tomas, Chen, Kai, Corrado, Greg, and Dean, Jeffrey, Efficient estimation of word representations in vector space, `arXiv:1301.3781`, (2013).

[35] Hegedüs, Gábor and Rónyai, Lajos, Gröbner Bases for Increasing Sequences, `arXiv:2208.00432`, (2022).

[36] Pennington, Jeffrey, Socher, Richard, and Manning, Christopher, GloVe: Global Vectors for Word Representation, Proceedings of the 2014 Conference on Empirical Methods in Natural Language Processing (EMNLP) 1532–1543, (2014), Association for Computational Linguistics.

[37] Bapat, Asilata, Brooks, Robyn, Hacker, Celia, Landi, Claudia, Mahler, Barbara I, and Stephenson, Elizabeth R, Computing the matching distance of 2-parameter persistence modules from critical values, `arXiv:2210.12868`, (2022).

[38] Boschert, Nicholas, Davis, Ethan, and Hiatt, Patrick, A Class of Freely Complemented von Neumann Subalgebras of $\mathcal{L}\mathbb{F}_n$, `arXiv:2411.05136`, (2024).

[39] Liu, Jiefeng, Zhou, Sihan, and Yuan, Lamei, Conformal r-matrix-Nijenhuis structures, symplectic-Nijenhuis structures, and ON-structures, Journal of Mathematical Physics **63** 10, (2022), AIP Publishing.

[40] Yadav, Pooja and Srivastava, Tanuja, Maximum Likelihood Estimation of the Parameters of Matrix Variate Symmetric Laplace Distribution, `arXiv:2502.04118`, (2025).

[41] Kurahashi, Taishi and Visser, Albert, Extensional Independence, `arXiv:2506.13524`, (2025).

[42] Zhao, Changsheng, Chang, Ernie, Liu, Zechun, Chang, Chia-Jung, Wen, Wei, Lai, Chen, Cao, Rick, Tian, Yuandong, Krishnamoorthi, Raghuraman, Shi, Yangyang, and others, MobileLLM-R1: Exploring the Limits of Sub-Billion Language Model Reasoners with Open Training Recipes, `arXiv:2509.24945`, (2025).

[43] Wang, Peng-Yuan, Liu, Tian-Shuo, Wang, Chenyang, Wang, Yi-Di, Yan, Shu, Jia, Cheng-Xing, Liu, Xu-Hui, Chen, Xin-Wei, Xu, Jia-Cheng, Li, Ziniu, and others, A Survey on Large Language Models for Mathematical Reasoning, `arXiv:2506.08446`, (2025).

[44] Mastroeni, Matthew, McCullough, Jason, Osborne, Andrew, Rice, Joshua, and Willis, Cole, Depth and singular varieties of exterior edge ideals, Rocky Mountain Journal of Mathematics **55** 4 1091–1110, (2025), Rocky Mountain Mathematics Consortium Tempe, AZ, USA.

[45] Barban, Lorenzo, Occhetta, Gianluca, and Conde, Luis E Solá, Quotients of flag varieties and their birational geometry, `arXiv:2509.05063`, (2025).

[46] Rizzi, Matteo and Peng, Xueqin, Normalized solutions for the nonlinear Schrödinger equation with potentials, arXiv:2507.20961, (2025).

[47] Lau, Gee-Choon and Shiu, Wai Chee, On local antimagic chromatic number of the join of two special families of graphs–II, arXiv:2410.17674, (2024).

[48] Nadimpalli, Santosh, Pattanayak, Santosha, and Prasad, Dipendra, Character theory at a torsion element, arXiv:2504.14684, (2025).

[49] Li, Jiaxin, Trung, Tran Nam, and Zhu, Guangjun, Associated primes of powers of edge ideals of edge-weighted trees, arXiv:2509.04774, (2025).

[50] Jacob, Cyril J, Lower bounds for Seshadri constants on blow ups of $\mathbb{P}^2$, arXiv:2404.11906, (2024).

[51] Cecchin, Alekos and Goffi, Alessandro, Convergence rates for the vanishing viscosity approximation of fully nonlinear, non-convex, second-order Hamilton-Jacobi equations, arXiv:2509.12144, (2025).

[52] Dorbec, Paul, Henning, Michael A, Tuza, Zsolt, and Versteegen, Leo, An exploration of the balance game, arXiv:2409.01796, (2024).

[53] Le, Nhat Hoang, The local twisted Gan-Gross-Prasad conjecture for $\mathrm{GL}(V)/U(V)$, arXiv:2504.21002, (2025).

[54] Apelblat, Alexander and González-Santander, Juan Luis, Infinite Series and Logarithmic Integrals Associated to Differentiation with Respect to Parameters of the Whittaker $W_{\kappa,\mu}$ (x) Function II, Axioms **12** 4 382, (2023), MDPI.

[55] Berestovskii, VN, The Gödel Universe as the Lie Group with left-invariant Lorentz metric, arXiv:2404.06866, (2024).

[56] Blanco, Víctor and Martínez-Antón, Miguel, Optimal Mediated Graphs: The role of Combinatorics in Conic Optimization, arXiv:2502.03288, (2025).

[57] Rokach, Lior and Maimon, Oded, Clustering methods, Data mining and knowledge discovery handbook 321–352, (2005), Springer.

[58] Kevin Leyton-Brown, Mausam, Yatin Nandwani, Hedayat Zarkoob, Chris Cameron, Neil Newman, and Dinesh Raghu, Matching Papers and Reviewers at Large Conferences, https://arxiv.org/abs/2202.12273, (2022).

[59] Xu, Yixuan Even, Fang, Fei, Tomczak, Jakub, Zhang, Cheng, Xue, Zhenyu Sherry, Paquet, Ulrich, and Belgrave, Danielle, Neurips 2024 experiment on improving the paper-reviewer assignment, (2024).

[60] Jhih-Yi Hsieh, Aditi Raghunathan, and Nihar B. Shah, Vulnerability of Text-Matching in ML/AI Conference Reviewer Assignments to Collusions, https://arxiv.org/abs/2412.06606, (2025).

[61] Yu Zhang, Yanzhen Shen, SeongKu Kang, Xiusi Chen, Bowen Jin, and Jiawei Han, Chain-of-Factors Paper-Reviewer Matching, https://arxiv.org/abs/2310.14483, (2025).

[62] Aitymbetov, Nurmukhammed and Zorbas, Dimitrios, Autonomous Machine Learning-Based Peer Reviewer Selection System, Proceedings of the 31st International Conference on Computational Linguistics: System Demonstrations 199–207, https://aclanthology.org/2025.coling-demos.20/, (2025).

[63] Fu, Yongfan, Luo, Jian, Nan, Guofang, and Li, Dahui, Peer review expert group recommendation: A multi-subject coverage-based approach, Expert Syst. Appl. **264** C, https://aclanthology.org/2025.coling-demos.20/, (2025), Pergamon Press, Inc..

[64] Jaeho Kim, Yunseok Lee, and Seulki Lee, Position: The AI Conference Peer Review Crisis Demands Author Feedback and Reviewer Rewards, Forty-second International Conference on Machine Learning Position Paper Track, https://openreview.net/forum?id=l8QemUZaIA, (2025).

[65] Zhu, Minjun, Weng, Yixuan, Yang, Linyi, and Zhang, Yue, Deepreview: Improving llm-based paper review with human-like deep thinking process, Forty-second International Conference on Machine Learning Position Paper Track, arXiv:2503.08569, (2025).

[66] Muennighoff, Niklas, Hongjin, SU, Wang, Liang, Yang, Nan, Wei, Furu, Yu, Tao, Singh, Amanpreet, and Kiela, Douwe, Generative representational instruction tuning, The Thirteenth International Conference on Learning Representations, (2024).

[67] Sun, Chenxi, Li, Hongyan, Li, Yaliang, and Hong, Shenda, Test: Text prototype aligned embedding to activate llm's ability for time series, arXiv:2308.08241, (2023).

[68] Liu, Weiming, Zheng, Xiaolin, Chen, Chaochao, Xu, Jiahe, Liao, Xinting, Wang, Fan, Tan, Yanchao, and Ong, Yew-Soon, Reducing item discrepancy via differentially private robust embedding alignment for privacy-preserving cross domain recommendation, Forty-first International Conference on Machine Learning, (2024).

[69] Lyu, Jiafei, Bai, Chenjia, Yang, Jingwen, Lu, Zongqing, and Li, Xiu, Cross-domain policy adaptation by capturing representation mismatch, arXiv:2405.15369, (2024).

[70] Stojanov, Petar, Li, Zijian, Gong, Mingming, Cai, Ruichu, Carbonell, Jaime, and Zhang, Kun, Domain adaptation with invariant representation learning: What transformations to learn?, Advances in Neural Information Processing Systems **34** 24791–24803, (2021).

[71] Cao, Jiaqi, Wang, Jiarui, Wei, Rubin, Guo, Qipeng, Chen, Kai, Zhou, Bowen, and Lin, Zhouhan, Memory decoder: A pretrained, plug-and-play memory for large language models, arXiv:2508.09874, (2025).

[72] Edward J. Hu, Yelong Shen, Phillip Wallis, Zeyuan Allen-Zhu, Yuanzhi Li, Shean Wang, Lu Wang, and Weizhu Chen, LoRA: Low-Rank Adaptation of Large Language Models, arXiv:2106.09685, (2021).

[73] Shuai Peng, Ke Yuan, Liangcai Gao, and Zhi Tang, MathBERT: A Pre-Trained Model for Mathematical Formula Understanding, arXiv:2105.00377, (2021).

[74] Amanpreet Singh, Mike D'Arcy, Arman Cohan, Doug Downey, and Sergey Feldman, SciRepEval: A Multi-Format Benchmark for Scientific Document Representations, Conference on Empirical Methods in Natural Language Processing, https://api.semanticscholar.org/CorpusID:254018137, (2022).

[75] Reimers, Nils and Gurevych, Iryna, Sentence-bert: Sentence embeddings using siamese bert-networks, Proceedings of the 2019 conference on empirical methods in natural language processing and the 9th international joint conference on natural language processing (EMNLP-IJCNLP) 3982–3992, (2019).

[76] Hallee, Logan, Kapur, Rohan, Patel, Arjun, Gleghorn, Jason P, and Khomtchouk, Bohdan B, Contrastive learning and mixture of experts enables precise vector embeddings in biological databases, Scientific Reports **15** 1 14953, (2025), Nature Publishing Group UK London.

[77] Weng, Yixuan, Zhu, Minjun, Xia, Fei, Li, Bin, He, Shizhu, Liu, Kang, and Zhao, Jun, Mastering symbolic operations: Augmenting language models with compiled neural networks, arXiv:2304.01665, (2023).

[78] Drozdov, Andrew, Schärli, Nathanael, Akyürek, Ekin, Scales, Nathan, Song, Xinying, Chen, Xinyun, Bousquet, Olivier, and Zhou, Denny, Compositional semantic parsing with large language models, arXiv:2209.15003, (2022).

[79] Lo, Kyle, Wang, Lucy Lu, Neumann, Mark, Kinney, Rodney, and Weld, Daniel S, S2ORC: The semantic scholar open research corpus, Proceedings of the 58th annual meeting of the association for computational linguistics 4969–4983, (2020).

[80] Karpukhin, Vladimir, Oguz, Barlas, Min, Sewon, Lewis, Patrick, Wu, Ledell, Edunov, Sergey, Chen, Danqi, and Yih, Wen-tau, Dense passage retrieval for open-domain question answering, Proceedings of the 2020 conference on empirical methods in natural language processing (EMNLP) 6769–6781, (2020).

[81] Humeau, Samuel, Shuster, Kurt, Lachaux, Marie-Anne, and Weston, Jason, Poly-encoders: Transformer architectures and pre-training strategies for fast and accurate multi-sentence scoring, arXiv:1905.01969, (2019).

[82] Muennighoff, Niklas, Tazi, Nouamane, Magne, Loïc, and Reimers, Nils, Mteb: Massive text embedding benchmark, Proceedings of the 17th Conference of the European Chapter of the Association for Computational Linguistics 2014–2037, (2023).

[83] Thakur, Nandan, Reimers, Nils, Rücklé, Andreas, Srivastava, Abhishek, and Gurevych, Iryna, Beir: A heterogenous benchmark for zero-shot evaluation of information retrieval models, arXiv:2104.08663, (2021).

[84] Bast, Hannah and Korzen, Claudius, A benchmark and evaluation for text extraction from PDF, 2017 ACM/IEEE joint conference on digital libraries (JCDL), IEEE 1–10, (2017).

[85] Habib, Raja and Afzal, Muhammad Tanvir, Sections-based bibliographic coupling for research paper recommendation, Scientometrics **119** 2 643–656, (2019), Springer.

J. Basic Sci. HUFS **62** (2026), pp. 51-98

ANALYSIS OF VAN HIELE LEVELS AND ACHIEVEMENTS FOR STUDENTS THROUGH VAN HIELE GEOMETRY TESTS

Young Rock Kim, Eon Woo Nam

Abstract. In this work we tested Van Hiele Geometry tests to 1500 students from primary schools, middle schools, and high schools in Korea. The methodology of Van Hiele model was used in questionnaires, and in analysis of data and results. We made question problems about general attitude concerning Van Hiele Geometry. In this work we present the results of the study applied to a students in schools in Korea about Van Hiele Geometry and its analysis. Therefore we determined the distribution of the 5 Van Hiele levels of thinking through 12 grades in schools in Korea. Appling this test to every students through 12 grades in schools, we analyised 5 Van Hiele levels of thinking (Visualization, Analysis, Informal Deduction, Deduction, and Rigor). The purpose of this study is to examine the relationship between attitudes toward mathematics and understanding of geometry through survey. The study targeted the 1st, 2nd grade students from elementary school, 2nd grade students from middle school, and 2nd grade students from high school. In this experiment, mathematical self-concepts, attitudes, and study habits of students were reviewed after the experiment was further examined through survey. Also, their understanding of geometry was analyzed. Survey of attitude towards mathematics' was used for the questionnaire. Later, EXCEL (spreadsheet program) and SPSS (Statistical Package for the Social Sciences) were used in order to analyze the results.

Key words and phrases. van Hiele Geometry tests, Mathematics Education, van Hiele Levels, survey.

Department of Mathematics Education, Graduate School of Education, Hankuk University of Foreign Studies. This research was supported by the research fund of Hankuk University of Foreign Studies, he second author, Eon Woo Nam, is conducting his graduate thesis research under the supervision of the first author. Parts of this work provide the foundation for the author's graduate thesis, with appropriate extensions and additional analyses presented in the thesis.

1. Introduction

1.1. **Necessity and Purpose of the Study.** The 2009 Revised National Curriculum stipulates the need to cultivate the character of all citizens and equip them with the ability to lead independent lives and the qualities required of democratic citizens, all based on the educational philosophy of *Hongik Ingan* (devotion to the welfare of humanity). The ultimate goal is to enable every individual to lead a truly humane life and to contribute to the development of a democratic nation and the realization of the ideal of universal human prosperity. The ideal human type envisioned by the 2009 Revised National Curriculum is as follows:

a. An individual who develops their unique personality and charts their own career path based on holistic growth.
b. An individual who demonstrates creativity through innovative ideas and challenges, grounded in fundamental competencies.
c. An individual who leads a dignified life based on cultural literacy and an understanding of diverse values.
d. An individual who participates in community development with a spirit of consideration and sharing as a global citizen.

From this, it is evident that the purpose of the current curriculum is not merely to produce individuals who excel at solving problems—or, in other words, those who simply achieve high academic grades [1].

In today's 21st-century knowledge-based information society, the core of education lies not in training individuals for mere technical skills, but in cultivating autonomous and creative talent capable of creating intellectual value through self-directed learning. Consequently, mathematics education must foster "mathematical power"—a concept encompassing the ability to explore, predict, and reason logically based on fundamental mathematical concepts, principles, and laws; the ability to utilize mathematics and process or exchange information through it; problem-solving skills (including formulating and solving problems by applying mathematical knowledge to real-life situations or other disciplines); creativity; a disposition for mathematical thinking; cognitive flexibility; and self-confidence [2].

Geometry is considered a crucial area for enhancing the mathematical abilities mentioned above. While the previous curriculum required 8th-grade students (second year of middle school) to learn geometric proofs presented in textbooks, the current 2009 revised curriculum shifted this topic to the 10th grade (first year of high school) to alleviate the students' academic burden. This shift led to the hypothesis that a disparity in Van Hiele levels of geometric thinking between students and teachers causes many students—despite diligent instruction—to resort to rote memorization rather than engaging in the necessary cognitive processes; consequently, the following study was conducted.

This study first surveyed 8th-grade (second year of middle school) and 11th-grade (second year of high school) students to understand their attitudes toward mathematics and perceptions of geometry. Subsequently, it analyzed the geometry achievement and geometric thinking levels—based on the Van Hiele model—of these students, as well as those in the first and second grades of elementary school. The study also examined the distribution of Van Hiele geometric thinking levels by categorizing students' geometry achievement levels according to grade and gender. Based on these findings, the relationships between students' mathematical attitudes, perceptions of geometry, and geometric thinking levels were investigated. Furthermore, the study summarized the geometry-related curriculum content for each grade group under the 2009 Revised National Curriculum and assessed which stage of the Van Hiele geometric thinking model corresponded to the content of each unit.

1.2. **Research Questions.** This study establishes the following research questions and aims to conduct a detailed investigation and analysis:

Q1. Examine the attitudes toward mathematics and perceptions of geometry held by students in grades 1 and 2 (elementary school), grade 8 (second year of middle school), and grade 11 (second year of high school).

Q2. Analyze the students' achievement levels in geometry and their levels of geometric thinking based on the Van Hiele Geometry Test.

Q3. Analyze differences in geometry achievement levels based on grade and gender, and examine the distribution of Van Hiele geometric thinking levels.

Q4. Investigate the relationships between the students' mathematical attitudes, perceptions of geometry, and levels of geometric thinking.

Q5. Examine the geometry-related curriculum content of the current 2009 Revised National Curriculum and determine how it is categorized according to Van Hiele geometric thinking levels.

2. Theoretical Background

The theory of geometric thinking levels proposed by Van Hiele originated from the doctoral dissertation submitted by the Dutch mathematics educator Pierre van Hiele to Utrecht University in 1957. While teaching at a middle school, Van Hiele observed that many students struggled to understand geometric proofs despite his instruction. This experience led him to investigate the nature of students' geometric thinking. Van Hiele proposed that geometric thinking develops through five hierarchical levels. He also argued that each level is characterized by its own unique language structure, making communication difficult between individuals reasoning at different levels. Consequently, differences between teachers' and students' levels of geometric thinking can create challenges in the teaching and learning of geometry. Teachers tend to explain concepts from their own level of understanding and expect students to comprehend them accordingly, whereas students often interpret these explanations using reasoning appropriate to a lower level. As a result, students may fail to understand the teacher's explanations. To address this issue, Van Hiele emphasized that teachers should carefully assess their students' levels of geometric thinking and provide instruction that is appropriate to those levels. In other words, teachers should encourage rich mathematical thinking by providing instruction suited to students' current levels and guide them progressively toward the next level of geometric thinking.

The main principles of Van Hiele's theory of mathematical learning levels can be summarized as follows. First, students cannot attain level n without first passing through level $n-1$; mathematical thinking develops sequentially through all levels. Second, students do not progress through the levels at the same rate. Advancement from one level to the next may be accelerated by effective instruction or delayed by inappropriate teaching. Third, ideas that are implicit at one level become explicit and consciously recognized at the next level. The mathematical thinking characteristic of each level investigates and organizes the internal structure of the preceding level. Fourth, progression through the levels is closely related to the development and expansion of language. Fifth, individuals who reason at different levels are generally unable to understand one another effectively [15].

2.1. **Components of Van Hiele's Theory.**

2.1.1. **Insight.** From the early stages of their research, the Van Hieles were interested in identifying ways to develop their students' intuitive insight. They defined insight as the ability to:

- perform a given task even in an unfamiliar situation;
- carry out the actions required in that situation skillfully (accurately and appropriately); and
- solve the problem deliberately and consciously (systematically) by selecting an appropriate method for the situation.

When students possess insight, they understand what they are doing, why they are doing it, and when they should apply it. Furthermore, students with insight are able to apply their knowledge effectively to problem-solving situations [28].

2.1.2. **Van Hiele's Levels of Geometric Thinking.** While accepting Piaget's theory of the developmental stages of geometry, Van Hiele shifted the emphasis from development to learning. According to Piaget, learning is of limited value until learners reach an appropriate stage of logical development. In contrast, Van Hiele argued that appropriate instruction can promote learners' progression from one developmental level to the next.

According to Van Hiele, mathematical thinking is an activity of organizing one's experiential world. At each level, the means used to organize experience at the previous level become the objects of thought at the next level, where they are reorganized and reinterpreted. This repeated process of reorganizing experience enables learners to make qualitative leaps to higher levels of thinking. Consequently, mathematics instruction should guide students through these discontinuous levels of thought so that they can continually reconstruct and rediscover mathematical ideas. Van Hiele classified geometric thinking into the following six levels. This hierarchical model demonstrates that a serious mismatch may occur when mathematics instruction is not aligned with students' levels of learning [17].

(1) **Level 0: Pre-recognition** At this level, children distinguish geometric shapes by attending to only one visual characteristic. They are unfamiliar with many common geometric figures and do not classify shapes into conventional categories. For example, they distinguish between straight and curved shapes rather than between quadrilaterals and triangles, classifying squares and circles as different simply because they appear different. Students at this level lack the visual imagery necessary to recognize common geometric figures.

Such imagery is based on internal representations formed through children's actions and serves as the foundation for later reasoning. Their judgments are based primarily on specific shapes or tactile stimuli, and they recognize figures only as visually "the same shape." This level generally corresponds to children before elementary school [31].

(2) **Level 1: Visual Recognition**

At the visual recognition level, students identify figures based on their overall appearance rather than on their properties. For example, when asked, "Why is this figure a square?" they may respond, "Because it looks like a square." Students perceive geometric figures as complete visual wholes and can mentally represent them as visual images. However, they pay little attention to the defining properties of the figures. Although geometric figures are mathematically defined by their properties, students at this level fail to recognize these characteristics. Thus, statements such as "This figure is a rhombus" simply mean "This figure has the same appearance as what I have learned to call a rhombus." As students progress from Level 1 to Level 2, visual images gradually become associated with the properties of geometric figures [31]. In summary, students at Level 1 classify figures solely according to their appearance and have little awareness of their defining properties. Their reasoning is based on whether shapes look alike or different.

(3) **Level 2: Descriptive/Analytic Recognition**

At the descriptive or analytic level, students focus on and analyze the properties of geometric figures. By examining visually perceived shapes, they identify their defining characteristics and classify figures according to these properties rather than their appearance. Geometric figures are viewed as collections of properties, while visual images become secondary. For example, a rhombus is recognized as a figure with four equal sides, and the term rhombus represents a set of defining properties rather than a familiar visual image. However, students still have difficulty understanding inclusion relationships among figures and may reject hierarchical classifications based on their personal conceptions. At this level, the object of thought is the set of properties that characterizes each figure [31]. In summary, students at Level 2 can identify and explain the properties of individual geometric figures. For example, they understand that the sum of the interior angles of a triangle is 180 degrees and that a quadrilateral has four vertices. However, although they recognize the properties of individual figures, they do not yet fully understand the hierarchical relationships among different classes of figures.

(4) **Level 3: Relational/Abstract Recognition**

At the relational or abstract level, geometric figures and their properties become logically organized. Students construct abstract definitions of concepts, distinguish between necessary and sufficient conditions, and engage in logical reasoning about geometry. Some properties become part of formal definitions, while others are derived through logical deduction. Students understand both the relationships among different geometric figures and the relationships among the properties of a single figure. They can organize figures into hierarchical classifications and justify these classifications through informal arguments. For example, students recognize that a square is simultaneously a rhombus, a rectangle, a parallelogram, and a trapezoid.

As students discover increasingly complex relationships among properties, they recognize the need to organize them systematically. Understanding that one property may imply another represents the first step toward deductive reasoning. Nevertheless, students at this level do not yet fully comprehend formal deductive proof or the complete structure of an axiomatic system. Their deductive reasoning remains local rather than global. For instance, they can reason that since a quadrilateral can be divided into two triangles and each triangle has interior angles summing to 180 degrees, the sum of the interior angles of a quadrilateral must be 360 degrees [31]. In summary, students at Level 3 are capable of abstract reasoning without relying on concrete examples. They understand hierarchical relationships among geometric figures and can derive simple properties from existing ones. However, they have not yet mastered formal deductive proof.

(5) **Level 4: Formal Deduction**

At the formal deduction level, students fully understand the nature of deductive reasoning. They appreciate the significance of the axiomatic method for constructing and developing geometric theory. Students are able to establish theorems within an axiomatic system and distinguish logically among undefined terms, axioms, definitions, and theorems. They understand deductive reasoning and can construct formal proofs. In other words, they are capable of producing a logically coherent sequence of propositions that justifies a conclusion from a given set of assumptions [31]. Thus, Level 4 represents the stage at which students can develop formal proofs through logical reasoning and derive new mathematical results. Van Hiele regarded this as the highest level that should be expected of students.

(6) **Level 5: Rigor**

At the highest level, students reason within fully abstract mathematical systems. The specific properties of objects and the concrete meanings of relationships among those properties are abstracted away. Learners are able to reason formally about different mathematical systems independently of particular interpretations or models. They can investigate geometry without relying on visual models and reason formally using axioms, definitions, and theorems. Students at this level appreciate the significance of different axiomatic and logical systems and can reason rigorously within multiple mathematical frameworks. Geometry is viewed as an abstract deductive system, and students possess a deep understanding of mathematical structures, enabling them to justify higher-order propositions about those structures. This level corresponds to the reasoning ability of professional mathematicians. Such reasoning leads not only to the development and refinement of axiomatic geometric systems but also to comparisons among systems such as Euclidean and non-Euclidean geometry [31]. In summary, Level 5 is characterized by the ability to reason abstractly without reference to concrete geometric objects. Students can investigate and develop geometric theories independently of specific figures. This level corresponds to the reasoning of professional mathematicians and generally exceeds the level expected of ordinary students.

2.2. **Characteristics of Van Hiele's Levels of Geometric Thinking.** First, thinking is regarded as a discontinuous activity consisting of hierarchical levels. In mathematics learning, learners cannot reach a higher level without first passing through the preceding level, and mathematical thinking develops sequentially through all levels. In other words, students cannot attain level n without first progressing through level $n-1$. Second, not all students progress through each level at the same rate. Advancement from one level to the next may be facilitated by appropriate instruction or delayed by inappropriate teaching. Progression between levels depends more on the content and methods of instruction than on age or physical maturation. Third, at a higher level, the actions performed at the previous level become the objects of analysis. In other words, what serves as the means of thinking at one level becomes the object of thought at the next level, and concepts that were implicitly understood at the previous level become explicitly recognized. More specifically, at Level 1, learners understand objects in the surrounding world through the medium of geometric figures. At Level 2, geometric figures themselves become the objects of thought, while their properties serve as the means of thinking. At Level 3, the properties of geometric figures become the objects of thought, and propositions become the means of reasoning about those properties. At Level 4, propositions become the objects of thought, and logic serves as the means of understanding them. Finally, at Level 5, logic itself becomes the object of study. Fourth, each level possesses its own linguistic symbols and a system of relationships connecting those symbols. Therefore, progression through the levels is closely related to the expansion of language. Fifth, two individuals reasoning at different levels are generally unable to understand one another. This phenomenon frequently occurs between teachers and students and constitutes one of the major obstacles to effective mathematics instruction.

	Object of Thought	Means of Thinking
Level 1	Objects in the Surrounding World	Geometric Figures
Level 2	Geometric Figures	Properties
Level 3	Properties	Propositions
Level 4	Propositions	Logic
Level 4	Logic	

Table 1. Objects and Means of Thinking at the Levels of Geometric Learning

As shown in Table 1, Van Hiele explained the process of learning mathematics through his theory of hierarchical levels, arguing that the means of thinking at one level become the objects of thought at the next level, thereby producing a qualitative leap in thinking (Clements & Battista, 1992; [31]).

2.3. **Educational Implications of Van Hiele's Theory.** A central concern of contemporary education is the development of thinking, and the learning process should involve learners' constructive activities and the rediscovery of knowledge. Like Piaget and Freudenthal, Van Hiele's theory emphasizes mathematical thinking. According to Van Hiele, mathematical thinking develops progressively through the descriptive level, the theoretical level, the deductive level, and the level of rigor. This perspective is consistent with the views of many mathematics educators, who argue that mathematics curricula and learning activities should be organized according to the logical structure and hierarchy of mathematics while taking students' cognitive development into account, progressing from concrete manipulative activities to formal mathematical reasoning.

Teachers often conduct instruction primarily through verbal explanations without considering the differences between their own levels of thinking and those of their students, paying little attention to students' mathematical thinking processes. Furthermore, by explaining the key ideas for solving problems before students have the opportunity to discover them independently, teachers may hinder students' creative learning and deprive them of valuable opportunities to develop their own mathematical thinking. From this perspective, instruction based on Van Hiele's levels of thinking provides learning experiences appropriate to students' cognitive levels, enabling them to reason at their own developmental stages while preventing stagnation or gaps in their cognitive development.

Van Hiele's ideas suggest that the development of geometric thinking depends more on the quality of instruction than on students' natural maturation. According to Van Hiele, mathematical thinking is an activity of organizing the world of experience. The means used to organize experience at one level become conscious objects of thought at the next level, where they are reorganized, resulting in a qualitative leap to a higher level. This process is repeated continuously, and mathematics instruction should therefore guide students through these discontinuous levels of thinking so that they may continually reconstruct mathematical ideas. Consequently, mathematics teaching that fails to consider Van Hiele's theory of geometric thinking levels may result in a serious mismatch between instruction and students' cognitive development.

Van Hiele's theory reflects the essential characteristics of mathematization, including transforming means of organizing phenomena into objects of study, making the internal order of thought explicit, identifying patterns, formalizing ideas, and repeatedly alternating between form and content. Consequently, the theory provides valuable implications for the development of geometry curricula and the improvement of geometry instruction.

The educational significance of Van Hiele's theory can be summarized as follows. First, it establishes levels of geometric learning based on profound insights into the developmental stages of geometric thinking. Second, it attempts to promote effective instruction in Euclidean geometry through local organization of geometric concepts. Third, by emphasizing the importance of Euclidean geometry and the implementation of developmental principles, it has contributed significantly to the improvement of geometry education. Fourth, Van Hiele argued that his theory is applicable not only to all areas of mathematics but also to disciplines beyond mathematics [14].

3. Van Hiele Geometry Test

3.1. **Research Methods and Procedures.**

(1) Participants

The participants in this study consisted of 146 first-grade students (Grade 1 of elementary school), 170 second-grade students (Grade 2 of elementary school), 122 eighth-grade students (Grade 2 of middle school), and 242 eleventh-grade students (Grade 2 of high school). The 146 first-grade and 170 second-grade elementary school students completed only the Van Hiele Geometry Test without participating in the questionnaire survey. In contrast, the 122 eighth-grade and 242 eleventh-grade students completed the questionnaire survey prior to taking the Van Hiele Geometry Test. The details of the participants are presented in the following table.

Grade	School	Number of Students
Grade 1	Elementary School A, Guri-si, Gyeonggi-do	71
Grade 1	Elementary School B, Dobong-gu, Seoul	75
Grade 2	Elementary School A, Guri-si, Gyeonggi-do	85
Grade 2	Elementary School B, Dobong-gu, Seoul	85
Grade 8	Middle School C, Uijeongbu-si, Gyeonggi-do	82
Grade 8	Middle School D, Seongbuk-gu, Seoul	40
Grade 11	High School E, Uijeongbu-si, Gyeonggi-do	102
Grade 11	High School F, Nowon-gu, Seoul	30
Grade 11	High School G, Seocho-gu, Seoul	34
Grade 11	High School H, Seongbuk-gu, Seoul	40
Grade 11	High School I, Songpa-gu, Seoul	36

Table 2. Participants

(2) Research Period: September 2014 – June 2015

(3) Research Procedures

(a) Selection of the research topic: September 2014

(b) Literature review and investigation of previous studies: October 2014 – November 2014
(c) Selection of participants: March 2015
(d) Development of research instruments: December 2014 – February 2015
(e) Implementation of the study and administration of the questionnaire survey: April 2015 – May 2015
(f) Statistical analysis and organization of the collected data: June 2015

(4) Research Methods
(a) Previous studies related to the research topic were reviewed.
(b) Relevant literature and teaching–learning theories proposed by mathematics education researchers were examined.
(c) The existing Van Hiele Geometry Test was translated and adapted to suit the Korean educational context.
(d) Questionnaires on mathematical attitudes and perceptions of geometry were developed.
(e) The questionnaire survey was administered before the geometry test. For elementary school students, however, the questionnaire on mathematical attitudes and perceptions of geometry was not administered. The testing time was 15 minutes (5 items) for first- and second-grade elementary students, 30 minutes (20 items) for middle school students, and 35 minutes (25 items) for high school students.
(f) The results of the Van Hiele Geometry Test and the questionnaires on mathematical attitudes and perceptions of geometry were analyzed and summarized.

(5) Research Instruments
(a) Van Hiele Geometry Test developed for each grade level
(b) Questionnaire Survey
The questionnaire items were developed based on the affective characteristics of Korean students toward mathematics. In addition, items related to students' perceptions of geometry were added to the existing questionnaire. The purpose of administering the questionnaire was to examine the relationship between students' mathematical attitudes and their levels of geometric thinking. The questionnaire was based on the *Mathematical Attitude Inventory* developed by the Korean Educational Development Institute (KEDI) in 1992.

The questionnaire consisted of four domains: *self-concept in mathematics*, *attitudes toward mathematics*, *mathematics learning habits*, and *perceptions of geometry*. It comprised a total of 60 items: 11 items on self-concept, 15 items on attitudes, 14 items on learning habits, and 20 items on perceptions of geometry.

Domain	Item Numbers	Number of Items
Self-concept	1, 4, 9, 11, 12, 17, 20, 25, 28, 33, 36	11
Attitude	2, 5, 7, 10, 13, 15, 18, 21 23, 26, 29, 31, 34, 37, 39	15
Learning Habits	3, 6, 8, 14, 16, 19, 22, 24, 27, 30, 32, 35, 38, 40	14
Perception of Geometry	41∼60	20

TABLE 3. Questionnaire Contents and Analysis Framework

(1) Data Processing

The questionnaire items measuring students' affective characteristics employed a five-point Likert scale: "① Strongly Agree, ② Agree, ③ Neutral, ④ Disagree, ⑤ Strongly Disagree." Responses of "Strongly Agree" were assigned 5 points, "Agree" 4 points, "Neutral" 3 points, "Disagree" 2 points, and "Strongly Disagree" 1 point. Invalid responses were assigned 0 points. Negatively worded items (Items 3, 8, 13, 18, 23, 28, 33, 38, 45, and 57) were reverse-scored.

(2) Statistical Analysis

The questionnaire survey was administered under the supervision of the classroom teachers to 122 eighth-grade students (Grade 2 of middle school) and 210 eleventh-grade students (Grade 2 of high school) prior to the administration of the geometry test, and all questionnaires were collected. After reviewing the collected data, 21 invalid responses were identified among the middle school students and 23 among the high school students. These were judged not to have a significant influence on the research results. Accordingly, the collected data were statistically processed and analyzed using Microsoft Excel and SPSS.

3.2. **Research Contents.** The Van Hiele Geometry Test was used as the primary instrument for collecting data to analyze students' levels of geometric thinking. The test, originally developed by Usiskin (1982) as part of the Chicago Project [32], consists of 25 items, with five items corresponding to each of Van Hiele's five levels of geometric thinking. Items 21 through 25 were designed to measure Level 5 of Van Hiele's theory. Although Usiskin argued that Level 5 neither exists among secondary school students nor can be meaningfully measured, the present study adopted all 25 items in accordance with the Korean mathematics curriculum. Different numbers of items were administered depending on the participants' grade levels, as shown below. This study included only Grades 1–2 (elementary school), Grade 8 (middle school), and Grade 11 (high school).

Grade	Items	Testing Time
Grades 1–2 (Elementary School)	Items 1–5	15 minutes
Grades 3–4 (Elementary School)	Items 1–10	20 minutes
Grades 5–6 (Elementary School)	Items 1–15	25 minutes
Grades 7–9 (Middle School)	Items 1–20	30 minutes
Grades 10–12 (High School)	Items 1–25	35 minutes

Table 4. Test Classification

The scoring procedure and the assignment of Van Hiele levels followed the method used in the Chicago Project (Usiskin, 1982). In determining students' levels, the Chicago Project compared two criteria: correctly answering three out of five items (3/5) and correctly answering four out of five items (4/5) within each level.

Probability of correctly answering 3 out of 5 items by random guessing = 0.0579

Probability of correctly answering 4 out of 5 items by random guessing = 0.0067

The Chicago Project concluded that the 4/5 criterion produced fewer classification errors than the 3/5 criterion. Accordingly, the present study adopted the same criterion and assigned scores as follows.

1) Level 1 (1–5): 1 point for answering at least 4 of the 5 items correctly.
2) Level 2 (6–10): 2 points for answering at least 4 of the 5 items correctly.
3) Level 3 (11–15): 4 points for answering at least 4 of the 5 items correctly.
4) Level 4 (16–20): 8 points for answering at least 4 of the 5 items correctly.
5) Level 5 (21–25): 16 points for answering at least 4 of the 5 items correctly.

Furthermore, in the Chicago Project, students whose responses did not follow the hierarchical sequence predicted by Van Hiele's theory were excluded from the analysis. In the present study, however, students were classified into those who progressed sequentially through the Van Hiele levels (*fitters*) and those who did not (*non-fitters*), and were treated as follows.

· **Fitter group**: Students who progressed sequentially through the levels were assigned the highest Van Hiele level they attained. Total scores of 1, 3, 7, 15, and 31 on the Van Hiele Level Test correspond to Van Hiele Levels 1, 2, 3, 4, and 5, respectively. Students who did not attain Level 1 were classified as Level 0.

· **Non-fitter group**: Students who did not progress sequentially through the levels were assigned the highest level they attained and were classified as belonging to a *quasi-level*. Specifically, a total score of 2 corresponds to Quasi-Level 2, scores of 4–6 correspond to Quasi-Level 3, scores of 8–14 correspond to Quasi-Level 4, and scores of 16–30 correspond to Quasi-Level 5.

3.3. **Analysis of the Van Hiele Geometry Thinking Level Test.**

3.3.1. *Grade 1 (Elementary School).*

Level	Male	Female	Total
Level 0	75 (51.4%)	70 (47.9%)	145 (99.3%)
Level 1	0 (0.0%)	1 (0.7%)	1 (0.7%)
Total	75 (51.4%)	71 (48.6%)	146 (100%)

Table 5. Grade 1 (Elementary School) – Fitter Group

The highest expected level of geometric thinking for first-grade elementary school students is Level 1. The analysis of 146 first-grade students showed that, with the exception of one female student who reached Level 1, all students were classified as Level 0. This result does not necessarily indicate that the participating students had poor geometric thinking abilities. Rather, the test was administered at the beginning of the school year before students had completed the relevant curriculum. Since there was virtually no difference between male and female students, a gender-based analysis was considered unnecessary.

Item	Correct Rate
1	35.6%
2	15.1%
3	31.5%
4	17.1%
5	4.1%

TABLE 6. Grade 1 (Elementary School) – Correct Response Rate by Item

Item 1, which asked students to identify the shape of a square, showed the highest correct response rate at 35.6%. In contrast, Item 5, which required students to identify a parallelogram, recorded the lowest correct response rate at 4.1%. Items 2 through 4 asked students to identify the shapes of an equilateral triangle, a rectangle, and a square, respectively. Although geometry is first introduced in Unit 2, "Various Shapes," during the second semester of Grade 1, none of the items had a correct response rate of 0%. This suggests that some students had been exposed to geometry through learning experiences outside the regular school curriculum.

3.3.2. *Grade 2 (Elementary School).*

Level	Male	Female	Total
Level 0	87 (51.2%)	74 (43.5%)	161 (94.7%)
Level 1	5 (2.9%)	4 (2.4%)	9 (5.3%)
Total	92 (54.1%)	78 (45.9%)	170 (100%)

TABLE 7. Grade 2 (Elementary School) – Fitter Group

The highest expected level of geometric thinking for second-grade elementary school students is also Level 1. Among the 170 students analyzed, the vast majority (94.7%) were classified as Level 0, similar to the first-grade students. However, nine students (5.3%), consisting of five boys and four girls, reached Level 1. This result is likely attributable to the additional year of learning completed by the second-grade students. As in Grade 1, no substantial gender difference was observed.

Item	Correct Rate
1	39.4%
2	47.1%
3	34.1%
4	28.2%
5	8.8%

TABLE 8. Grade 2 (Elementary School) – Correct Response Rate by Item

As in Grade 1, Item 1, which asked students to identify the shape of a square, showed the highest correct response rate (39.4%), whereas Item 5, which asked students to identify a parallelogram, had the lowest correct response rate (8.8%). Items 2 through 4 asked students to identify the shapes of an equilateral triangle, a rectangle, and a square, respectively. Compared with the first-grade students, the second-grade students demonstrated considerably higher correct response rates. This improvement is likely because second-grade students had already studied the relevant geometry unit, "Various Geometric Figures," during the first semester.

3.3.3. *Grade 8 (Second Year of Middle School).*

Level	Male	Female	Total
Level 0	9 (11.7%)	5 (11.1%)	14 (14.3%)
Level 1	13 (16.9%)	12 (26.7%)	25 (25.5%)
Level 2	14 (18.2%)	10 (22.2%)	24 (24.5%)
Level 3	24 (31.2%)	10 (22.2%)	34 (34.7%)
Level 4	1 (1.3%)	0 (0.0%)	1 (1.0%)
Total	61 (79.2%)	45 (82.2%)	98 (100%)

Table 9. Grade 8 (Second Year of Middle School) – Fitter Group

Level	Male	Female	Total
Quasi-Level 2	2 (2.6%)	1 (2.2%)	3 (12.5%)
Quasi-Level 3	13 (16.9%)	7 (15.6%)	20 (83.3%)
Quasi-Level 4	1 (1.3%)	0 (0.0%)	1 (4.2%)
Total	16 (20.8%)	8 (17.8%)	24 (100%)

Table 10. Grade 8 (Second Year of Middle School) – Non-fitter Group

Among the 122 eighth-grade students analyzed, 98 belonged to the fitter group and 24 to the non-fitter group. The highest expected level of geometric thinking for eighth-grade students is Level 4. However, only one male student reached Level 4, probably because the participants had not yet completed the Grade 9 mathematics curriculum.

Within the fitter group, the largest proportion of students (34.7%) was classified at Level 3. This result appears to have been influenced primarily by the male students, among whom Level 3 was the most common level, whereas the largest proportion of female students was classified at Level 1. These findings suggest that male students in Grade 8 exhibited higher levels of geometric thinking than female students.

Analysis of the non-fitter group showed that most students were classified as Quasi-Level 3. Similar to the fitter group, in which Level 3 was the most common, these students appear to possess an average level of geometric thinking despite not progressing through the Van Hiele levels sequentially.

Item	Correct Rate	Item	Correct Rate
1	96.7%	11	62.3%
2	81.1%	12	49.2%
3	89.3%	13	76.2%
4	78.7%	14	61.5%
5	72.1%	15	54.1%
6	77.0%	16	24.6%
7	91.8%	17	39.3%
8	50.8%	18	27.0%
9	88.5%	19	18.0%
10	46.7%	20	18.0%

Table 11. Grade 8 (Second Year of Middle School) – Correct Response Rate by Item

Items 1–5 assessed students' recognition of the shapes of plane figures, while Items 6–9 examined their understanding of the properties of plane figures. Items 10, 16, and 18–20 focused on geometric proofs. Finally, Items 11–15 and Item 17 assessed students' understanding of inclusion relationships among plane figures.

The analysis of the correct response rates revealed that the proof-related items had the lowest success rates. This result is likely attributable to the removal of formal geometric proof from the revised 2009 mathematics curriculum, whereas it had been included in the previous curriculum.

3.3.4. *Grade 11 (Second Year of High School).*

Level	Male	Female	Total
Level 0	7 (6.7%)	13 (9.4%)	20 (11.1%)
Level 1	4 (3.8%)	17 (12.3%)	21 (11.7%)
Level 2	3 (2.9%)	12 (8.7%)	15 (8.3%)
Level 3	33 (31.7%)	55 (39.9%)	88 (48.9%)
Level 4	5 (4.8%)	8 (5.8%)	13 (7.2%)
Level 5	18 (17.3%)	5 (3.6%)	23 (12.8%)
Total	70 (67.3%)	110 (79.7%)	180 (100%)

Table 12. Grade 11 (Second Year of High School) – Fitter Group

Level	Male	Female	Total
Quasi-Level 2	2 (1.9%)	7 (5.1%)	9 (14.5%)
Quasi-Level 3	10 (9.6%)	11 (8.0%)	21 (33.9%)
Quasi-Level 4	4 (3.8%)	1 (0.7%)	5 (8.1%)
Quasi-Level 5	18 (17.3%)	9 (6.5%)	27 (43.5%)
Total	34 (32.7%)	28 (20.3%)	62 (100%)

Table 13. Grade 11 (Second Year of High School) – Non-fitter Group

Among the 242 Grade 11 (second-year high school) students analyzed, 180 were classified as belonging to the fitter group and 62 to the non-fitter group. The highest expected level of geometric thinking for Grade 11 students is Level 5.

Since the geometry test was administered before the students had completed the Grade 11 curriculum, it was expected that relatively few students would reach Level 5. However, in the fitter group, 12.8% of the students attained Level 5, a proportion comparable to those of the other levels except Level 3. This finding suggests that a considerable number of students had engaged in advanced learning through private education beyond the regular school curriculum.

In particular, Quasi-Level 5 was the most common classification in the non-fitter group. This suggests that many of these students focused on accelerated learning through private education rather than progressing through the Van Hiele levels sequentially via conceptual understanding, as intended in formal school instruction.

Item	Correct Rate	Item	Correct Rate
1	96.3%	14	68.6%
2	88.0%	15	76.0%
3	93.4%	16	40.9%
4	83.1%	17	60.3%
5	81.0%	18	48.8%
6	86.8%	19	22.3%
7	90.5%	20	38.8%
8	70.2%	21	50.0%
9	93.0%	22	37.2%
10	59.5%	23	41.3%
11	80.6%	24	23.6%
12	78.9%	25	54.5%
13	84.7%		

Table 14. Grade 11 (Second Year of Middle School) – Correct Response Rate by Item

Items 1–5 assessed students' recognition of the shapes of plane figures, while Items 6–9 examined their understanding of the properties of plane figures. Items 10, 16, and 18–20 focused on geometric proofs. Items 11–15 and Item 17 assessed students' understanding of inclusion relationships among plane figures. Finally, Items 21–25 assessed students' understanding of propositions and logical reasoning. The analysis of the correct response rates revealed that, as was also observed among the Grade 8 (second-year middle school) students, the proof-related items had the lowest correct response rates. However, compared with the Grade 8 students, the correct response rates for Items 10 and 16 increased by approximately 13 and 16 percentage points, respectively. This improvement is likely attributable to the fact that formal geometric proofs, which were omitted from the middle school curriculum, are introduced in the high school mathematics curriculum.

3.4. **Questionnaire Analysis.**

3.4.1. *Reliability Analysis.*

Factor	Self-concept	Attitude	Study Habits	Geometry Classes
Cronbach's α	.935	.936	.913	.960
N of Items	11	15	14	20

Table 15. Reliability and Number of Items for Affective Factors and Geometry Classes – Grade 8 (Second Year of Middle School)

The reliability analysis for the Grade 8 (second-year middle school) students showed that, among the four domains, the perception (satisfaction) of geometry classes had the highest reliability, with a Cronbach's α of .960, whereas study habits had the lowest reliability, with a Cronbach's α of .913. Since the reliability coefficients for all four domains exceeded .75, the questionnaire was considered sufficiently reliable, and the collected data were regarded as meaningful for subsequent analyses.

Factor	Self-concept	Attitude	Study Habits	Geometry Classes
Cronbach's α	.919	.928	.874	.959
N of Items	11	15	14	20

Table 16. Reliability and Number of Items for Affective Factors and Geometry Classes – Grade 11 (Second Year of High School)

The reliability analysis for the Grade 11 (second-year high school) students showed that, among the four domains, the perception (satisfaction) of geometry classes had the highest reliability, with a Cronbach's α of .959, whereas study habits had the lowest reliability, with a Cronbach's α of .874. Since the reliability coefficients for all four domains exceeded .75, the questionnaire was considered sufficiently reliable, and the collected data were regarded as meaningful for further analysis.

3.4.2. *Frequency Analysis.*

a. Frequency Analysis of Self-concept Items

	Frequency	Percentage	Cumulative Percentage
Strongly Agree	208	16%	16%
Agree	281	21%	37%
Neutral	448	34%	70%
Disagree	250	19%	89%
Strongly Disagree	150	11%	100%
Total	1337	100%	

Table 17. Frequency Analysis of Self-concept – Grade 8 (Second Year of Middle School)

Among the Grade 8 (second-year middle school) students, 37% demonstrated a positive mathematical self-concept, whereas 30% showed a negative mathematical self-concept. Therefore, students with a positive self-concept outnumbered those with a negative one.

	Frequency	Percentage	Cumulative Percentage
Strongly Agree	179	8%	8%
Agree	508	22%	30%
Neutral	749	32%	62%
Disagree	585	25%	88%
Strongly Disagree	287	12%	100%
Total	2308	100%	

Table 18. Frequency Analysis of Self-concept – Grade 11 (Second Year of High School)

Among the Grade 11 (second-year high school) students, 38% exhibited a positive mathematical self-concept, while 37% exhibited a negative mathematical self-concept. Although the difference was small, students with a positive self-concept slightly outnumbered those with a negative one.

b. Frequency Analysis of Attitude Items

	Frequency	Percentage	Cumulative Percentage
Strongly Agree	363	20%	20%
Agree	420	23%	43%
Neutral	560	31%	73%
Disagree	319	17%	91%
Strongly Disagree	166	9%	100%
Total	1828	100%	

Table 19. Frequency Analysis of Attitude – Grade 8 (Second Year of Middle School)

Among the Grade 8 (second-year middle school) students, 43% demonstrated a positive attitude toward mathematics, whereas 26% demonstrated a negative attitude. Thus, students with a positive attitude toward mathematics outnumbered those with a negative attitude.

	Frequency	Percentage	Cumulative Percentage
Strongly Agree	641	20%	20%
Agree	1024	33%	53%
Neutral	821	26%	79%
Disagree	424	13%	93%
Strongly Disagree	234	7%	100%
Total	3144	100%	

Table 20. Frequency Analysis of Attitude – Grade 11 (Second Year of High School)

Among the Grade 11 (second-year high school) students, 53% exhibited a positive attitude toward mathematics, indicating that slightly more than half of the students held favorable attitudes. In contrast, only 20% demonstrated a negative attitude toward mathematics. Overall, students with positive attitudes toward mathematics clearly outnumbered those with negative attitudes.

c. Frequency Analysis of Learning Habit Items

	Frequency	Percentage	Cumulative Percentage
Strongly Agree	253	15%	15%
Agree	353	21%	36%
Neutral	600	35%	71%
Disagree	370	22%	93%
Strongly Disagree	127	7%	100%
Total	1703	100%	

Table 21. Frequency Analysis of Learning Habits – Grade 8 (Second Year of Middle School)

Among Grade 8 (second-year middle school) students, 36% showed positive learning habits, whereas 29% showed negative learning habits. These results indicate that students with positive learning habits outnumber those with negative learning habits.

	Frequency	Percentage	Cumulative Percentage
Strongly Agree	340	12%	12%
Agree	813	28%	39%
Neutral	987	34%	73%
Disagree	565	19%	92%
Strongly Disagree	227	8%	100%
Total	2932	100%	

TABLE 22. Frequency Analysis of Learning Habits – Grade 11 (Second Year of High School)

Among Grade 11 (second-year high school) students, 40% demonstrated positive learning habits, whereas 27% demonstrated negative learning habits. Therefore, students with positive learning habits outnumber those with negative learning habits.

d. Frequency Analysis of Geometry Class Perception Items

	Frequency	Percentage	Cumulative Percentage
Strongly Agree	291	12%	12%
Agree	495	20%	32%
Neutral	922	38%	70%
Disagree	501	21%	91%
Strongly Disagree	219	9%	100%
Total	2428	100%	

TABLE 23. Frequency Analysis of Perceptions of Geometry Classes – Grade 8 (Second Year of Middle School)

Among Grade 8 (second-year middle school) students, 32% held positive perceptions of geometry classes, whereas 30% held negative perceptions. These results indicate that students with positive perceptions of geometry classes slightly outnumber those with negative perceptions.

	Frequency	Percentage	Cumulative Percentage
Strongly Agree	400	10%	10%
Agree	984	23%	33%
Neutral	1703	41%	74%
Disagree	737	18%	91%
Strongly Disagree	364	9%	100%
Total	4188	100%	

TABLE 24. Frequency Analysis of Perceptions of Geometry Classes – Grade 11 (Second Year of High School)

Among Grade 11 (second-year high school) students, 33% held positive perceptions of geometry classes, whereas 27% held negative perceptions. Therefore, students with positive perceptions of geometry classes outnumber those with negative perceptions. Overall, the results indicate that both Grade 8 (second-year middle school) and Grade 11 (second-year high school) students generally exhibit positive tendencies across all measured domains.

3.4.3. *Correlation Analysis.* Correlation analysis was conducted to investigate how mathematical self-concept, attitude toward mathematics, and study habits influence students' perceptions of geometry classes among Grade 8 (second year of middle school) and Grade 11 (second year of high school) students. The results of the item-by-item analysis are as follows.

(1) Correlation Analysis between Self-Concept and Perception of Geometry Classes

	Geometry Class			Geometry Class	
Study Habit 1	Correlation Coefficient	.283**	Study Habit 8	Correlation Coefficient	.517**
	P	.002		P	.000
	N	122		N	122
Study Habit 2	Correlation Coefficient	.399**	Study Habit 9	Correlation Coefficient	.404**
	P	.000		P	.000
	N	122		N	122
Study Habit 3	Correlation Coefficient	.301**	Study Habit 10	Correlation Coefficient	.543**
	P	.001		P	.000
	N	122		N	122
Study Habit 4	Correlation Coefficient	.603**	Study Habit 11	Correlation Coefficient	.610**
	P	.000		P	.000
	N	122		N	122
Study Habit 5	Correlation Coefficient	.640**	Study Habit 12	Correlation Coefficient	.295**
	P	.000		P	.001
	N	122		N	122
Study Habit 6	Correlation Coefficient	.395**	Study Habit 13	Correlation Coefficient	.236**
	P	.000		P	.009
	N	122		N	122
Study Habit 7	Correlation Coefficient	.528**	Study Habit 14	Correlation Coefficient	.473**
	P	.000		P	.000
	N	122		N	122

Table 25. Correlation between Study Habits and Perceptions of Geometry Classes (Grade 8) (**$p < .01$, *$p < .05$)

The table above presents the correlation between mathematical self-concept and perceptions of geometry classes among Grade 8 (second year of middle school) students. The correlation coefficients for each item were .488, .438, .460, .501, .486, .417, .465, .481, .189, −.033, and .533, respectively. Overall, mathematical self-concept showed a positive correlation with perceptions of geometry classes. This suggests that students with a higher level of mathematical self-concept are more likely to have positive perceptions of geometry classes.

	Geometry Class			Geometry Class	
Self-Concept1	Correlation Coefficient	.461**	Self-Concept7	Correlation Coefficient	.473**
	P	.000		P	.000
	N	210		N	210
Self-Concept2	Correlation Coefficient	.326**	Self-Concept8	Correlation Coefficient	.473**
	P	.000		P	.000
	N	210		N	210
Self-Concept3	Correlation Coefficient	.518**	Self-Concept9	Correlation Coefficient	.419**
	P	.000		P	.000
	N	210		N	210
Self-Concept4	Correlation Coefficient	.396**	Self-Concept10	Correlation Coefficient	.050
	P	.000		P	.473
	N	210		N	210
Self-Concept5	Correlation Coefficient	.553**	Self-Concept11	Correlation Coefficient	.466**
	P	.000		P	.000
	N	210		N	210
Self-Concept6	Correlation Coefficient	.381**			
	P	.000			
	N	210			

Table 26. Correlation between Self-Concept and Perception of Geometry Classes (Grade 11) (**p¡.01, *p¡.05)

The table above presents the correlation between mathematical self-concept and perceptions of geometry classes among Grade 11 (second year of high school) students. The correlation coefficients for each item were .461, .326, .518, .396, .553, .381, .473, .473, .419, .050, and .466, respectively. Overall, mathematical self-concept showed a positive correlation with perceptions of geometry classes. This suggests that students with a higher level of mathematical self-concept are more likely to have positive perceptions of geometry classes.

(2) Correlation Analysis between Attitude and Perception of Geometry Classes

	Geometry Class			Geometry Class	
Attitude1	Correlation Coefficient	.591**	Attitude9	Correlation Coefficient	.278**
	P	.000		P	.002
	N	122		N	122
Attitude2	Correlation Coefficient	.565**	Attitude10	Correlation Coefficient	.592**
	P	.000		P	.000
	N	122		N	122
Attitude3	Correlation Coefficient	.622**	Attitude11	Correlation Coefficient	.525**
	P	.000		P	.000
	N	122		N	122
Attitude4	Correlation Coefficient	.582**	Attitude12	Correlation Coefficient	.415**
	P	.000		P	.000
	N	122		N	122
Attitude5	Correlation Coefficient	.422**	Attitude13	Correlation Coefficient	.511**
	P	.000		P	.000
	N	122		N	122
Attitude6	Correlation Coefficient	.287**	Attitude14	Correlation Coefficient	.560**
	P	.001		P	.000
	N	122		N	122
Attitude7	Correlation Coefficient	.408**	Attitude15	Correlation Coefficient	.598**
	P	.000		P	.000
	N	122		N	122
Attitude8	Correlation Coefficient	.523**			
	P	.000			
	N	122			

TABLE 27. Correlation between Attitude and Perception of Geometry Classes (Grade 8) (**p¡.01, *p¡.05)

The table above presents the correlation between students' attitudes toward mathematics and their perceptions of geometry classes among Grade 8 (second year of middle school) students. The correlation coefficients for each item were .591, .565, .622, .582, .422, .287, .408, .523, .278, .592, .525, .415, .511, .560, and .598, respectively. Overall, students' attitudes toward mathematics showed a positive correlation with their perceptions of geometry classes. This suggests that students with more positive attitudes toward mathematics are more likely to have favorable perceptions of geometry classes.

	Geometry Class			Geometry Class	
Attitude1	Correlation Coefficient	.572**	Attitude9	Correlation Coefficient	.255**
	P	.000		P	.000
	N	210		N	210
Attitude2	Correlation Coefficient	.529**	Attitude10	Correlation Coefficient	.530**
	P	.000		P	.000
	N	210		N	210
Attitude3	Correlation Coefficient	.577**	Attitude11	Correlation Coefficient	.495**
	P	.000		P	.000
	N	210		N	210
Attitude4	Correlation Coefficient	.498**	Attitude12	Correlation Coefficient	.400**
	P	.000		P	.000
	N	210		N	210
Attitude5	Correlation Coefficient	.289**	Attitude13	Correlation Coefficient	.636**
	P	.000		P	.000
	N	210		N	210
Attitude6	Correlation Coefficient	.296**	Attitude14	Correlation Coefficient	.371**
	P	.000		P	.000
	N	210		N	210
Attitude7	Correlation Coefficient	.525**	Attitude15	Correlation Coefficient	.371**
	P	.000		P	.000
	N	210		N	210
Attitude8	Correlation Coefficient	.493**			
	P	.000			
	N	210			

Table 28. Correlation between Attitude and Perception of Geometry Classes (Grade 11) (**p¡.01, *p¡.05)

The table above presents the correlation between students' attitudes toward mathematics and their perceptions of geometry classes among Grade 11 (second year of high school) students. The correlation coefficients for each item were .572, .529, .577, .498, .289, .296, .525, .493, .255, .530, .495, .400, .636, .371, and .371, respectively. Overall, students' attitudes toward mathematics showed a positive correlation with their perceptions of geometry classes. This suggests that students with more positive attitudes toward mathematics are more likely to have favorable perceptions of geometry classes.

(3) Correlation Analysis between Study Habits and Perceptions of Geometry Classes

	Geometry Class			Geometry Class	
Study Habit 1	Correlation Coefficient	.283**	Study Habit 8	Correlation Coefficient	.517**
	P	.002		P	.000
	N	122		N	122
Study Habit 2	Correlation Coefficient	.399**	Study Habit 9	Correlation Coefficient	.404**
	P	.000		P	.000
	N	122		N	122
Study Habit 3	Correlation Coefficient	.301**	Study Habit 10	Correlation Coefficient	.543**
	P	.001		P	.000
	N	122		N	122
Study Habit 4	Correlation Coefficient	.603**	Study Habit 11	Correlation Coefficient	.610**
	P	.000		P	.000
	N	122		N	122
Study Habit 5	Correlation Coefficient	.640**	Study Habit 12	Correlation Coefficient	.295**
	P	.000		P	.001
	N	122		N	122
Study Habit 6	Correlation Coefficient	.395**	Study Habit 13	Correlation Coefficient	.236**
	P	.000		P	.009
	N	122		N	122
Study Habit 7	Correlation Coefficient	.528**	Study Habit 14	Correlation Coefficient	.473**
	P	.000		P	.000
	N	122		N	122

TABLE 29. Correlation between Study Habits and Perceptions of Geometry Classes (Grade 8) (**p¡.01, *p¡.05)

The table above presents the correlation between mathematics study habits and perceptions of geometry classes among Grade 8 (second-year middle school) students. The correlation coefficients for the individual items are .283, .399, .301, .603, .640, .395, .528, .517, .404, .543, .610, .295, .236, and .473, respectively. Therefore, mathematics study habits and perceptions of geometry classes are generally positively correlated. This suggests that students with better mathematics study habits are more likely to have positive perceptions of geometry classes.

	Geometry Class			Geometry Class	
Study Habit 1	Correlation Coefficient	.276**	Study Habit 8	Correlation Coefficient	.425**
	P	.000		P	.000
	N	210		N	210
Study Habit 2	Correlation Coefficient	.382**	Study Habit 9	Correlation Coefficient	.420**
	P	.000		P	.000
	N	210		N	210
Study Habit 3	Correlation Coefficient	.140*	Study Habit 10	Correlation Coefficient	.484**
	P	.043		P	.000
	N	210		N	210
Study Habit 4	Correlation Coefficient	.438**	Study Habit 11	Correlation Coefficient	.549**
	P	.000		P	.000
	N	210		N	210
Study Habit 5	Correlation Coefficient	.500**	Study Habit 12	Correlation Coefficient	.170*
	P	.000		P	.014
	N	210		N	210
Study Habit 6	Correlation Coefficient	.193**	Study Habit 13	Correlation Coefficient	.301**
	P	.005		P	.000
	N	210		N	210
Study Habit 7	Correlation Coefficient	.416**	Study Habit 14	Correlation Coefficient	.441**
	P	.000		P	.000
	N	210		N	210

Table 30. Correlation between Study Habits and Perceptions of Geometry Classes (Grade 11) (**p¡.01, *p¡.05)

The table above presents the correlation between mathematics study habits and perceptions of geometry classes among Grade 11 (second-year high school) students. The correlation coefficients for the individual items are .276, .382, .140, .438, .500, .193, .416, .425, .420, .484, .549, .170, .301, and .441, respectively. Therefore, mathematics study habits and perceptions of geometry classes are generally positively correlated. This suggests that students with better mathematics study habits are more likely to have positive perceptions of geometry classes. The correlation analysis indicates that, for both Grade 8 (second-year middle school) and Grade 11 (second-year high school) students, all four affective factors related to mathematics are generally positively correlated with perceptions of geometry classes.

3.4.4. *Analysis of Satisfaction with Geometry Classes.*

Geometry Class 1	M	3.11	Geometry Class 11	M	3.04
	SD	1.12		SD	1.12
	N	122		N	122
Geometry Class 2	M	3.02	Geometry Class 12	M	2.89
	SD	1.04		SD	1.04
	N	122		N	122
Geometry Class 3	M	3.00	Geometry Class 13	M	3.29
	SD	1.11		SD	1.10
	N	122		N	122
Geometry Class 4	M	3.05	Geometry Class 14	M	2.98
	SD	1.11		SD	1.14
	N	122		N	122
Geometry Class 5	M	3.48	Geometry Class 15	M	3.04
	SD	1.08		SD	1.17
	N	122		N	122
Geometry Class 6	M	3.08	Geometry Class 16	M	2.84
	SD	1.06		SD	1.16
	N	122		N	122
Geometry Class 7	M	3.11	Geometry Class 17	M	3.55
	SD	1.05		SD	1.11
	N	122		N	122
Geometry Class 8	M	3.09	Geometry Class 18	M	2.83
	SD	1.11		SD	1.13
	N	122		N	122
Geometry Class 9	M	3.21	Geometry Class 19	M	2.65
	SD	1.12		SD	1.30
	N	122		N	122
Geometry Class 10	M	2.92	Geometry Class 20	M	2.77
	SD	1.10		SD	1.18
	N	122		N	133

TABLE 31. Analysis of Satisfaction with Geometry Classes–Grade 8 (Second-Year Middle School)

Geometry Class 1	M	3.00	Geometry Class 11	M	3.07
	SD	1.08		SD	1.07
	N	210		N	210
Geometry Class 2	M	2.93	Geometry Class 12	M	3.18
	SD	1.05		SD	1.09
	N	210		N	210
Geometry Class 3	M	2.97	Geometry Class 13	M	3.42
	SD	1.03		SD	1.04
	N	210		N	210
Geometry Class 4	M	3.09	Geometry Class 14	M	3.03
	SD	1.06		SD	1.07
	N	210		N	210
Geometry Class 5	M	3.09	Geometry Class 15	M	3.07
	SD	1.07		SD	1.08
	N	210		N	210
Geometry Class 6	M	3.11	Geometry Class 16	M	2.89
	SD	1.01		SD	1.06
	N	210		N	210
Geometry Class 7	M	3.33	Geometry Class 17	M	3.13
	SD	1.02		SD	1.13
	N	210		N	210
Geometry Class 8	M	3.29	Geometry Class 18	M	2.80
	SD	0.97		SD	0.89
	N	210		N	210
Geometry Class 9	M	3.51	Geometry Class 19	M	2.61
	SD	1.07		SD	1.00
	N	210		N	210
Geometry Class 10	M	3.05	Geometry Class 20	M	2.76
	SD	1.12		SD	1.19
	N	210		N	210
Overall Perception of Geometry Classes	M	3.07			
	SD	1.06			
	N	210			

Table 32. Analysis of Satisfaction with Geometry Classes–Grade 11 (Second-Year High School)

Table 31 shows that the average level of satisfaction with geometry classes among Grade 8 (second-year middle school) students was 3.04, indicating a moderate level of satisfaction. Among the survey items, Item 17, “I am not afraid of learning geometry," had the highest mean score of 3.55, followed by Item 5, "I am not intimidated when solving geometry problems," with a mean score of 3.48. These findings indicate that Grade 8 students generally do not have a strong aversion to solving geometry problems. In contrast, Item 19, "Geometry has increased my interest in mathematics," had the lowest mean score of 2.65. This suggests that although students may not dislike geometry, studying geometry itself does not necessarily increase their interest in mathematics as a whole.

Table 32 shows that the average level of satisfaction with geometry classes among Grade 11 (second-year high school) students was 3.07, also indicating a moderate level of satisfaction. Item 9, "Geometry helps me think about mathematics from a wider variety of perspectives," received the highest mean score of 3.51, while Item 13, "I believe geometry is worth learning in the future," had the second-highest mean score of 3.42. These results suggest that students recognize geometry as an important subject that promotes diverse mathematical thinking and perceive it as worthwhile to study. In contrast, Item 19, "Geometry has increased my interest in mathematics," had the lowest mean score of 2.61, indicating that learning geometry does not necessarily enhance students' overall interest in mathematics.

Overall, both Grade 8 (second-year middle school) and Grade 11 (second-year high school) students recognize the importance of geometry classes. However, this recognition does not appear to translate into greater intrinsic interest in geometry classes or increased motivation and interest in mathematics as a whole.

4. Conclusion

This study investigated the mathematical attitudes of Grade 1 and Grade 2 (elementary school), Grade 8 (second year of middle school), and Grade 11 (second year of high school) students through a questionnaire survey. In addition, the students' levels of geometric thinking were assessed using the Van Hiele Geometry Test developed by Usiskin (1982) as part of the Chicago Project. Based on these results, the following analyses were conducted.

(1) To investigate the mathematical attitudes and perceptions of geometry among Grade 1 and Grade 2 (elementary school), Grade 8 (second year of middle school), and Grade 11 (second year of high school) students.

(2) To analyze students' achievement levels in geometry and their levels of geometric thinking based on the Van Hiele Geometry Test.
(3) To analyze differences in students' achievement levels in geometry according to grade level and gender, and to examine the distribution of Van Hiele levels of geometric thinking.
(4) To investigate the relationship between students' mathematical attitudes, their perceptions of geometry, and their levels of geometric thinking.
(5) To examine the geometry-related contents of the current 2009 Revised Mathematics Curriculum and classify them according to the Van Hiele levels of geometric thinking.

The questionnaire was designed with a particular emphasis on students' attitudes toward geometry. The results of the Van Hiele Geometry Test were statistically analyzed by classifying students into the fitter and non-fitter groups and calculating their percentages. The questionnaire responses were categorized according to the domains of mathematical attitudes, and correlation analyses were conducted among these domains. The participants consisted of 146 Grade 1 (first year of elementary school) students, 170 Grade 2 (second year of elementary school) students, 122 Grade 8 (second year of middle school) students, and 242 Grade 11 (second year of high school) students. However, Grade 1 and Grade 2 students were excluded from the questionnaire survey. Based on the findings of this study, the following conclusions were drawn.

(1) Mathematical self-concept, attitude toward mathematics, and study habits all showed positive correlations with perceptions of geometry classes. This indicates that students with higher mathematical self-concept, more positive attitudes toward mathematics, and better study habits tend to have more positive perceptions of geometry classes.
(2) The analysis of satisfaction with geometry classes revealed that both Grade 8 (second year of middle school) and Grade 11 (second year of high school) students generally recognized the importance of geometry classes. However, this recognition did not necessarily lead to voluntary interest in geometry classes or increased interest in mathematics as a whole.
(3) The analysis of the 2009 Revised Mathematics Curriculum showed that, for Grade 1 and Grade 2 (elementary school), where the geometry test was

administered in this study, most instructional content focuses on recognizing the shapes of geometric figures. Although learning about the components of geometric figures after recognizing their shapes corresponds to Level 2, the majority of the content concerns identifying shapes. Therefore, most students appeared to be at Van Hiele Level 0.

(4) For Grade 8 (second year of middle school), the curriculum covers the properties of geometric figures and similarity, which mostly correspond to Van Hiele Level 3. Therefore, it was expected that most students would be at Level 2 unless they had received advanced instruction. However, the largest proportion of students was found at Level 3, suggesting that many students had engaged in advanced learning prior to formal instruction.

(5) For Grade 11 (second year of high school), the curriculum mainly deals with coordinate geometry and equations of geometric figures, which largely correspond to Van Hiele Level 4. Therefore, it was expected that no students would reach Level 5 unless they had thoroughly mastered the preceding levels through sequential learning. Although the largest proportion of students was indeed at Level 3, as expected, the proportion of students at Level 5 was not substantially different from those at the other levels (excluding Level 3). This suggests that a considerable number of students had received advanced instruction through private education in addition to their regular school education.

In addition to the fitter group, which demonstrated sequential developmental progress, students in the non-fitter group, who did not exhibit such sequential development, are also expected to improve their levels of geometric thinking if their deficiencies are appropriately addressed. Therefore, students in the non-fitter group should not necessarily be regarded as having low levels of geometric thinking.

Furthermore, the Van Hiele Geometry Test proposed by Usiskin revealed that Grade 8 (second year of middle school) students demonstrated relatively weak abilities in constructing geometric proofs. Although the 2009 Revised Mathematics Curriculum reduced students' burden by omitting formal geometric proof, the findings of this study suggest that instruction on geometric proof should be reintroduced into the middle school curriculum.

References

[1] 교육과학기술부 (2011):「수학과 교육과정 」, 교육과학기술부 고시 제2011-361호.

[2] 교육부 (2000):「중학교 교육 과정 해설 」, (주)대한 교과서.

[3] 김남희 (1999):「van Hiele 이론을 기초로 한 중학교 기하학습에 관한 연구」, 서강대학교 교육대학원 석사학위논문.

[4] 김남희 외 5인(2006), 수학교육과정과 교재연구, 경문사

[5] 김량군(2010), 중학교 수학과 기하영역에서의 반 힐레 수준 분석과 교수 학습 지도 방안, 아주대학교 교육대학원 석사학위논문.

[6] 김미경(1993), VAN HIELE 이론에 의한 중학생들의 기하적 사고 수준에 관한 연구, 이화여자대학교 교육대학원 석사학위논문.

[7] 김미희 (1994):「van Hiele 이론을 기초로 한 교과서 기하내용의 연계성 분석」, 연세대학교 교육대학원 석사학위논문.

[8] 김효정 외 4인 (1993):「van Hiele 이론에 근거한 우리 나라 중학생의 기하 사고수준 고찰.」,대한수학교육학회.

[9] 김혜민(2008), 함수에 대학 학습수준이 함수 성취도에 미치는 영향-반힐레의 기하학습 수준이론 적용-, 아주대학교 교육대학원 석사학위논문.

[10] 문지혜(2010), 중학교 학생들의 van Hiele 수준을 통한 효과적인 기하교육방법 연구, 중앙대학교 교육대학원 석사학위논문.

[11] 박지혜 (2000):「van Hiele 이론에 의한 중학생들의 기하 인지 수준과 교재 선정에 관한 연구」, 연세대학교 교육대학원 석사학위 논문.

[12] 백은자 (2006):「초등수학에서 유시스킨의 반힐레 수준검사지의 문제점 분석 및 개선 연구」, 전주교육대학교 교육대학원 석사학위 논문.

[13] 신진수(2008), Van Hiele 이론에 기초한 기하영역 분석 및 지도 방안 고찰-중학교 기하 영역을 중심으로, 아주대학교 교육대학원 석사학위논문.

[14] 양규모 (2002):「van Hiele 이론에 근거한 도형학습 수준 분석과 자료 개발에 관한 연구」, 부산교육대학교 교육대학원 석사학위 논문.

[15] 우정호 (1999):「학교 수학의 교육적 기초」, 서울대학교 출판부.

[16] 우정호 (1986):「Van Hiele의 수학학습 수준이론에 대한 소고」, 서울대학교 사범대학 논총 제33집.

[17] 우정호 (2000):「수학학습-지도 원리와 방법」, 서울대학교출판부.

[18] 이금주 (2007):「Van Hiele 이론에 기초한 교과서 분석과 효과적인 기하 학습에 관한 연구」, 중앙대학교 교육대학원 석사학위논문.

[19] 이소진 (2001):「V반 힐레 모형에 따른 교과서의 재구성 및 그에 따른 학습효과」, 충북대학교 교육대학원 석사학위논문.

[20] 이영웅(2012), Van Hiele 기하수준이론을 적용한 중학교 기하영역 지도방법에 관한 연구, 전남대학교 교육대학원 석사학위논문.

[21] 이중권 (2006):「van Hiele의 기하 인지발달이론에 따른 중학교 기하교육과정 및 우리나라 중학생들의 기하수준에 관한 연구. 한국교육문제연구 제17집」, 동국대학교 교육연구원.

[22] 이창연(2010), van Hiele 이론과 GSP를 활용한 중학교 기하영역에 관한 연구-8-나 단계의 사각형의 성질을 중심으로-, 한국수학교육학회지 시리즈 A 제 49권 제 1호 pp.85 ~109.

[23] 이택근(2010), van Hiele의 기하수준에 따른 GSP 활용에서 학생들의 기하 학습 과정에 관한 연구-8-나 여러 가지 삼각형-, 단국대학교 교육대학원 석사학위논문.
[24] 최민정(2014), 수학 학습부진아의 반힐레 기하수준 판별을 통한 기하 학습지도 방법에 관한 연구, 전북대학교 교육대학원 석사학위논문.
[25] 최현호 (1990):「van Hiele의 기하인지 발달이론과 증명능력에 관한 기초 연구」, 연세대학교 교육대학원 석사학위논문.
[26] 최혜정 (1990):「van Hiele 이론을 통한 기하학의 개념이해 및 문제풀이 연구」, 이화여자대학교 교육대학원 석사학위논문.
[27] 한규태(2007), 중학교 기하영역에 관한 연구-Van Hiele 이론을 중심으로, 한양대학교 교육대학원 석사학위논문.
[28] 한태식 (1995):「van Hiele 이론에 대한 대표적 연구의 비교 」, 대한 수학교육학회 논문집 제 5권 제1호.
[29] 황선욱 외 10인(2013), 중학교 교과서 수학 ①, 수학 ②, 수학 ③, (주) 좋은책신사고
[30] 황혜정 외 5인(2007), 수학교육학신론, 문음사.
[31] 황혜정, 나귀수, 최승현, 박경미, 임재훈, 서동엽 (2012):「 수학교육학신론 」, 문음사.
[32] Usiskin(1982), Van Hiele levels and achievement in Secondary School Geometry: final Report of CDASSG, University of Chicago.

Appendix A: Mathematics Attitude Questionnaire

Item No.	Statement	Strongly Disagree	Disagree	Neutral	Agree	Strongly Agree
1	Mathematics is easy for me.	①	②	③	④	⑤
2	I enjoy studying mathematics.	①	②	③	④	⑤
3	I often think about other things during mathematics class.	①	②	③	④	⑤
4	I can be praised because I do well in mathematics.	①	②	③	④	⑤
5	I want to learn more about mathematics.	①	②	③	④	⑤
6	I always preview mathematics lessons.	①	②	③	④	⑤
7	I want to apply what I learn in mathematics class.	①	②	③	④	⑤
8	I study mathematics hard only during exam periods.	①	②	③	④	⑤
9	I think I have a talent for mathematics.	①	②	③	④	⑤
10	The harder I study mathematics, the more enjoyable it becomes.	①	②	③	④	⑤
11	I think my mathematics teacher recognizes my ability.	①	②	③	④	⑤
12	I am confident that I can do well in mathematics.	①	②	③	④	⑤
13	When mathematics class is over, I often do not know what I have learned.	①	②	③	④	⑤
14	I study mathematics well on my own without being told.	①	②	③	④	⑤
15	After taking a mathematics test, I want to know my score as soon as possible.	①	②	③	④	⑤
16	After mathematics class, I organize in my mind what I learned.	①	②	③	④	⑤
17	I think I am a good mathematics student.	①	②	③	④	⑤
18	Mathematics class is boring.	①	②	③	④	⑤
19	I do not fool around with other students during mathematics class.	①	②	③	④	⑤
20	I can get good grades on mathematics tests.	①	②	③	④	⑤

Item No.	Statement	Strongly Disagree	Disagree	Neutral	Agree	Strongly Agree
21	Mathematics is an essential subject for my future studies.	①	②	③	④	⑤
22	I always review what I learned in mathematics class.	①	②	③	④	⑤
23	I think it is enough to study mathematics only enough to avoid being scolded by the teacher.	①	②	③	④	⑤
24	I make sure I fully understand what I learned in mathematics class before moving on.	①	②	③	④	⑤
25	I am good at mathematics.	①	②	③	④	⑤
26	I look forward to mathematics class.	①	②	③	④	⑤
27	I sit properly and study attentively during mathematics class.	①	②	③	④	⑤
28	I am not good at mathematics.	①	②	③	④	⑤
29	I would like to study mathematics more.	①	②	③	④	⑤
30	I enjoy answering questions during mathematics class.	①	②	③	④	⑤
31	I want to do better in mathematics than other students.	①	②	③	④	⑤
32	Once I start studying mathematics, I work hard until I finish.	①	②	③	④	⑤
33	I think there are many things in mathematics that I do not know.	①	②	③	④	⑤
34	I wish there were more mathematics classes.	①	②	③	④	⑤
35	I often do not notice when mathematics class is over.	①	②	③	④	⑤
36	I believe I can achieve good grades in mathematics in the future.	①	②	③	④	⑤
37	I intend to study mathematics harder than I do now.	①	②	③	④	⑤
38	Even if I do not understand something in mathematics class, I usually do not ask questions.	①	②	③	④	⑤
39	I try to make study plans to improve my mathematics achievement.	①	②	③	④	⑤
40	I summarize the important points when studying mathematics.	①	②	③	④	⑤

Appendix B: Geometry Perception Questionnaire

Item No.	Statement	Strongly Disagree	Disagree	Neutral	Agree	Strongly Agree
41	Geometry is more interesting than other areas of mathematics.	①	②	③	④	⑤
42	Geometry increases my interest in mathematics.	①	②	③	④	⑤
43	I can concentrate better on geometry than on other areas of mathematics.	①	②	③	④	⑤
44	Geometry lessons are more effective for understanding other mathematical concepts.	①	②	③	④	⑤
45	I enjoy solving geometry problems.	①	②	③	④	⑤
46	Geometry classes help me understand mathematics more quickly.	①	②	③	④	⑤
47	Geometry helps me solve problems in other areas of mathematics.	①	②	③	④	⑤
48	Studying geometry improves my learning ability.	①	②	③	④	⑤
49	Geometry helps me think about mathematics from multiple perspectives.	①	②	③	④	⑤
50	I would recommend studying geometry to other students.	①	②	③	④	⑤
51	I would like to learn more about geometry.	①	②	③	④	⑤
52	I would encourage younger students to study geometry.	①	②	③	④	⑤
53	I believe geometry is worth learning in the future as well.	①	②	③	④	⑤
54	Geometry classes have made me realize the importance of mathematics.	①	②	③	④	⑤
55	I enjoy the process of solving geometry problems.	①	②	③	④	⑤
56	Geometry increases my motivation to learn.	①	②	③	④	⑤
57	I am not afraid of learning geometry.	①	②	③	④	⑤
58	I always enjoy geometry classes at school.	①	②	③	④	⑤
59	Geometry has increased my interest in mathematics.	①	②	③	④	⑤
60	I have applied geometry to objects and situations in everyday life.	①	②	③	④	⑤

Appendix C: Van Hiele Geometry Test for Grade 11 (High School, Grade 2)

고등학교 시험지

1–3학년 **반힐레 기하 영역**

'가' 형 | 성명 | 수험 번호 | *1*

- 자신이 선택한 학년의 문제지인지 확인하시오.
- 문제지의 해당란에 성명과 수험 번호를 정확히 쓰시오.
- 답안지의 해당란에 성명과 수험 번호를 쓰고, 또 수험 번호와 답을 정확히 표시하시오.
- 이 시험은 25 문항으로 이루어져 있습니다. 모르는 문항이 있을 수도 있습니다.
- 각 문항을 주의 깊게 읽으시오.
- 각 문항의 답을 생각해 본 후 각자 나눠준 답지의 해당 문항에 맞춰 답을 적으시오. 모든 문항의 답은 1개입니다.
- 그림을 그려야 하는 경우에는 제공된 답지의 빈 공간을 활용하시오.
- 답지에 기입한 답을 바꾸고 싶은 경우, 처음 기입한 답을 확실히 지우고 작성하시오.
- 시험 시간은 35분입니다. 교사가 시작하라고 할 때까지 기다리시오.

1. 다음 중 어떤 도형이 정사각형인가?

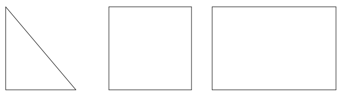

(1) (2) (3)

① (1)만 정사각형이다. ② (2)만 정사각형이다. ③ (3)만 정사각형이다.
④ (2)과 (3)만 정사각형이다. ⑤ 모두 정사각형이다.

2. 다음 중 어떤 도형이 삼각형인가?

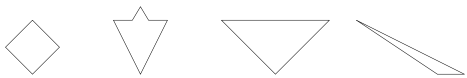

(1) (2) (3) (4)

① 어떤 그림도 삼각형이 아니다. ② (2)만 삼각형이다. ③ (3)만 삼각형이다.
④ (3)과 (4)만 삼각형이다. ⑤ (2)과 (3)만 삼각형이다.

3. 다음 중 어떤 도형이 직사각형인가?

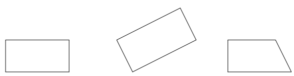

(1) (2) (3)

① (1)만 직사각형이다. ② (2)만 직사각형이다. ③ (1)과 (2)만 직사각형이다.
④ (1)과 (3)만 직사각형이다. ⑤ 세개 모두 직사각형이다.

1/7

Figure 1. Geometry Test for Grade 11 (High School, Grade 2): Page 1

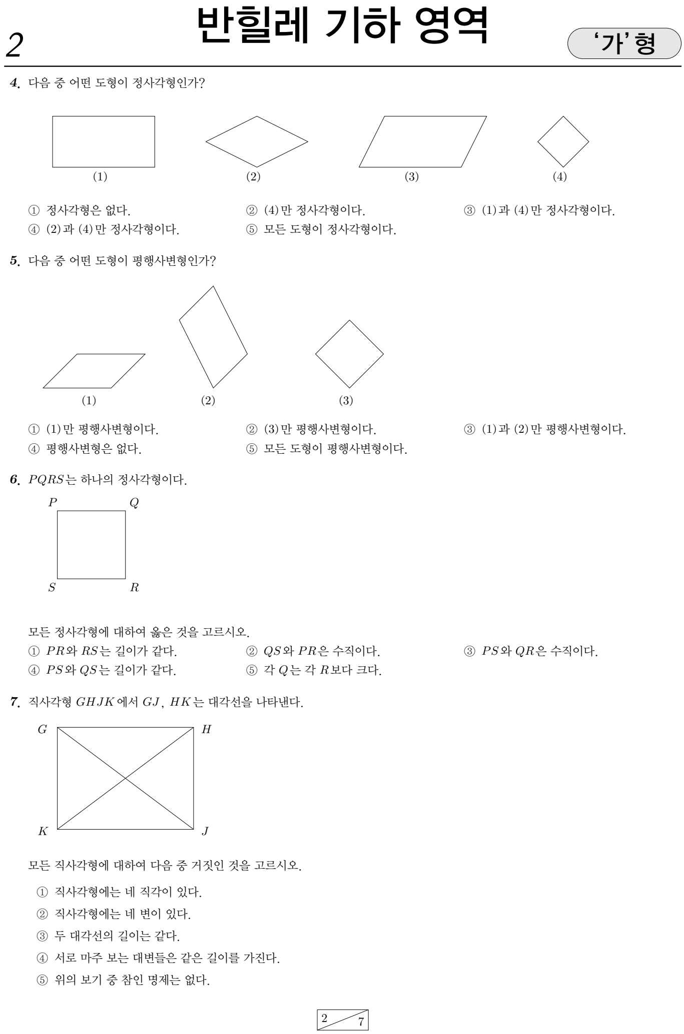

2 반힐레 기하 영역 '가'형

4. 다음 중 어떤 도형이 정사각형인가?

(1) (2) (3) (4)

① 정사각형은 없다. ② (4)만 정사각형이다. ③ (1)과 (4)만 정사각형이다.
④ (2)과 (4)만 정사각형이다. ⑤ 모든 도형이 정사각형이다.

5. 다음 중 어떤 도형이 평행사변형인가?

(1) (2) (3)

① (1)만 평행사변형이다. ② (3)만 평행사변형이다. ③ (1)과 (2)만 평행사변형이다.
④ 평행사변형은 없다. ⑤ 모든 도형이 평행사변형이다.

6. $PQRS$는 하나의 정사각형이다.

P Q S R

모든 정사각형에 대하여 옳은 것을 고르시오.
① PR와 RS는 길이가 같다. ② QS와 PR은 수직이다. ③ PS와 QR은 수직이다.
④ PS와 QS는 길이가 같다. ⑤ 각 Q는 각 R보다 크다.

7. 직사각형 $GHJK$에서 GJ, HK는 대각선을 나타낸다.

G H K J

모든 직사각형에 대하여 다음 중 거짓인 것을 고르시오.

① 직사각형에는 네 직각이 있다.
② 직사각형에는 네 변이 있다.
③ 두 대각선의 길이는 같다.
④ 서로 마주 보는 대변들은 같은 길이를 가진다.
⑤ 위의 보기 중 참인 명제는 없다.

2 / 7

FIGURE 2. Geometry Test for Grade 11 (High School, Grade 2): Page 2

'가'형

반힐레 기하 영역

3

8. 마름모는 네 변의 길이가 모두 같은 사각형이다.

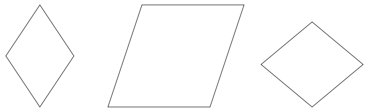

모든 마름모에 대하여 다음 중 거짓인 명제를 고르시오.

① 두 대각선은 같은 길이를 가진다.
② 대각선은 마름모의 각을 이등분한다.
③ 두 대각선은 서로 수직이다.
④ 마주 보는 각들의 크기는 같다.
⑤ 모든 마름모에 대하여 위의 네 명제 중 거짓인 명제가 있다.

9. 이등변삼각형은 두 변의 길이가 같은 삼각형이다. 이등변삼각형의 예들은 아래 그림과 같다.

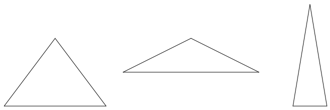

모든 이등변삼각형에 대하여 다음 중 참인 문장을 고르시오.

① 세 변은 반드시 같은 길이를 가진다.
② 한 변은 반드시 다른 변의 길이의 두 배이다.
③ 적어도 두 각의 크기는 반드시 같아야 한다.
④ 세 각이 모두 같아야 한다.
⑤ 이등변삼각형에 대한 위의 네 명제 중 어떤 것도 참이 아니다.

10. 중심이 P, Q인 두 원이 두 점 R과 S에서 만나 다음과 같이 사각형 $PRQS$을 이룬다.
다음 그림과 같이 두 가지 예가 있다.

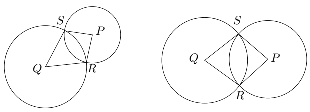

다음 명제 중 항상 참이 아닌 문장은?

① $PRQS$는 같은 길이를 가지는 두 쌍의 변을 가진다.
② $PRQS$는 적어도 두 각이 같은 크기를 가진다.
③ 직선 $\overline{PQ}$과 $\overline{RS}$는 서로 수직이다.
④ 각 P와 Q는 크기가 같다.
⑤ 위의 네 보기 중 참이 아닌 문장은 없다.

3/7

FIGURE 3. Geometry Test for Grade 11 (High School, Grade 2): Page 3

4

반힐레 기하 영역

'가'형

11. 다음과 같은 두 문장에 대하여 옳은 것을 고르시오.

문장 1: 도형 F는 직사각형이다.
문장 2: 도형 F는 삼각형이다.

① 문장 1이 참이면 문장 2가 참이다.
② 문장 1이 거짓이면 문장 2는 참이다.
③ 문장 1과 문장 2가 동시에 참이 될 수 없다.
④ 문장 1과 문장 2가 동시에 거짓이 될 수 없다.
⑤ 위의 네 보기 모두 옳지 않다.

12. 다음 두 문장에 대하여 옳은 것을 고르시오.

문장 S: 삼각형 $\triangle ABC$의 세 변의 길이가 같다.
문장 T: 삼각형 $\triangle ABC$에서 $\angle B$와 $\angle C$의 크기는 같다.

① 문장 S과 문장 T가 동시에 참이 될 수 없다.
② 문장 S가 참이면, 문장 T도 참이다.
③ 문장 T가 참이면, 문장 S도 참이다.
④ 문장 S가 거짓이면, 문장 T도 거짓이다.
⑤ 위의 네 보기 모두 옳지 않다.

13. 다음 도형 중 어떤 것들이 직사각형이라 할 수 있는가?

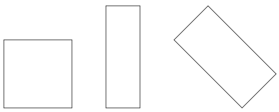

(1) (2) (3)

① 세 도형 모두 직사각형이다. ② (2)만 직사각형이다. ③ (3)만 직사각형이다.
④ (1), (2)만 직사각형이다. ⑤ (2), (3)만 직사각형이다.

14. 어떤 것이 참인지 고르시오.

① 직사각형들이 만족하는 성질들은 정사각형들도 모두 만족한다.
② 정사각형들이 만족하는 성질들은 직사각형들도 모두 만족한다.
③ 직사각형들이 만족하는 성질들은 평행사변형들도 모두 만족한다.
④ 정사각형들이 만족하는 성질들은 평행사변형들도 모두 만족한다.
⑤ 위 네 개 문장들 중 어떤 것도 참이 아니다.

4/7

FIGURE 4. Geometry Test for Grade 11 (High School, Grade 2): Page 4

‘가’형

반힐레 기하 영역

5

15. 다음 중 직사각형들은 만족하지만 평행사변형들은 만족하지 않는 성질은?

① 서로 마주 보는 변들이 같다. ② 두 대각선이 같다. ③ 서로 마주 보는 변들은 평행이다.
④ 서로 마주 보는 각들은 같다. ⑤ 해당 사항 없다.

16. $\triangle ABC$ 는 직각삼각형이고, $\triangle ACE, \triangle ABF, \triangle BCD$ 는 $\triangle ABC$ 의 각 변 위에 만들어진 이등변 삼각형이면 $\overline{AD}, \overline{BE}, \overline{CF}$ 가 공통으로 만나는 점이 있다라고 증명할 수 있다. 이 증명으로부터 우리가 알 수 있는 것은?

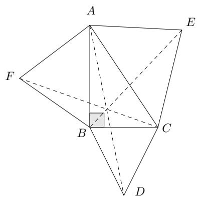

① 위의 그림에 있는 삼각형에 대해서만 $\overline{AD}, \overline{BE}, \overline{CF}$ 가 공통으로 만나는 점이 있다는 것을 확신할 수 있다.
② 모든 직각삼각형에 대해서는 아니고 특별한 직각삼각형에 대해서만 $\overline{AD}, \overline{BE}, \overline{CF}$ 가 공통으로 만나는 점이 있다.
③ 모든 직각삼각형에 대하여 $\overline{AD}, \overline{BE}, \overline{CF}$ 가 공통으로 만나는 점이 있다.
④ 모든 삼각형에 대하여 $\overline{AD}, \overline{BE}, \overline{CF}$ 가 공통으로 만나는 점이 있다.
⑤ 모든 이등변삼각형에 대하여 $\overline{AD}, \overline{BE}, \overline{CF}$ 가 공통으로 만나는 점이 있다.

17. 다음은 어떤 도형이 가지는 세가지 성질이다.

성질 D: 이 도형의 대각선은 같은 길이를 가진다.
성질 S: 이 도형은 정사각형이다.
성질 R: 이 도형은 직사각형이다.

다음 중 어떤 것이 참인가?

① 성질 D를 만족하면 성질 S도 만족하여 성질 R도 만족한다.
② 성질 D를 만족하면 성질 R도 만족하여 성질 S도 만족한다.
③ 성질 S를 만족하면 성질 R도 만족하여 성질 D도 만족한다.
④ 성질 R을 만족하면 성질 D도 만족하여 성질 R도 만족한다.
⑤ 성질 R을 만족하면 성질 S도 만족하여 성질 D도 만족한다.

18. 다음 두 문장에 대하여 옳은 것을 고르시오.

문장 I: 어느 도형이 직사각형이면, 그 대각선은 서로 다른 것을 이등분한다.
문장 II: 어느 도형의 대각선이 서로 다른 것을 이등분하면, 그 도형은 직사각형이다.

① 문장 I이 참임을 증명하려면 문장 II가 참임을 증명하면 된다.
② 문장 II가 참임을 증명하려면 문장 I이 참임을 증명하면 된다.
③ 문장 II가 참임을 증명하려면 대각선이 서로 다른 것을 이등분하는 직사각형을 찾으면 된다.
④ 문장 II가 거짓임을 증명하려면 대각선이 서로 다른 것을 이등분하는 직사각형이 아닌 도형을 찾으면 된다.
⑤ 위의 보기들 모두 옳지 않다.

5/7

FIGURE 5. Geometry Test for Grade 11 (High School, Grade 2): Page 5

6 반힐레 기하 영역 '가'형

19. 기하 영역에 대하여 옳은 것을 고르시오.

① 모든 용어는 정의될 수 있고, 모든 참인 명제는 참이라는 것을 증명할 수 있다.
② 모든 용어는 정의될 수 있지만, 어떤 명제들은 참이라고 가정하는 것이 필요하다.
③ 어떤 용어들은 정의되지 않은 채 남아 있지만, 모든 참인 명제들은 참이라는 것을 증명할 수 있다.
④ 어떤 용어들은 정의되지 않은 채 남아 있지만, 어떤 명제들은 참이라고 가정하는 것이 필요하다.
⑤ 위의 보기들 모두 옳지 않다.

20. 다음 세 명제에 대하여 생각해 보자.

(1) : 같은 직선에 수직인 두 직선은 평행하다.
(2) : 평행한 두 직선 중 어느 하나의 직선과 수직인 직선은 다른 직선과도 수직이다.
(3) : 만약 두 직선이 똑같은 거리에 있다면 이 두직선은 평행하다.

다음과 같이 직선 m과 p가 서로 수직이고, 직선 n과 p도 수직이라고 하자. 직선 m과 n이 평행이라는 결론을 낼 때 사용된 명제는 위의 세 명제 중 어떤 것들인가?

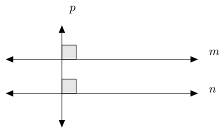

① (1) 명제만　② (2) 명제만　③ (3) 명제만
④ (1) 명제 또는 (2) 명제　⑤ (2) 명제 또는 (3) 명제

21. F-기하에서는 여러분들이 사용해오던 것과는 다르게 정확히 4개의 점과 6개의 직선만 있다. 모든 직선은 정확히 2개의 점만 포함하고 있다. 4개의 점을 P, Q, R, S라 하면 직선들은 다음과 같다.

$$\{P,Q\},\{P,R\},\{P,S\},\{Q,R\},\{Q,S\},\{R,S\}$$

F-기하에서는 두 직선이 만난다와 평행하다를 다음과 같이 정의한다. 두 직선 $\{P,Q\}$와 $\{P,R\}$은 점 P를 공통으로 가지기 때문에 두 직선 $\{P,Q\}$와 $\{P,R\}$은 P에서 만난다라고 정의한다. 또한 두 직선 $\{P,Q\}$와 $\{R,S\}$는 공통으로 가지는 점이 없기 때문에 두 직선 $\{P,Q\}$와 $\{R,S\}$는 평행하다라고 한다.
이와 같은 정보를 이용하면 다음 중 어떤 것이 옳은 것인가?

① $\{P,R\}$와 $\{Q,S\}$는 만난다.
② $\{P,R\}$와 $\{Q,S\}$는 평행하다.
③ $\{Q,R\}$와 $\{R,S\}$는 평행하다.
④ $\{P,S\}$와 $\{Q,R\}$는 만난다.
⑤ 앞의 네 명제 중 어느 것도 참이 아니다.

6/7

FIGURE 6. Geometry Test for Grade 11 (High School, Grade 2): Page 6

‘가’형

반힐레 기하 영역

7

22. 임의의 각을 삼등분하는 것은 각을 똑 같은 크기의 3개의 각으로 나눈다는 것을 의미한다. 1847년에 P.L. Wantzel은 일반적으로 눈금없는 자와 컴퍼스 만을 사용하여서는 임의의 각을 삼등분하는 것이 불가능하다는 것을 증명하였다. 그의 증명으로부터 여러분은 어떤 결론을 낼 수 있는가?

① 일반적으로 눈금없는 자와 컴퍼스 만을 사용하여서는 임의의 각을 이등분하는 것은 불가능하다.
② 일반적으로 눈금이 있는 자와 컴퍼스 만을 사용하여 임의의 각을 삼등분하는 것은 불가능하다.
③ 일반적으로 임의의 작도 도구를 사용하여서 임의의 각을 삼등분하는 것은 불가능하다.
④ 눈금없는 자와 컴퍼스 만을 사용하여 임의의 각을 삼등분하는 일반적인 방법을 어떤 사람이 미래에 찾을 수 있는 것은 여전히 가능하다.
⑤ 눈금없는 자와 컴퍼스 만을 사용하여서는 임의의 각을 삼등분하는 일반적인 방법을 어떤 사람도 발견하는 것이 불가능하다.

23. 어떤 수학자 J가 다음 가정이 참인 기하를 창조하였다.

“삼각형의 세 내각의 합은 180° 보다 작다.”

다음 중 옳은 것을 고르시오.

① J는 삼각형의 각을 측정하는데 실수하였다.
② J는 논리적인 추론에서 실수하였다.
③ J는 참이라는 것의 의미에 대해 잘못 이해하고 있다.
④ J는 보통의 기하에서 가정하고 있는 것과는 다른 가정으로부터 시작하였다.
⑤ 앞의 네 명제 중 어느 것도 참이 아니다.

24. 서로 다른 기하책에서 직사각형을 각각 다른 방법으로 정의하고 있다. 옳은 것을 고르시오.

① 두 권의 책 중 하나의 책은 오류가 있다.
② 두 권의 책 중 어느 하나의 책의 정의는 잘못되었다. 직사각형에 대한 두 개의 서로 다른 정의는 있을 수 없다.
③ 두 책 중 어느 하나의 책의 직사각형의 성질은 다른 책의 직사각형의 성질과 다르다.
④ 어느 한 책의 직사각형은 다른 책의 직사각형과 같은 성질을 갖는다.
⑤ 두 책의 직사각형의 성질들은 다를 수 있다.

25. 만약 여러분이 문장 I과 문장 II를 증명했다고 가정하자.

문장 I : p이면 q이다.
문장 II : s이면 q가 아니다.

문장 I과 문장 II에 대하여 옳은 것을 고르시오.

① p이면 s이다.
② p가 아니면 q가 아니다.
③ p 또는 q이면 s이다.
④ s이면 p가 아니다.
⑤ s가 아니면 p이다.

7 / 7

FIGURE 7. Geometry Test for Grade 11 (High School, Grade 2): Page 7

수험 번호

반 힐레 기하 시험

답지

성명 (한글) ________________ (영문) ________________ 학기 ________________

수학선생님 성함 ____________________ 학교명____________________

학년 : 7 8 9 10 11 12 성별 : 남 여

생년월일 :

시험날짜 :

알맞은 답을 체크하시오.

1.	①	②	③	④	⑤
2.	①	②	③	④	⑤
3.	①	②	③	④	⑤
4.	①	②	③	④	⑤
5.	①	②	③	④	⑤
6.	①	②	③	④	⑤
7.	①	②	③	④	⑤
8.	①	②	③	④	⑤
9.	①	②	③	④	⑤
10.	①	②	③	④	⑤
11.	①	②	③	④	⑤
12.	①	②	③	④	⑤
13.	①	②	③	④	⑤
14.	①	②	③	④	⑤
15.	①	②	③	④	⑤
16.	①	②	③	④	⑤
17.	①	②	③	④	⑤
18.	①	②	③	④	⑤
19.	①	②	③	④	⑤
20.	①	②	③	④	⑤
21.	①	②	③	④	⑤
22.	①	②	③	④	⑤
23.	①	②	③	④	⑤
24.	①	②	③	④	⑤
25.	①	②	③	④	⑤

FIGURE 8. Answer Key for the Van Hiele Geometry Test

J. Basic Sci. HUFS **62** (2026), pp. 99-114

FRENET FORMULA OF NULL AND PSEUDO NULL CURVES IN MINKOWSKI SPACES $\mathbb{R}^{2,1}$ AND $\mathbb{R}^{3,1}$

SUNG-HO PARK*

Abstract. We prove Frenet formula of null or pseudo null curves in 3 or 4 dimensional Minkowski space $\mathbb{R}^{2,1}$ or $\mathbb{R}^{3,1}$. As an application, we classify k-type pseudo null curves in $\mathbb{R}^{2,1}$.

1. Introduction

The Frenet formula is the fundamental concept and the starting point of differential geometry and Riemannian geometry. The Frenet formula for a smooth regular curve $c : I \to \mathbb{R}^3$, with unit tangent vector field T, principal normal vector field N and binormal vector field B, states that

$$\begin{pmatrix} T' \\ N' \\ B' \end{pmatrix} = \begin{pmatrix} 0 & \kappa & 0 \\ -\kappa & 0 & \tau \\ 0 & -\tau & 0 \end{pmatrix} \begin{pmatrix} T \\ N \\ B \end{pmatrix}, \tag{1}$$

where $' = \frac{d}{ds} = \left(1/\left|\frac{dc}{dt}\right|\right)\frac{d}{dt}$ is the differentiation with respect to the arc-length (cf. §2). Note that the Frenet frame field T, N, B can be considered as the Gram-Schmidt orthogonalization of $\frac{dc}{dt}$, $\frac{d^2c}{dt^2}$, $\frac{d^3c}{dt^3}$, and (1) is the orthogonal decomposition of $\{T', N', B'\}$ in terms of the orthonormal basis $\{T, N, B\}$ of $\mathbb{R}^3$. An interesting viewpoint of (1) is that it describes the behavior of the unit vector field T in $\mathbb{R}^3$.

We consider the Frenet formula in the Minkowski space. The $(n+1)$-dimensional Minkowski space $\mathbb{R}^{n,1}$ is $\mathbb{R}^{n+1}$ equipped with the Lorentzian

---

*Professor, Major in Mathematics, Graduate School of Education, Hankuk University of Foreign Studies, Seoul, Republic of Korea. E-mail: sunghopark@hufs.ac.kr
This work was supported by the Research Fund 2026 of Hankuk University of Foreign Studies.

scalar product

$$\langle (x_1,\ldots,x_{n+1}),(y_1,\ldots,y_{n+1})\rangle_L = x_1y_1+\cdots+x_ny_n - x_{n+1}y_{n+1}.$$

A vector $v \in \mathbb{R}^{n,1}$ is said to be

i) spacelike if $\langle v,v\rangle_L > 0$,

ii) timelike if $\langle v,v\rangle_L < 0$,

iii) null or lightlike if $\langle v,v\rangle_L = 0$.

For a vector $v \in \mathbb{R}^{n,1}$, let

$$\|v\|_L = |\langle v,v\rangle_L|^{\frac{1}{2}}.$$

Unlike curves in the Euclidean space $\mathbb{R}^n$, curves ($c : I \to \mathbb{R}^{n,1}$) are classified according to the causal characters of $\frac{d^kc}{dt^k}$. For example, c is spacelike or timelike or lightlike (or null) if $\frac{dc}{dt}$ is spacelike or timelike or null on I respectively. If c is spacelike or timelike, then c can be reparametrized to satisfy $\left\|\frac{dc}{dt}\right\|_L = 1$, said to be parametrized by arc-length.

In the following, we deal with *null* and *pseudo null* curves in $\mathbb{R}^{2,1}$ and $\mathbb{R}^{3,1}$. For a null curve c in $\mathbb{R}^{2,1}$ and $\mathbb{R}^{3,1}$, c'' is either identically null or spacelike. If c'' is identically null, then c' and c'' are collinear (cf. §2). When c'' is spacelike, we assume that c is parametrized to satisfy

$$\langle c'',c''\rangle_L = 1.$$

In this case, c is said to be parametrized by *pseudo arc-length.*

A pseudo null curve is a spacelike curve $c : I \to \mathbb{R}^{n,1}$, assumed to be parametrized by arc-length, that has null c'', or, null principal normal N. Bonnor obtained Frenet formulas of null or pseudo null curves in $\mathbb{R}^{3,1}$ [2, 3]. Walrave prove Frenet formulas for various types of curves in $\mathbb{R}^{2,1}$ and $\mathbb{R}^{3,1}$ including null and pseudo null curves and give interesting applications [9]. There were related researches [1, 4, 5, 6, 8]. But some of the works lack in mathematical details and backgrounds.

In this paper, we give mathematically rigorous and detailed proofs of the Frenet formula of null or pseudo null curves in $\mathbb{R}^{2,1}$ and $\mathbb{R}^{3,1}$. We also give more mathematically rigorous proof of the theorems. Specially, we apply the Frenet formula to classify j-type pseudo null Darboux helix in $\mathbb{R}^{2,1}$.

2. Frenet formula for null curves in $\mathbb{R}^{2,1}$ and $\mathbb{R}^{3,1}$

We start by introducing a new approach for the Frenet formula of a smooth regular curve $c : I \to \mathbb{R}^3$. We assume that c is regular and we let $c^{(i)} = \frac{d^i c}{dt^i}$ and $' = \frac{1}{|c^{(1)}|}\frac{d}{dt}$ be the differentiation with respect to the arc-length. For the unit tangent vector field $T = \frac{c^{(1)}}{|c^{(1)}|}$, define the unit vector field N and a nonnegative function κ by

$$\kappa N = T' - \langle T', T\rangle T = T'.$$

As a result, N is the principal normal of c. Hence N is the direction of infinitesimal change of T and κ is the rate of change. If $\kappa \equiv 0$, then T is constant and c is a straight line. Since

$$T' = \frac{1}{|c^{(1)}|}\frac{dT}{dt} = \frac{1}{|c^{(1)}|}\frac{d}{dt}\left(\frac{c^{(1)}}{|c^{(1)}|}\right) = \frac{1}{|c^{(1)}|^2}\left(c^{(2)} - \left(c^{(2)}\cdot T\right)T\right),$$

we have

$$\kappa = |T'| = \frac{\left|c^{(2)} - \left(c^{(2)}\cdot T\right)T\right|}{|c^{(1)}|^2}$$

and

$$N = \frac{c^{(2)} - \left(c^{(2)}\cdot T\right)T}{|c^{(2)} - (c^{(2)}\cdot T)T|}. \tag{2}$$

A unit vector field B and a nonnegative function τ are defined by

$$\tau B = N' - \langle N', T\rangle T - \langle N', N\rangle N = N' + \kappa T.$$

Hence B is perpendicular to the osculating plane $\langle T, N\rangle$, that is, B is the binormal vector of c up to sign.

Note that $\langle T, N\rangle = \left\langle c^{(1)}, c^{(2)}\right\rangle$ and τB is the component of N', perpendicular to $\langle T, N\rangle$. From (2), we may write

$$N' = \frac{c^{(3)}}{|c^{(1)}|\,|c^{(2)} - (c^{(2)}\cdot T)T|} + \alpha T + \beta N.$$

Then

$$B = \frac{c^{(3)} - (c^{(3)} \cdot T)T - (c^{(3)} \cdot N)N}{|c^{(3)} - (c^{(3)} \cdot T)T - (c^{(3)} \cdot N)N|} \tag{3}$$

and

$$\begin{aligned}\tau = N' \cdot B &= \frac{c^{(3)} \cdot B}{|c^{(1)}|\,|c^{(2)} - (c^{(2)} \cdot T)T|} \\ &= \frac{\left|c^{(3)} - (c^{(3)} \cdot T)T - (c^{(3)} \cdot N)N\right|}{|c^{(1)}|\,|c^{(2)} - (c^{(2)} \cdot T)T|}.\end{aligned}$$

Note that the equations for T, N, B are actually the Gram–Schmidt orthogonalization of $c^{(1)}, c^{(2)}, c^{(3)}$. Since c is a curve in $\mathbb{R}^3$, one may let $B = T \times N$ and, as a result, the sign of τ may change.

Example 1. For constants $a > 0, b$ with $a^2+b^2 = 1$, let $c(t) = (a\cos t, a\sin t, bt)$, i.e., a helix. Then $T = (-a\sin t, a\cos t, b)$ and $T' = (-a\cos t, -a\sin t, 0)$. Hence $N = (-\cos t, -\sin t, 0)$ with $\kappa = a$.

Since

$$\tau B = N' + \kappa T = (\sin t, -\cos t, 0) + a(-a\sin t, a\cos t, b) = b(b\sin t, -b\cos t, a),$$

we have $\tau = |b|$ and $B = \frac{b}{|b|}(b\sin t, -b\cos t, a)$. On the other hand, if we let $B = T \times N$, then $\tau = b$.

Example 2. Let $c(t) = (3t - t^3, 3t^2, 3t + t^3)$. Then $c'(t) = (3 - 3t^2, 6t, 3 + 3t^2)$ and

$$T = \frac{1}{\sqrt{2}(1+t^2)}\left(1 - t^2, 2t, 1 + t^2\right).$$

From $c^{(2)}(t) = (-6t, 6, 6t)$, we have

$$c^{(2)} - \left(c^{(2)} \cdot T\right)T = \frac{6}{1+t^2}\left(-2t, 1 - t^2, 0\right).$$

Hence

$$N = \frac{1}{1+t^2}\left(-2t, 1-t^2, 0\right), \quad \kappa = \frac{1}{3(1+t^2)^2}.$$

From $c^{(3)}(t) = (-6, 0, 6)$, we get

$$c^{(3)} - (c^{(3)} \cdot T)T - (c^{(3)} \cdot N)N = \frac{6}{(1+t^2)^2}\left(-1 + t^2, -2t, 1 + t^2\right)$$

Hence

$$B = \frac{1}{\sqrt{2}(1+t^2)}\left(-1+t^2, -2t, 1+t^2\right), \ \ \tau = \frac{1}{3(1+t^2)^2}.$$

For a curve $c : I \to \mathbb{R}^4$, we define the unit tangent T, principal normal N, the firs binormal B_1 and the second binormal B_2 and smooth functions κ, τ_1 and τ_2 inductively by

$$\begin{aligned} T &= \frac{c^{(1)}}{|c^{(1)}|}, \ \ \kappa N = T' \\ \tau_1 B_1 &= N' - \langle N', T\rangle T = N' + \kappa T \\ \tau_2 B_2 &= B_1' - \langle B_1', T\rangle T - \langle B_1', N\rangle N = B_1' + \tau_1 N. \end{aligned}$$

Then

$$B_2' = \langle B_2', B_1\rangle B_1 = -\tau_2 B_1.$$

If $\kappa\tau_1\tau_2 \neq 0$, then we may argue as in the case of $\mathbb{R}^3$ to get

$$\begin{aligned} B_1 &= \frac{c^{(3)} - (c^{(3)}\cdot T)T - (c^{(3)}\cdot N)N}{|c^{(3)} - (c^{(3)}\cdot T)T - (c^{(3)}\cdot N)N|}, \\ B_2 &= \frac{c^{(4)} - (c^{(4)}\cdot T)T - (c^{(4)}\cdot N)N - (c^{(4)}\cdot B_1)B_1}{|c^{(4)} - (c^{(4)}\cdot T)T - (c^{(4)}\cdot N)N - (c^{(4)}\cdot B_1)B_1|} \end{aligned}$$

and

$$\begin{aligned} \tau_1 &= \frac{\left|c^{(3)} - (c^{(3)}\cdot T)T - (c^{(3)}\cdot N)N\right|}{|c^{(1)}|\,|c^{(2)} - (c^{(2)}\cdot T)T|}, \\ \tau_2 &= \frac{\left|c^{(4)} - (c^{(4)}\cdot T)T - (c^{(4)}\cdot N)N - (c^{(4)}\cdot B_1)B_1\right|}{|c^{(1)}|\,|c^{(3)} - (c^{(3)}\cdot T)T - (c^{(3)}\cdot N)N|}. \end{aligned}$$

Note that T, N, B_1, B_2 are actually the Gram–Schmidt orthogonalization of $c^{(1)}, c^{(2)}, c^{(3)}, c^{(4)}$. Moreover, if $\tau_2 \equiv 0$, then c lies on a 3-dimensional Affine hyperplane.

THEOREM 2.1. *Let $c : I \to \mathbb{R}^4$ be a regular curve parametrized by arc-length. The Frenet formula of c with respect to T, N, B_1 and B_2, defined* *above, is*

$$\begin{pmatrix} T' \\ N' \\ B_1' \\ B_2' \end{pmatrix} = \begin{pmatrix} 0 & \kappa & 0 & 0 \\ -\kappa & 0 & \tau_1 & 0 \\ 0 & -\tau_1 & 0 & \tau_2 \\ 0 & 0 & -\tau_2 & 0 \end{pmatrix} \begin{pmatrix} T \\ N \\ B_1 \\ B_2 \end{pmatrix}.$$

Now we consider smooth regular curves in the Minkowski space $\mathbb{R}^{n,1}$. A simple case is a curve $c : I \to \mathbb{R}^{2,1}$ with spacelike $c' = \frac{dc}{dt}$, $\left\| \frac{dc}{dt} \right\|_L = 1$ and spacelike c'' and timelike c'''. For $T = c'$, define a unit vector N and κ by

$$\kappa N = T'.$$

Note that N' and $N' + \kappa T$ are timelike. Define a timelike vector B with $\langle B, B \rangle_L = -1$ by

$$\tau B = N' - \langle N', T \rangle_L T = N' + \kappa T.$$

Then

$$B' = \tau N.$$

The Frenet formula of c with respect to T, N and B is

$$\begin{pmatrix} T' \\ N' \\ B' \end{pmatrix} = \begin{pmatrix} 0 & \kappa & 0 \\ -\kappa & 0 & \tau \\ 0 & \tau & 0 \end{pmatrix} \begin{pmatrix} T \\ N \\ B \end{pmatrix}.$$

In the remaining of this section, we consider null curves in $\mathbb{R}^{2,1}$ or in $\mathbb{R}^{3,1}$, that is, curves with null tangent vector. Let c be a null curve in $\mathbb{R}^{2,1}$ or in $\mathbb{R}^{3,1}$. Then c'' is either identically null or spacelike: note that $\langle c', c'' \rangle_L = 0$. There are constants a and b such that the last component of $ac'' - bc'$ is 0. Hence $ac'' - bc'$ is either zero or spacelike. If $ac'' - bc'$ is zero, then c' and c'' are collinear. If $ac'' - bc'$ is spacelike, then

$$\|ac'' - bc'\|_L = |a| \, \|c''\|_L > 0.$$

If c'' is identically null, then c' and c'' are collinear. Hence

$$c' = e^{\int f} (a, b, c)$$

for a smooth function f and constant (a, b, c). Hence c is a straight line.

In the following, we assume that c'' is spacelike and c is parametrized by pseudo arc-length. A natural choice of T and N for a null curve c is

$$T = c' \text{ and } N = c'' = T'.$$

THEOREM 2.2. *Let $c : I \to \mathbb{R}^{2,1}$ be a null curve (with spacelike c'') parametrized by pseudo arc-length. Let $T = c'$ and $N = c''$, and define B by*

$$B = -N' - \frac{\|c'''\|_L^2}{2} T.$$

Then B is null and satisfies $\langle T, B\rangle_L = 1, \langle N, B\rangle_L = 0$.

The Frenet formula of c with respect to T, N, B is

$$\begin{pmatrix} T' \\ N' \\ B' \end{pmatrix} = \begin{pmatrix} 0 & 1 & 0 \\ -\frac{\|c'''\|_L^2}{2} & 0 & -1 \\ 0 & \frac{\|c'''\|_L^2}{2} & 0 \end{pmatrix} \begin{pmatrix} T \\ N \\ B \end{pmatrix}.$$

Proof. From $\langle c', c'\rangle_L = 0$ and $\langle c'', c''\rangle_L = 1$, we have

$$\langle c', c''\rangle_L = \langle c'', c'''\rangle_L = 0 \text{ and } \langle c', c'''\rangle_L = -1.$$

Hence $T = c'$ and $N' = c'''$ lies on the plane $P_N = \langle c'', (x_1, x_2, x_3)\rangle_L = 0$, and there is a null vector $\tilde{B}$ such that

$$c''' = uT - \tilde{B}.$$

From $\|c''' - uT\|_L = 0$, we have

$$u = -\frac{\|c'''\|_L^2}{2}$$

and $\tilde{B} = B$. It follows that $\langle T, B\rangle_L = 1$, which is the cause of the choice of $-\tilde{B}$ in $c''' = uT - \tilde{B}$. Then

$$B' = \langle B', B\rangle_L T + \langle B', N\rangle_L N + \langle B', T\rangle_L B = \frac{\|c'''\|_L^2}{2} N.$$

This completes the proof. $\square$

Now we consider null curves in $\mathbb{R}^{3,1}$. We use the ideas and computations of the above Theorem 2.2 and its proof.

THEOREM 2.3. *Let $c : I \to \mathbb{R}^{3,1}$ be a null curve parametrized by pseudo arc-length. Let $T = c'$ and $N = c''$. Then*

$$B_1 := -N' - \frac{\|c'''\|_L^2}{2} T$$

is null and satisfies $\langle T, B_1 \rangle_L = 1$. The vector

$$\mathcal{B} := B_1' - \frac{\|c'''\|_L^2}{2} N$$

is spacelike and $\mathcal{B} \perp T, N, B_1$.

For the spacelike unit vector B_2 defined by

$$B_2 = \frac{\mathcal{B}}{\|\mathcal{B}\|_L},$$

the Frenet formula of c with respect to T, N, B_1 and B_2 is

$$\begin{pmatrix} T' \\ N' \\ B_1' \\ B_2' \end{pmatrix} = \begin{pmatrix} 0 & 1 & 0 & 0 \\ -\frac{\|c'''\|_L^2}{2} & 0 & -1 & 0 \\ 0 & \frac{\|c'''\|_L^2}{2} & 0 & u \\ -u & 0 & 0 & 0 \end{pmatrix} \begin{pmatrix} T \\ N \\ B_1 \\ B_2 \end{pmatrix},$$

where $u = \|\mathcal{B}\|_L = \left\| -c'''' - \langle c'''', c''' \rangle_L c' - \|c'''\|_L^2 c'' \right\|_L$.

Proof. As in the proof of Theorem 2.2, we have

$$\langle c', c'' \rangle_L = \langle c'', c''' \rangle_L = 0 \text{ and } \langle c', c''' \rangle_L = -1.$$

We also have

$$\langle c', c'''' \rangle_L = 0.$$

The vectors $T = c'$ and $N' = c'''$ lies on the hyperplane

$$P_N = \langle c'', (x_1, x_2, x_3, x_4) \rangle_L = 0.$$

As in the proof of Theorem 2.2, B_1 defined by

$$c''' = -\frac{\|c'''\|_L^2}{2} T - B_1$$

is null and satisfies $\langle T, B_1 \rangle_L = 1$, $\langle N, B_1 \rangle_L = 0$.

It is straightforward to see that

$$\langle B_1', T\rangle_L = \langle B_1', B_1\rangle_L = 0 \text{ and } \langle B_1', N\rangle_L = \frac{\|c'''\|_L^2}{2}.$$

Hence $\mathcal{B}$ satisfies

$$\langle \mathcal{B}, T\rangle_L = \langle \mathcal{B}, N\rangle_L = \langle \mathcal{B}, B_1\rangle_L = 0.$$

It follows that $\mathcal{B}$ is spacelike. Then $B_2 = \frac{\mathcal{B}}{\|\mathcal{B}\|_L}$ satisfies

$$B_2' = -uT.$$

This completes the proof. $\square$

3. Frenet formula for pseudo null curves in $\mathbb{R}^{2,1}$ and $\mathbb{R}^{3,1}$

For a pseudo null curve c in $\mathbb{R}^{2,1}$ or in $\mathbb{R}^{3,1}$ parametrized by arc-length, let $T = c'$ and $N = c'' = T'$.

Theorem 3.1. *Let $c : I \to \mathbb{R}^{2,1}$ be a pseudo null curve parametrized by arc-length. Then c lies on a Euclidean plane, which is parallel to the osculating plane $\langle T, N\rangle$. For $T = c'$ and $N = c''$, the Frenet formula is*

$$\begin{pmatrix} T' \\ N' \end{pmatrix} = \begin{pmatrix} 0 & 1 \\ 0 & \tau \end{pmatrix} \begin{pmatrix} T \\ N \end{pmatrix},$$

where τ is a smooth function.

There are constant null vector (p, q, r) and constant spacelike unit vector (α, β, γ) such that

$$c' = \left(\int e^{\int \tau}\right)(p, q, r) + (\alpha, \beta, \gamma),$$

which determines c up to constant vector.

Introducing a null vector field B satisfying

$$\langle T, B\rangle_L = 0, \ \langle N, B\rangle_L = 1,$$

we have

$$\begin{pmatrix} T' \\ N' \\ B' \end{pmatrix} = \begin{pmatrix} 0 & 1 & 0 \\ 0 & \tau & 0 \\ -1 & 0 & -\tau \end{pmatrix} \begin{pmatrix} T \\ N \\ B \end{pmatrix}.$$

The above $\{T, N, B\}$ is called a *pseudo-orthonormal* basis of $\mathbb{R}^{2,1}$.

Proof. For each fixed $s \in I$, we claim that c''' is a constant multiple of c''. By applying a Lorentzian isometry of $\mathbb{R}^{2,1}$, we may assume that

$$c' = (1, 0, 0).$$

From $\langle c', c'' \rangle_L = 0$ and $\langle c'', c'' \rangle_L = 0$, we have

$$c'' = (0, a, a) \text{ or } (0, a, -a)$$

for some $a \neq 0$. From $\langle c', c''' \rangle_L = 0$ and $\langle c'', c''' \rangle_L = 0$, we have

$$c''' = (0, b, b) \text{ or } (0, b, -b)$$

for some $b \neq 0$ respectively, which proves our claim.

It follows that there is a smooth function τ such that

$$c''' = \tau c'' \text{ or } N' = \tau N. \tag{4}$$

Hence

$$c'' = \left(e^{\int \tau}\right)(p, q, r),$$

for some constant null vector (p, q, r). Then

$$c' = \left(\int e^{\int \tau}\right)(p, q, r) + (\alpha, \beta, \gamma)$$

for some constant vector (α, β, γ). Since $\langle c', c'' \rangle_L = 0$ and $\|c'\|_L = 1$, we have $\langle (p, q, r), (\alpha, \beta, \gamma) \rangle_L = 0$ and (α, β, γ) is spacelike with $|(\alpha, \beta, \gamma)|_L = 1$.

Hence c lies on the Euclidean plane parallel to $\langle T(s_0), N(s_0) \rangle$ and passing through $c(s_0)$ for fixed $s_0 \in I$. The Frenet formula is straightforward from the choice of T, N and τ.

The Frenet formula of c with respect to the pseudo-orthonormal basis $\{T, N, B\}$ follows from

$$B' = \langle B', T\rangle_L T + \langle B', B\rangle_L N + \langle B', N\rangle_L B = -T - \tau B.$$

□

For a pseudo null curve in $\mathbb{R}^{2,1}$, the Darboux vector field D is defined by [6]

$$D = \tau T - N.$$

A pseudo null curve in $\mathbb{R}^{2,1}$ is called a *pseudo null Darboux helix* if there is a constant vector V such that

$$\langle D, V\rangle_L = constant.$$

COROLLARY 3.2. [6] *A pseudo null curve in $\mathbb{R}^{2,1}$ is a pseudo null Darboux helix.*

Proof. Using the results of Theorem 3.1, we have

$$\langle D, (p, q, r)\rangle_L = 0.$$

Hence, c is a pseudo null Darboux helix with $V = (p, q, r)$. □

A pseudo null Darboux helix is said to be of j-type ($j = 1, 2, 3$) [6] if there is a constant vector U_k ($k = 1, 2, 3$), which is not collinear with V, such that

$$\langle U_1, T\rangle_L = c_1, \text{ if } j = 1,$$
$$\langle U_2, N\rangle_L = c_2, \text{ if } j = 2,$$
$$\langle U_3, B\rangle_L = c_3, \text{ if } j = 3.$$

We point out that there are missing cases in Theorem 3 of [6] (cf. (3) of the following theorem.). We use the results of Theorem 3.1 in the following

THEOREM 3.3. [6] *Let c be a pseudo null Darboux helix in $\mathbb{R}^{2,1}$ with non-constant τ. Then*

(1) *if c is 1-type with $c_1 \neq 0$, then*

$$U_1 = d_1 (p, q, r) + c_1 (\alpha, \beta, \gamma),$$

where d_1 is a constant.

(2) *every 2-type pseudo null Darboux helix is 1-type pseudo null Darboux helix.*

(3) *if c is 3-type, then $\tau' - \frac{1}{2}\tau^2$ is a constant and we have three cases with*

$$U_3 = c_3\left(-\tau T + N - \tau' B\right):$$

i. *if $\tau' - \frac{1}{2}\tau^2$ is a positive constant C, then*

$$\tau = \sqrt{2C}\tan\left(\frac{\sqrt{2C}}{2}(s+d_3)\right).$$

ii. *if $\tau' - \frac{1}{2}\tau^2 = 0$, then*

$$\tau = -\frac{2}{s+d_4}.$$

iii. *if $\tau' - \frac{1}{2}\tau^2$ is a negative constant C, then*

$$\tau = \sqrt{-2C}\tanh\left(\frac{\sqrt{-2C}}{2}(s+d_5)\right).$$

where d_3, d_4 and d_5 are constants.

Proof. (1). Let

$$U_1 = k_1 T + l_1 N + m_1 B.$$

Since $\langle U_1, T\rangle_L = c_1$, $k_1 = c_1$. From $U_1' = 0$, we have $k_1' - m_1 = 0$, $m_1' - \tau m_1 = 0$ and $k_1 + l_1' + \tau l_1 = 0$. Hence $m_1 = 0$ and $c_1 + l_1' + \tau l_1 = 0$. The solution of the ordinary differential equation $c_1 + l_1' + \tau l_1 = 0$ is

$$l_1 = e^{-\int\tau}\left(d_1 - c_1\int e^{\int\tau}\right)$$

for a constant d_1. Using the results of Theorem 3.1, we have

$$U_1 = d_1\left(p, q, r\right) + c_1\left(\alpha, \beta, \gamma\right).$$

Hence V and U_1 are collinear only if $c_1 = 0$.

(2). From

$$\langle U_2, N\rangle_L' = 0,$$

we have $\tau c_2 = 0$. Hence $c_2 = 0$, and

$$U_2 = k_2 T + l_2 N.$$

Arguing as in (1), we have $k_2 = constant$, which proves (2).

(3). We may let

$$U_3 = k_3 T + c_3 N + m_3 B.$$

From $U_3' = 0$, we have $k_3' - m_3 = 0$, $k_3 + c_3\tau = 0$, $m_3' - m_3\tau = 0$. If $c_3 = 0$, then $k_3 = m_3 = 0$, that is, $U_3 = 0$. Hence we should have $c_3 \neq 0$. Then τ satisfies $\tau'' - \tau\tau' = 0$, or,

$$\tau' - \frac{\tau^2}{2} = C(constant).$$

Depending on the sign of C, we have three cases:

i. if $C > 0$, then

$$\tau = \sqrt{2C}\tan\left(\frac{\sqrt{2C}}{2}(s + d_3)\right)$$

where d_3 is a constant.

ii. if $C = 0$, then

$$\tau = -\frac{2}{s + d_4},$$

where d_4 is a constant.

iii. if $C < 0$, then

$$\tau = \sqrt{-2C}\tanh\left(\frac{\sqrt{-2C}}{2}(s + d_5)\right),$$

where d_5 is a constant.

□

We give examples for the case ii. and case iii. of (3).

Example 3. Let $\tau = \frac{2}{s+1}$ with $(p,q,r) = (0,1,1)$ and $(\alpha,\beta,\gamma) = (1,0,0)$ in Theorem 3.1. Then

$$N = c'' = \left(e^{\int \frac{2}{s+1}}\right)(0,1,1) = (s+1)(0,1,1)$$

and

$$T = c' = \frac{(s+1)^2}{2}(0,1,1) + (1,0,0).$$

Hence

$$D = \tau T - N = \frac{2}{s+1}(1,0,0).$$

satisfies $\langle D, (0,1,1)\rangle_L = 0$. For a constants c_1 and d_1, let

$$U_1 = (c_1, d_1, d_1).$$

Then

$$\langle U_1, T\rangle_L = c_1.$$

Hence the curve

$$c(s) = \frac{(s+1)^3}{6}(0,1,1) + s\,(1,0,0) + C$$

is a 1-type pseudo null Darboux helix.

Example 4. Let $\tau = 2\tanh s$ with $(p,q,r) = (0,1,1)$ and $(\alpha,\beta,\gamma) = (1,0,0)$ in Theorem 3.1. Then

$$N = c'' = \left(e^{\int 2\tanh s}\right)(0,1,1) = \cosh^2 s\,(0,1,1)$$

and

$$\begin{aligned} T = c' &= \left(\frac{\sinh(2s)}{4} + \frac{s}{2}\right)(0,1,1) + (1,0,0) \\ &= \left(\frac{1}{2}\cosh s \sinh s + \frac{s}{2}\right)(0,1,1) + (1,0,0). \end{aligned}$$

Hence

$$D = \tau T - N = (s\tanh s - 1)(0,1,1) + 2\tanh s\,(1,0,0).$$

satisfies $\langle D, (0,1,1)\rangle_L = 0$.

Now we consider pseudo null curves in $\mathbb{R}^{3,1}$. We remark that a pseudo null curve c in $\mathbb{R}^{3,1}$ is similar to a null curve lying in the hyperplane $T^\perp \subset \mathbb{R}^{3,1}$, which is not parametrized by pseudo arc-length. If c''' is identically null, then c is a pseudo null curve in some hyperplane of $\mathbb{R}^{3,1}$. Actually, c'' and c''' are collinear.

THEOREM 3.4. *Let $c : I \to \mathbb{R}^{3,1}$ be a pseudo null curve parametrized by arc-length with spacelike c'''. Let $T = c'$, $N = c''$. Define a spacelike unit vector B_1 by*

$$N' = \|c'''\|_L B_1.$$

For

$$v = -\frac{1}{2\,\|c'''\|_L^3}\left(\|c''''\|_L^2 - \frac{\langle c'''', c'''\rangle_L^2}{\|c'''\|_L^2}\right),$$

a vector B_2 defined by

$$B_1' = vN - \|c'''\|_L\, B_2$$

is null and satisfies $\langle N, B_2\rangle_L = 1$.

The Frenet formula of c with respect to T, N, B_1 and B_2 is

$$\begin{pmatrix} T' \\ N' \\ B_1' \\ B_2' \end{pmatrix} = \begin{pmatrix} 0 & 1 & 0 & 0 \\ 0 & 0 & \|c'''\|_L & 0 \\ 0 & v & 0 & -\|c'''\|_L \\ -1 & 0 & -v & 0 \end{pmatrix} \begin{pmatrix} T \\ N \\ B_1 \\ B_2 \end{pmatrix}.$$

Proof. From $\langle c', c'\rangle_L = 1$ and $\langle c'', c''\rangle_L = 0$, it follows that

$$\langle c', c''\rangle_L = \langle c'', c'''\rangle_L = \langle c', c'''\rangle_L = \langle c', c''''\rangle_L = 0.$$

Hence $\langle T, N\rangle_L = \langle T, B_1'\rangle_L = 0$ and $\langle B_1, N\rangle_L = \langle B_1, B_1'\rangle_L = 0$. Note that c''' is either spacelike or identically null. If c''' is identically null, then c'' and c''' are collinear, which amounts to Theorem 3.1. Hence there is a null vector B_2 defined by

$$B_1' = \mu N + \nu B_2$$

that satisfies $\langle N, B_2\rangle_L = 1$. It is straightforward to see that $B_1' - vN$ is null and $\langle N, B_2\rangle_L = 1$ for $wB_2 = vN - B_1'$.

We also have

$$B_2' = \langle B_2', T\rangle_L\, T + \langle B_2', B_2\rangle_L\, N + \langle B_2', B_1\rangle_L\, B_1 + \langle B_2', N\rangle_L\, B_2 = -T - vB_1.$$

This completes the proof. □

References

[1] A. Ali, R. Lopez and M. Turgut, *k-type partially null and pseudo null slant helices in Minkowski 4-space*, Math. Commun. **17** (2012), 93-103.

[2] W. Bonnor, *Null curves in a minkowski space-time*, Tensor **20** (1969), 229-242.

[3] W. Bonnor, *Curves with null normals in Minkowski spacetime*, A random walk in relativity and cosmology, Wiley Eastern Ltd (1985), 33-47.

[4] M. Grbović, K. İlarslan and E. Nešović, *On null and pseudo null Mannheim curves in Minkowski 3-space*, J. Geom. **105** (2014), 177–183.

[5] K. İlarslan and E. Nešović, *Some Characterizations of Null, Pseudo null and Partially null Rectifying Curves in Minkowski space-time* Taiwanese J. of Math. **12** no. 5 (2008) 1035-1044.

[6] E. Nešovića, U. Öztürk and E. Öztürk, *On k-type pseudo null Darboux helices in Minkowski 3-space* J. Math. Anal. Appl. **439** (2016), 690–700.

[7] B. O'Neil, *Semi-Riemannian Geometry*, Academic Press, New York-London, 1983.

[8] U. Öztürk and E. Nešović, *On pseudo null and null cartan darboux helices in minkowski 3-space* Kuwait J. Sci. **43** (2016), 64-82.

[9] J. Walrave, *Curves and surfaces in Minkowski space*, Doctoral thesis, K. U. Leuven, Fac. of Science, Leuven, (1995)

4. Author Information

Sung-Ho Park (E-mail: sunghopark@hufs.ac.kr)

Professor, Major in Mathematics, Graduate School of Education, Hankuk University of Foreign Studies, Republic of Korea.

J. Basic Sci. HUFS **62** (2026), pp. 115–124

A GENERALIZED KRONECKER CONGRUENCE FOR MODULAR FUNCTIONS OF ARBITRARY LEVEL

DONG HWA SHIN

Abstract. Let N be a positive integer and let f be a meromorphic modular function of level N whose Fourier coefficients lie in the Nth cyclotomic field. For a prime p not dividing N, define a function f_p on the complex upper half-plane $\mathbb{H}$ by

$$f_p(\tau) = f\left(\frac{\tau}{p}\right) \quad (\tau \in \mathbb{H}).$$

Let j be the elliptic modular function. We show that if f is integral over $\mathbb{Z}[j]$, then

$$\frac{1}{p}\left(f_p^p - f^{\left[\begin{smallmatrix}1&0\\0&p\end{smallmatrix}\right]}\right)\left(f_p - \left(f^{\left[\begin{smallmatrix}p^{e(N,\,p)-1}&0\\0&p^{e(N,\,p)}\end{smallmatrix}\right]}\right)^p\right)$$

is also integral over $\mathbb{Z}[j]$, where $e(N,\,p)$ is the order of p in the group $(\mathbb{Z}/N\mathbb{Z})^\times/\langle -1\rangle$. Consequently, we establish a Kronecker-type congruence for modular functions of arbitrary level. In particular, the result recovers the previously known congruence when $p \equiv \pm 1 \pmod{N}$.

1. Introduction

Let $\mathbb{H} = \{\tau \in \mathbb{C} \mid \mathrm{Im}(\tau) > 0\}$ be the complex upper half-plane. The elliptic modular function j on $\mathbb{H}$ has the Fourier expansion

$$j(\tau) = \frac{1}{q} + 744 + 196884q + 21493760q^2 + \cdots \quad (q = e^{2\pi \mathrm{i}\tau},\ \tau \in \mathbb{H}).$$

It is a weakly holomorphic (that is, holomorphic on $\mathbb{H}$ but may have poles at the cusps) modular function for the full modular group $\mathrm{SL}_2(\mathbb{Z})$; see [10, §3.3].

Let p be a prime. Weber [14] proved that if $\Phi_p(x,\,y)$ is the modular polynomial for j, so that

$$\Phi_p(j(\tau),\,j(p\tau)) = 0 \quad (\tau \in \mathbb{H}),$$

2020 *Mathematics Subject Classification.* Primary 11F03; Secondary 12J25, 13F25.

then it satisfies the *Kronecker congruence relation*

$$\Phi_p(x,\, y) \equiv (x^p - y)(x - y^p) \pmod{p\mathbb{Z}[x,\, y]}. \tag{1}$$

See also [5, Theorem 11.18]. This congruence has been further investigated and extended to certain genus-zero Hauptmoduln other than j for special primes p, via the q-expansion principle. See, for example, Chen-Yui [2], Cais-Conrad [1], Cho [3, 4], and others.

Let N be a positive integer, and let $\zeta_N = e^{2\pi\mathrm{i}/N}$ be a primitive Nth root of unity. For a meromorphic modular function f of level N, define a function f_p on $\mathbb{H}$ by

$$f_p(\tau) = f\left(\frac{\tau}{p}\right) \quad (\tau \in \mathbb{H}).$$

Using class field theory (see [6, Chapter V] and [12, Chapters 5–6]), Jung et al. [7] generalized the Kronecker congruence relation (1) to functions on modular curves of higher level and higher genus as follows.

Theorem A ([7, Theorem 7.1]). *Let f be a weakly holomorphic modular function for $\Gamma_1(N)$ with rational Fourier coefficients. Let p be a prime such that $p \equiv 1$ or $-1 \pmod{N}$. If f is integral over $\mathbb{Z}[j]$, then we have*

$$\prod_{\delta\in R_{N,\,p}} \left\{(f_p^p - f)(f_p - f^p)\right\} \circ \delta \equiv 0 \pmod{p\mathcal{O}_{N,\,p}}.$$

Here, $R_{N,p}$ is a set of representatives for the right cosets of $\Gamma_1(N)\cap\Gamma^0(p)$ in $\Gamma_1(N)$, and $\mathcal{O}_{N,p}$ is the integral closure of $\mathbb{Z}[j]$ in the field of meromorphic modular functions for $\Gamma_1(N)$ with Fourier coefficients in $\mathbb{Q}(\zeta_{Np})$.

Recently, Jung et al. [8] refined Theorem A by using valuation-theoretic ideas in the sense of Tate [13] and Serre [11], together with Katz's q-expansion principle [9]. Let $\mathcal{F}_N$ be the field of meromorphic modular functions of level N whose Fourier coefficients belong to $\mathbb{Q}(\zeta_N)$. It is well known that $\mathcal{F}_N$ is a Galois extension of $\mathcal{F}_1$ and that

$$\mathrm{Gal}(\mathcal{F}_N/\mathcal{F}_1) \simeq \mathrm{GL}_2(\mathbb{Z}/N\mathbb{Z})/\langle -I_2\rangle$$

(see §2). We write f^γ for the corresponding Galois action on $f \in \mathcal{F}_N$, as recalled in Proposition 2.1. Denote by $\mathcal{O}_{\mathcal{F}_N}$ the integral closure of $\mathbb{Z}[j]$ in $\mathcal{F}_N$.

Theorem B ([8, Theorem 8.1]). *Let $f \in \mathcal{F}_N$, and let p be a prime such that*

$$p \equiv 1 \ \textit{or}\ -1 \pmod{N}.$$

If f is integral over $\mathbb{Z}[j]$, then the function

$$\frac{1}{p}\left(f_p^p - f^{\left[\begin{smallmatrix}1&0\\0&p\end{smallmatrix}\right]}\right)\left(f_p - (f^{\left[\begin{smallmatrix}1&0\\0&p\end{smallmatrix}\right]})^p\right)$$

is also integral over $\mathbb{Z}[j]$. Consequently, one obtains the Kronecker-type congruence

$$\left(f_p^p - f^{\left[\begin{smallmatrix}1&0\\0&p\end{smallmatrix}\right]}\right)\left(f_p - (f^{\left[\begin{smallmatrix}1&0\\0&p\end{smallmatrix}\right]})^p\right) \equiv 0 \pmod{p\mathcal{O}_{\mathcal{F}_{Np}}}.$$

The purpose of this paper is to remove the congruence condition

$$p \equiv 1 \text{ or } -1 \pmod{N}$$

from Theorem B. More precisely, we prove the following result.

Theorem C. *Let N be a positive integer, let $f \in \mathcal{F}_N$, and let p be a prime not dividing N. If f is integral over $\mathbb{Z}[j]$, then*

$$\frac{1}{p}\left(f_p^p - f^{\left[\begin{smallmatrix}1&0\\0&p\end{smallmatrix}\right]}\right)\left(f_p - \left(f^{\left[\begin{smallmatrix}p^{e(N,\,p)-1}&0\\0&p^{e(N,\,p)}\end{smallmatrix}\right]}\right)^p\right)$$

is integral over $\mathbb{Z}[j]$, where $e(N,\,p)$ is the order of p in the group $(\mathbb{Z}/N\mathbb{Z})^\times/\langle -1\rangle$.

Our approach relies on the valuation-theoretic integrality criterion established in [8, Proposition 6.2]. This criterion allows us to reduce the integrality question to analyzing the Fourier coefficients of the corresponding functions under the action of $\mathrm{SL}_2(\mathbb{Z})$.

2. Preliminaries on modular function fields and integrality

In this section, we recall some basic facts on modular function fields and an integrality criterion that will be used in the proof of the main theorem.

Unless otherwise stated, N denotes a positive integer. For a lattice L in $\mathbb{C}$, the Weierstrass $\wp$-function $\wp(\,\cdot\,;\,L)$ on $\mathbb{C}$ is defined by

$$\wp(z;\,L) = \frac{1}{z^2} + \sum_{w\in L\setminus\{0\}}\left\{\frac{1}{(z-w)^2} - \frac{1}{w^2}\right\} \quad (z \in \mathbb{C}).$$

We also put

$$g_2(L) = 60 \sum_{w \in L \setminus \{0\}} \frac{1}{w^4},$$

$$g_3(L) = 140 \sum_{w \in L \setminus \{0\}} \frac{1}{w^6}.$$

For basic properties of the Weierstrass $\wp$-function, one may refer to [5, §10.A]. For $\mathbf{v} = \begin{bmatrix} v_1 & v_2 \end{bmatrix} \in M_{1,2}(\mathbb{Q}) \setminus M_{1,2}(\mathbb{Z})$, the Fricke function $f_{\mathbf{v}}$ on $\mathbb{H}$ is given by

$$f_{\mathbf{v}}(\tau) = -2^7 3^5 \frac{g_2([\tau,\, 1])g_3([\tau,\, 1])}{g_2([\tau,\, 1])^3 - 27 g_3([\tau,\, 1])^2} \wp(v_1\tau + v_2;\, [\tau,\, 1]) \quad (\tau \in \mathbb{H})$$

where $[\tau,\, 1]$ denotes the $\mathbb{Z}$-lattice generated by τ and 1. For each positive integer N, define

$$\mathcal{F}_N = \begin{cases} \mathbb{Q}(j) & \text{if } N = 1, \\ \mathbb{Q}\left(j,\, f_{\mathbf{v}} \mid \mathbf{v} \in \dfrac{1}{N} M_{1,2}(\mathbb{Z}) \setminus M_{1,2}(\mathbb{Z})\right) & \text{if } N \geq 2. \end{cases}$$

Then the field $\mathcal{F}_N$ is a Galois extension of $\mathcal{F}_1$ whose Galois group is isomorphic to

$$\mathrm{GL}_2(\mathbb{Z}/N\mathbb{Z})/\langle -I_2 \rangle.$$

Moreover, $\mathcal{F}_N$ coincides with the field of meromorphic modular functions for the principal congruence subgroup

$$\Gamma(N) = \{\gamma \in \mathrm{SL}_2(\mathbb{Z}) \mid \gamma \equiv I_2 \pmod{N M_2(\mathbb{Z})}\}$$

whose Fourier coefficients lie in the Nth cyclotomic field $\mathbb{Q}(\zeta_N)$; see [12, Theorem 6.6 (1), (2) and Proposition 6.9 (1)].

Proposition 2.1. *Let $f \in \mathcal{F}_N$ have the Fourier expansion*

$$f(\tau) = \sum_{n \gg -\infty} a_n q^{n/N} \text{ with } a_n \in \mathbb{Q}(\zeta_N) \quad (\tau \in \mathbb{H})$$

with respect to $q^{1/N} = e^{2\pi \mathrm{i}\tau/N}$. Let $\gamma \in \mathrm{GL}_2(\mathbb{Z}/N\mathbb{Z})/\langle -I_2 \rangle$ ($\simeq \mathrm{Gal}(\mathcal{F}_N/\mathcal{F}_1)$).

(i) *If γ is represented by $\begin{bmatrix} 1 & 0 \\ 0 & d \end{bmatrix}$ for some integer d relatively prime to N, then*

$$f^\gamma(\tau) = \sum_{n \gg -\infty} a_n^{\sigma_{N,d}} q^{n/N},$$

where $\sigma_{N,d}$ is the automorphism of $\mathbb{Q}(\zeta_N)$ defined by $\zeta_N^{\sigma_{N,d}} = \zeta_N^d$.

(ii) *If* γ *is represented by an element* α *of* $\mathrm{SL}_2(\mathbb{Z})$*, then*

$$f^{\gamma} = f \circ \alpha.$$

Proof. See [12, Theorem 6.6 (3) and Proposition 6.21 (3)]. □

PROPOSITION 2.2. *Let* $g \in \mathcal{F}_M$ *for a positive integer* M*. Then* g *is integral over* $\mathbb{Z}[j]$ *if and only if* g *is weakly holomorphic and* $g \circ \alpha$ *has algebraic integer Fourier coefficients for every* $\alpha \in \mathrm{SL}_2(\mathbb{Z})$*.*

Proof. See [8, Proposition 6.2]. □

3. A generalization of the Kronecker congruence relation

We now prove our main theorem concerning the integrality over $\mathbb{Z}[j]$ of certain modular functions.

LEMMA 3.1. *Let* $f \in \mathcal{F}_N$*. For a prime* p*, the function* f_p *belongs to* $\mathcal{F}_{Np}$ *and has Fourier coefficients in* $\mathbb{Q}(\zeta_N)$*.*

Proof. See [7, Lemma 4.2]. □

LEMMA 3.2. *Let* $K = \mathbb{Q}(\zeta_N)$*. If* p *is a prime not dividing* N*, then*

$$c^p \equiv c^{\sigma_{N,\,p}} \pmod{p\mathcal{O}_K} \quad \textit{for all } c \in \mathcal{O}_K.$$

Proof. See [8, Lemma 7.2]. □

LEMMA 3.3. *Let* M *be a positive integer and let* $L = \mathbb{Q}(\zeta_M)$*. Let* $g \in \mathcal{F}_M$ *have the Fourier expansion*

$$g(\tau) = \sum_{n \gg -\infty} a_n q^{n/M} \quad (\tau \in \mathbb{H})$$

with $a_n \in \mathcal{O}_L$ *for all* $n \in \mathbb{Z}$*. Then, for any prime* p*,*

$$g(\tau)^p \equiv \sum_{n \gg -\infty} a_n^p q^{pn/M} \pmod{p\mathcal{O}_L((q^{1/M}))}.$$

Proof. See [8, Lemma 7.3]. □

THEOREM 3.4. *Let* N *be a positive integer, let* $f \in \mathcal{F}_N$*, and let* p *be a prime not dividing* N*. If* f *is integral over* $\mathbb{Z}[j]$*, then*

$$\frac{1}{p}\left(f_p^p - f^{\left[\begin{smallmatrix}1 & 0\\ 0 & p\end{smallmatrix}\right]}\right)\left(f_p - \left(f^{\left[\begin{smallmatrix}p^{e(N,\,p)-1} & 0\\ 0 & p^{e(N,\,p)}\end{smallmatrix}\right]}\right)^p\right)$$

is integral over $\mathbb{Z}[j]$*, where* $e(N,\,p)$ *is the order of* p *in the group* $(\mathbb{Z}/N\mathbb{Z})^{\times}/\langle -1\rangle$*.*

Proof. Put

$$K = \mathbb{Q}(\zeta_N), \quad L = \mathbb{Q}(\zeta_{Np}), \quad e = e(N,\, p) \quad \text{and} \quad D = \begin{bmatrix} 1 & 0 \\ 0 & p \end{bmatrix}.$$

Set

$$h_0 = f^D \quad \text{and} \quad h = f^{\left[\begin{smallmatrix} p^{e-1} & 0 \\ 0 & p^e \end{smallmatrix}\right]}.$$

Define a function G on $\mathbb{H}$ by

$$G = \left(f_p^p - h_0\right)\left(f_p - h^p\right).$$

We shall prove that

$$F = \frac{1}{p}G$$

is integral over $\mathbb{Z}[j]$.

By Lemma 3.1, we have $f_p \in \mathcal{F}_{Np}$. Since h_0 and h belong to $\mathcal{F}_N$, they also belong to $\mathcal{F}_{Np}$, and hence

$$F \in \mathcal{F}_{Np}.$$

Moreover, since f is integral over $\mathbb{Z}[j]$, both h_0 and h are integral over $\mathbb{Z}[j]$ because they are Galois conjugates of f over $\mathcal{F}_1$. Therefore h_0 and h are weakly holomorphic by Proposition 2.2. Since f is weakly holomorphic, so is f_p. Consequently, F is weakly holomorphic. It remains to show that for every $\alpha \in \mathrm{SL}_2(\mathbb{Z})$ the Fourier coefficients of $F \circ \alpha$ are algebraic integers.

Let

$$\alpha = \begin{bmatrix} a & b \\ c & d \end{bmatrix} \in \mathrm{SL}_2(\mathbb{Z}).$$

It suffices to show that the Fourier coefficients of $G \circ \alpha$ with respect to $q^{1/(Np)}$ belong to $p\mathcal{O}_L$. We distinguish two cases, depending on whether

$$p \nmid a \quad \text{or} \quad p \mid a.$$

Case 1. Assume first that $p \nmid a$. Choose an integer t such that

$$at \equiv b \pmod{p}.$$

Then the matrix

$$\beta = \begin{bmatrix} a & (b-at)/p \\ pc & d-ct \end{bmatrix}$$

belongs to $\mathrm{SL}_2(\mathbb{Z})$ and satisfies

$$D\alpha = \beta \begin{bmatrix} 1 & t \\ 0 & p \end{bmatrix}. \tag{2}$$

It follows that

$$(3)\qquad (f_p \circ \alpha)(\tau) = (f \circ D \circ \alpha)(\tau) = (f \circ \beta)\left(\frac{\tau + t}{p}\right) \quad (\tau \in \mathbb{H}).$$

Since f is integral over $\mathbb{Z}[j]$, Propositions 2.1 and 2.2 give the Fourier expansion

$$(4)\qquad (f \circ \beta)(\tau) = \sum_{n \gg -\infty} b_n q^{n/N} \quad \text{with } b_n \in \mathcal{O}_K \quad (\tau \in \mathbb{H}).$$

Thus (3) and (4) give

$$(5)\qquad (f_p \circ \alpha)(\tau) = \sum_{n \gg -\infty} b_n \zeta_{Np}^{nt} q^{n/(Np)}.$$

Applying Lemma 3.3 with $M = Np$ and Lemma 3.2 to $b_n \in \mathcal{O}_K$, we deduce that

$$(6)\qquad (f_p \circ \alpha)(\tau)^p \equiv \sum_{n \gg -\infty} b_n^{\sigma_{N,p}} \zeta_N^{nt} q^{n/N} \pmod{p\mathcal{O}_L((q^{1/(Np)}))}.$$

On the other hand, the identity (2) can also be written as

$$D\alpha = \beta D \begin{bmatrix} 1 & t \\ 0 & 1 \end{bmatrix}.$$

Thus Proposition 2.1 implies that

$$(h_0 \circ \alpha)(\tau) = (f^D \circ \alpha)(\tau) = f^{D\alpha}(\tau) = \left((f \circ \beta)^D\right)(\tau + t).$$

Using Proposition 2.1 again, we obtain from (4) that

$$(7)\qquad (h_0 \circ \alpha)(\tau) = \sum_{n \gg -\infty} b_n^{\sigma_{N,p}} \zeta_N^{nt} q^{n/N}.$$

Combining (6) and (7), it follows that

$$(8)\qquad \left(f_p^p - h_0\right) \circ \alpha \equiv 0 \pmod{p\mathcal{O}_L((q^{1/(Np)}))}.$$

Furthermore, (5) shows that $f_p \circ \alpha$ has Fourier coefficients in $\mathcal{O}_L$. Since h is integral over $\mathbb{Z}[j]$, Proposition 2.2 implies that $h \circ \alpha$ has algebraic integer Fourier coefficients. Hence

$$(f_p - h^p) \circ \alpha = f_p \circ \alpha - (h \circ \alpha)^p$$

has Fourier coefficients in $\mathcal{O}_L$. Therefore, by (8), the Fourier coefficients of $G \circ \alpha$ with respect to $q^{1/(Np)}$ belong to $p\mathcal{O}_L$ in this case.

Case 2. Assume next that $p \mid a$. Then the matrix

$$\beta = \begin{bmatrix} a/p & b \\ c & pd \end{bmatrix}$$

belongs to $\mathrm{SL}_2(\mathbb{Z})$ and satisfies

$$D\alpha = \beta \begin{bmatrix} p & 0 \\ 0 & 1 \end{bmatrix}. \tag{9}$$

Thus we have

$$(f_p \circ \alpha)(\tau) = (f \circ D \circ \alpha)(\tau) = (f \circ \beta)(p\tau) \quad (\tau \in \mathbb{H}). \tag{10}$$

Let

$$S = pI_2 = \begin{bmatrix} p & 0 \\ 0 & p \end{bmatrix}.$$

Then we get the identity

$$D\alpha D = S\beta. \tag{11}$$

Since h is integral over $\mathbb{Z}[j]$, Proposition 2.2 yields the Fourier expansion

$$(h \circ \alpha)(\tau) = \sum_{n \gg -\infty} c_n q^{n/N} \quad \text{with } c_n \in \mathcal{O}_K \quad (\tau \in \mathbb{H}). \tag{12}$$

Applying Lemmas 3.2 and 3.3 to (12), we obtain

$$(h \circ \alpha)(\tau)^p \equiv \sum_{n \gg -\infty} c_n^{\sigma_{N,\,p}} q^{pn/N} \pmod{p\mathcal{O}_K((q^{1/N}))}. \tag{13}$$

On the other hand, Proposition 2.1 applied to (12) gives

$$((h \circ \alpha)^D)(p\tau) = \sum_{n \gg -\infty} c_n^{\sigma_{N,\,p}} q^{pn/N}. \tag{14}$$

Since e is the order of p in $(\mathbb{Z}/N\mathbb{Z})^\times/\langle -1 \rangle$, we have

$$S^e = I_2 \quad \text{in } \mathrm{GL}_2(\mathbb{Z}/N\mathbb{Z})/\langle -I_2 \rangle. \tag{15}$$

Note that

$$h = f^{S^{e-1}D}. \tag{16}$$

Using Proposition 2.1, together with (11), (15) and (16), we derive that

$$(h \circ \alpha)^D = (f^{S^{e-1}D})^{\alpha D} = f^{S^{e-1}D\alpha D} = f^{S^{e-1}S\beta} = f^{S^e\beta} = f^\beta = f \circ \beta.$$

Therefore, (10) implies that

$$((h \circ \alpha)^D)(p\tau) = (f \circ \beta)(p\tau) = (f_p \circ \alpha)(\tau). \tag{17}$$

Combining (13), (14), and (17), we get

$$(h \circ \alpha)(\tau)^p \equiv (f_p \circ \alpha)(\tau) \pmod{p\mathcal{O}_L(\!(q^{1/(Np)})\!)},$$

from which it follows that

$$(f_p - h^p) \circ \alpha \equiv 0 \pmod{p\mathcal{O}_L(\!(q^{1/(Np)})\!)}. \tag{18}$$

By (10), the function $f_p \circ \alpha = (f \circ \beta)(p\tau)$ has Fourier coefficients in $\mathcal{O}_K$ since f is integral over $\mathbb{Z}[j]$ and $\beta \in \mathrm{SL}_2(\mathbb{Z})$. Hence $(f_p \circ \alpha)^p$ has Fourier coefficients in $\mathcal{O}_K$. Also, since $h_0 = f^D$ is integral over $\mathbb{Z}[j]$, the function $h_0 \circ \alpha$ has algebraic integer Fourier coefficients. Therefore,

$$\left(f_p^p - h_0\right) \circ \alpha = (f_p \circ \alpha)^p - h_0 \circ \alpha$$

has Fourier coefficients in $\mathcal{O}_L$. Together with (18), this shows that the Fourier coefficients of $G \circ \alpha$ belong to $p\mathcal{O}_L$ in this case.

We have shown that for every $\alpha \in \mathrm{SL}_2(\mathbb{Z})$, the Fourier coefficients of $G \circ \alpha$ with respect to $q^{1/(Np)}$ belong to $p\mathcal{O}_L$. Therefore the Fourier coefficients of

$$F \circ \alpha = \frac{1}{p}(G \circ \alpha)$$

are algebraic integers for every $\alpha \in \mathrm{SL}_2(\mathbb{Z})$. Finally, Proposition 2.2 implies that F is integral over $\mathbb{Z}[j]$. □

Remark 3.5. Theorem 3.4 yields a Kronecker-type congruence

$$\left(f_p^p - f^{\left[\begin{smallmatrix} 1 & 0 \\ 0 & p \end{smallmatrix}\right]}\right)\left(f_p - \left(f^{\left[\begin{smallmatrix} p^{e(N,p)-1} & 0 \\ 0 & p^{e(N,p)} \end{smallmatrix}\right]}\right)^p\right) \equiv 0 \pmod{p\mathcal{O}_{\mathcal{F}_{Np}}}.$$

References

[1] B. Cais and B. Conrad, *Modular curves and Ramanujan's continued fraction*, J. Reine Angew. Math. 597 (2006), 27–104.

[2] I. Chen and N. Yui, *Singular values of Thompson series*, Ohio State Univ. Math. Res. Inst. Publ., 4, Walter de Gruyter & Co., Berlin, 1996, 255–326.

[3] B. Cho, *Modular equations for congruence subgroups of genus zero*, Ramanujan J. 51 (2020), no. 1, 187–204.

[4] B. Cho, *Modular equations for congruence subgroups of genus zero (II)*, J. Number Theory 231 (2022), 48–79.

[5] D. A. Cox, *Primes of the Form $x^2 + ny^2$: Fermat, Class field theory, and Complex Multiplication*, 3rd ed. with solutions, with contributions by Roger Lipsett, AMS Chelsea Publishing, Providence, R.I., 2022.
[6] G. J. Janusz, *Algebraic Number Fields*, 2nd ed., Grad. Studies in Math. 7, Amer. Math. Soc., Providence, R.I., 1996.
[7] H. Y. Jung, J. K. Koo and D. H. Shin, *A Kronecker congruence relation for modular functions of higher level and genus*, J. Number Theory 278 (2026), 875–892.
[8] H. Y. Jung, C. H. Kim, J. K. Koo and D. H. Shin, *On the integrality of modular functions over $\mathbb{Z}[j]$ and Kronecker-type congruences*, submitted.
[9] N. M. Katz, p-adic properties of modular schemes and modular forms, Modular functions of one variable, III (Proc. Internat. Summer School, Univ. Antwerp, Antwerp, 1972), pp. 69–190, Lecture Notes in Math., Vol. 350, Springer-Verlag, Berlin-New York, 1973.
[10] S. Lang, *Elliptic Functions*, With an appendix by J. Tate, 2nd ed., Grad. Texts in Math. 112, Springer-Verlag, New York, 1987.
[11] J.-P. Serre, *Formes modulaires et fonctions zêta p-adiques*, Modular functions of one variable, III (Proc. Internat. Summer School, Univ. Antwerp, Antwerp, 1972), pp. 191–268, Lecture Notes in Math., Vol. 350, Springer-Verlag, Berlin-New York, 1973.
[12] G. Shimura, *Introduction to the Arithmetic Theory of Automorphic Functions*, Iwanami Shoten and Princeton University Press, Princeton, N.J., 1971.
[13] J. Tate, *Rigid analytic spaces*, Invent. Math. 12 (1971), 257–289.
[14] H. Weber, *Zur Theorie der Elliptischen Functionen*, Acta Math. 6 (1885), no. 1, 329–416.

4. Author Information

Dong Hwa Shin (dhshin@hufs.ac.kr)
Professor, Department of Mathematics, Hankuk University of Foreign Studies, South Korea.

J. Basic Sci., HUFS, **62** (2026), pp. 125-131

Review of two kinds of Infrared Spectrometer based on Fourier transformation [1]

Chang Uk JUNG[2]

Spectrometer measures the interaction between the light and matter. Since light has a very long range of wavelength, each region can be covered by very special kind of spectrometer. If the light source is strong enough and a sensitive detector is available, then light beams with very narrow wavelength region is selectively incident on the sample and the reflection and transmission is measured to get the complex value of index of refraction. A grating using a single crystal is used for this purpose. The beam satisfying the Bragg condition can be selectively used. For larger wavelength region, the spectrometer meets harsh conditions on the availability of light source, and sensitive detector. The four-transformation spectroscopy using a beam splitter is generally good to overcome these difficulties. But in the region where wavelength is around 1 mm, this method is no longer effective. A novel technique of wavefront division method now comes in. In this report, I will review the characteristics of these two methods; beam splitter vs wavefront division method. Also, I will include my big achievements in the wavefront division method.

Grating spectrometer

A spectrometer is used to measure the interaction between the light and matter. One typically measures the refection, absorption, and transmission and calculate the optical constants such as n and k. For shorter wavelengths including visible light, the light intensity is strong enough and sensitive detector is available. So Grating shown in Fig. 1 is widely used to select the a (narrow range of) wavelength and this beam is incident on the sample. The incident angle of light on the grating is varied such that light having each wavelength can arrive at the sample. Thus, wavelength dependent reflection, absorption, and transmission can be directly measured, which gives directly the optical constant vs wavelength. In other words, we scan the wavelengths one by one and get the response of sample at each wavelength. By the way, the prism also can selectively separate the visible region to make a rainbow pattern. This method has disadvantage due to loss of absorption, reflection, and variable efficiency vs wavelength.

---

[1] This research was supported by the research fund 2025 of Hankuk University of Foreign Studies.

[2] Department of Physics, Hankuk University of Foreign Studies, Yongin 17035, Republic of Korea. E-mail: cu-jung@hufs.ac.kr

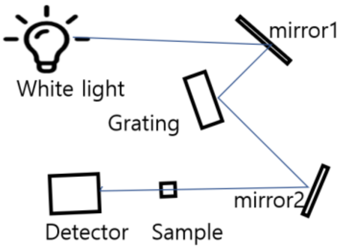

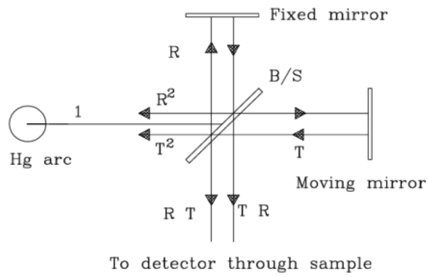

Figure 1, Structure of grating spectrometer Figure 2, Structure of Michelson interferometer

Fourier transform infrared spectrometer: conventional

In the infrared region, the intensity of the light source is not enough and the grating methos is no longer efficient. A Fourier transform infrared spectrometer (FTIR spectrometer) using Michelson interferometer should be used. FT spectrometer can give high-resolution optical properties over a wide spectral range from visible to IR region. Also, this method is fast compared to the grating spectrometer.

Michelson interferometer as shown in Fig. 2 shows that a source beam with a wide wavelength region is incident together on the beam splitter and then split into two beams which interfere with each other. At first, the beam enters into a beam splitter. Then R($0<R<1$, ideally R=0.5 but R depends on wavelength) of total beam is reflected toward the fixed mirror and then fully reflected beam enters the beam splitter. Then R^2 of beam is returned toward the light source and TR($0<TR<0.25$, TR=0.25 at R=T=(1-R)=0.5) of beam go toward the sample. Now we must consider another beam path. T($0<T<1$, ideally T=0.5 but T depends on wavelength) of total beam is transmitted at the beam splitter and move toward the moving mirror and then fully reflected beam reenter the beam splitter again. Then T^2 of beam is returned toward the light source and RT($0<RT<0.25$, RT=0.25 at R=T=(1-R)=0.5) of beam go toward the sample. This total 2TR($0<2TR<0.5$) intensity of light can move toward the sample.

Depending on the optical path difference between the two split beams, the 2TR values depends on the wavelength itself. At a value of optical path difference, a group of light has a constructive interference and the other group of light has a destructive interference. Of course, at another value of optical path difference, we have different sets of light having a constructive interference and a destructive interference.

Basic of Fourier transform spectroscopy

When coherent two beams made by Michelson interferometer are incident on the sample, the response intensity as a function of the path length difference p and wavenumber k is given by

$$I(p,k) = I(k)[1 + \cos(2\pi kp)]$$

p= path length difference in the interferometer, wavenumber k=1/λ

$I(k)$ is a response(reflection spectrum for example) of a sample when a beam with only one k is incident on the sample. Since not monochromatic but white light are incident on the sample, the so-called interferogram at a path length difference p is integral sum of $I(p,k)$ over all wavenumber k.

$$I(p) = \int_0^\infty I(k)[1 + \cos(2\pi kp)]dk$$

Then $I(k)$ can be obtained by a mathematical procedure called Fourier transform and is given as follows. [We must consider there is an error due to finite scan size of p, which is however tolerable compared to the advantage of FTIR technique.]

$$I(k) = 4\int_0^\infty [I(p) - \frac{1}{2}I(p = 0)]\cos(2\pi kp)\,dp$$

While FTIR spectrometer is strong tool at IR region, it has serious disadvantages to cover Far-IR region; a fundamental disadvantage and practical disadvantage. As we see in Fig. 3, More than half of beam return to the source and can not be incident on the sample. $R^2 + T^2 = R^2 + (1-R)^2 < 0.5$ where $0<R<1$.

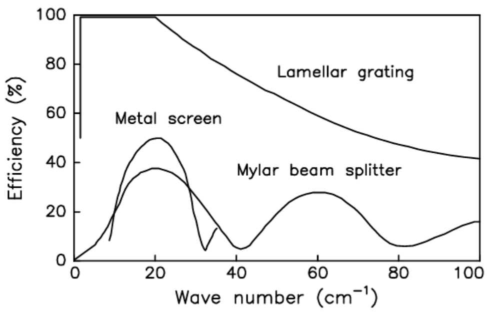

Figure 3, Modulation efficiency of various beam splitter

Yet, a more serious problem comes from the beam splitter itself. The above figure shows efficiency (=2*TR*) value of the typical Mylar beam splitter vs wave number *k*. As show in the figure, the efficiency is much smaller than ideal value of 0.5 and even shows strong modulation with wave number. This is due to the non-zero absorption of light and finite thickness effect. Even with metal screen type beam splitter having a negligible absorption problem, there is a strong modulation of efficiency over the different wavelength region as shown above. Compared to the conventional beam splitter, the Lamellar grating has a superior efficiency over almost all region $2<k$ (cm^{-1})<100.

Lamellar grating Fourier transform Far−IR spectrometer(LGFTIR): Principle

A lamellar grating Fourier transform far-infrared (LGFTIR) spectrometer can solve the disadvantage due to use of beam splitter.[Ref. 1] To generate the two interfering beams, LGFTIR use a set of interleaved, interlocking reflective metal mirror sets. Metal mirror has almost 100% reflection of light over the Far-Infrared region; no absorption and no modulation of efficiency with wavelength. One set remains stationary while the other moves, creating a path difference that generates an interferogram. While beam splitter divides amplitude of incident light, lamellar grating divides wavefront of light. Recently this technique extended into the extreme ultraviolet regions.[Ref. 2]

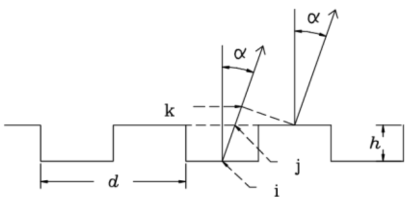

optical path difference = $h + l_{ij} + l_{jk}$

$l_{ij} = h/\cos\alpha$

$l_{jk} = (d/2-h\tan\alpha)\sin\alpha$

$\phi = (2\pi h/\lambda)[(1+\cos\alpha) + (d/2h)\sin\alpha]$

Figure 4, Interference at lamellar grating

Figure 4 shows a schematic diagram of the side view of lamellar grating. The intensity of light for a monochromatic plane wave beam with wavelength λ enter the lamellar grating with normal incidence is give as follows. Here, *d* is lattice constant of the lamellar grating and *h* is depth of grating and varies during scanning.

$$I = K^2\left(\frac{\sin\left(\frac{\pi d sin\alpha}{2\lambda}\right)}{\frac{\pi d sin\alpha}{2\lambda}}\right)^2\left(\frac{\sin\left(\frac{N\pi d sin\alpha}{\lambda}\right)}{\left(\frac{\pi d sin\alpha}{\lambda}\right)}\right)^2 cos^2\left(\frac{\phi}{2}\right) = A^2B^2C^2$$

A: corresponding to one grating surface.

B: corresponding to *N* array of grating surfaces.

C: corresponding to interference between upper and lower grating surfaces.

Grating equation is given by *B* and *B* has maximum value of N^2 when all *N* grating contributes to the constructive interference; when denominator is zero, as shown below.

$$\frac{\pi d sin\alpha}{\lambda} = m\pi,\ m = \text{integer}$$

But *A* is zero when non-zero *m* is even integer. When *m*=0, *A* is 1, *B* is N^2 and *I* is given as below. One can notice that this has the same form as the intensity of light when two light with ω are incident at the two reflection planes having an optical path difference of *x=2h* with each other.

$$I_0 \propto N^2 cos^2(2\pi\omega h) \propto cos^2(\pi\omega x) = \frac{1}{2}[1 + \cos(2\pi\omega x)]$$

If we compare the above equation with the previous basic equation of FTIR, one can find that LGFTIR use the 0th order diffracted beam.

$$B_\omega = (consant)\int_0^\infty \left[I_R(x) - \frac{1}{2}I_R(x=0)\right]\cos(2\pi\omega x)\,dx$$

$I_R(x)$: interferogram, response(reflection, transmission) of sample to the two coherent white lights having optical path difference of *x*. When *m* is odd integer, the intensity I_m is much smaller than I_0. Also, this beam can be eliminated by optical design (use of suitable size of light pipe).

$$I_{m,\,odd} = \left(\frac{2}{\pi m}\right)^2 I_0\quad m = odd\ interger$$

Lamellar grating Fourier transform Far-IR spectrometer: my new contribution

Most progress at the interferometer part of LGFTIR has been focused on the interferometer part. Large scan length increase resolution[Ref. 3-5], Double beam difference mode could measure absolute spectrum directly[Ref. 3] Double pass optical design was reported to give increased dispersion and the increased efficiency at shorter wavelength regions. Also, use of a concave surface of the lamellar grating removed the necessity of concave reflecting mirrors.[Ref. 6] However, BEFORE MY WORK, there was no significant improvement related to the intensity of light incident on the lamellar grating interferometer.

I adopted the on-axis elliptic mirror for maximum use of the light source (Hg arc lamp). Before my progress, they used very small(order of 1 steradian angle or even smaller) part of irradiation of Hg arc lamp and my designed used much larger part of radiation(order of 10 steradian angle), which is really a huge progress. This technique was shared by world top leading researchers.

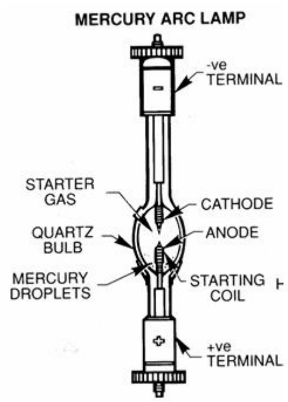

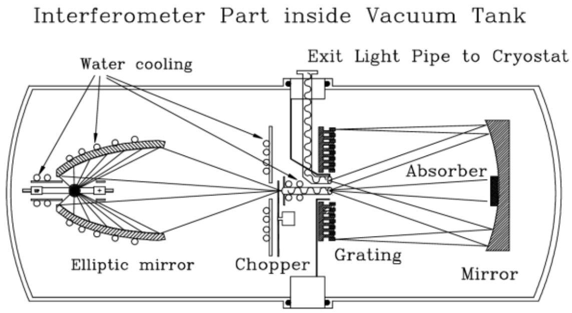

Figure 5, Hg arc lamp Figure 6, Lamellar grating interferometer with my design

As a light source at Far-IR region, high pressure Hg arc lamp has been generally used. Inside the lamp, there is a certain amount of Ha and Ar gas. The Ar gas act as a starter gas when Hg is vaporized. When lamp is cold the pressure inside the lamp is lower than one atmospheric pressure and one can see small globules of liquid Hg. The gap between the two electrode is insualting. In order to turn on the lamp, we must apply 35 kV high voltage pulse. This high voltage pulse can ignite the lamp when lamp is positioned such that anode is lower and cathode is higher. To avoid the absorption of the Far-IR light due to moisture, all the interferometer should be kept inside a big vacuum chamber (500~700 liter).

Previous design kept the vertical position all the ways. But I used a rotation stage and I could make the lamp with elliptic mirror horizontally after full ignition process is finished. This rotation design and use of elliptic mirror simple increased the use of light irradiation by more than 10 times.

Acknowledgements
이 연구는 2025년 한국외국어대학교 학술연구비 지원에 의해 이루어진 것임.

References

[1] K. Sakai, H. Masumoto, K. Ichimura, and H. Kojima, "High-resolution lamellar-grating Fourier-transform spectrometer for the suhmillimeter region," Appl. Opt. **17**, 1709-1715 (1978) https://opg.optica.org/ao/abstract.cfm?URI=ao-17-11-1709.

[2] H. R. Seren et al., "Lamellar grating based MEMS Fourier Transform Spectrometer," 2010 International Conference on Optical MEMS and Nanophotonics, Sapporo, Japan, 2010, pp. 105-106, doi: 10.1109/OMEMS.2010.5672163.

[3] R. L. Henry, D. B. Tanner, A lamellar grating interferometer for the far-infrared, Infrared Physics, Volume 19, Issue 2, (1979), Pages 163-174.

[4] "Spectroscopic Studies Using Fourier Transformations," Rev. Opt. 40 (no.2): 45 (1961) [in French] // "Spectroscopic Studies Using Fourier Transformations," Rev. Opt. 40 (no.3): 116 (1961) [in French] // "Spectroscopic Studies Using Fourier Transformations," Rev. Opt. 40 (no.4): 171 (1961) [in French] // "Spectroscopic Studies Using Fourier Transformations," Rev. Opt. 40 (no.5): 231 (1961) [in French] //"Fourier Transform Spectroscopy: Introductory Report," Mem. Soc. Roy. Sci. Liège 9: 81 (1964) [in French].

[5] Yahiko Yamada, Akiyoshi Mitsuishi, and Hiroshi Yoshinaga, "Transmission Filters in the Far-Infrared Region," J. Opt. Soc. Am. 52, 17-19 (1962).

[6] Bell, R.J., IntroductionFourier Transform Spectroscopy ,. Academic Press,. New York, 1972.

저자정보

주저자: 정창욱 / 한국외국어대학교 전자물리학과 / 교수

J. Basic Sci. HUFS **62** (2026), pp. 132–139

A VARIABLE SELECTION ALGORITHM IN PRICING POLICY WITH RELATIVE ERROR[1]

HEUNGSUN PARK*

Abstract. To make efficient investment, it is crucial to predict the future values properly for the assets. Least squares estimation or least absolute value deviation method have been used as the basic predicting tool. However, the relative error loss rather than the error itself is considered more importantly in many areas, in such stock market or appraisal industry where relative error prediction could be applied. In this article, a variable selection algorithm based on Mallow's Cp statistic is presented concerning relative error prediction. This algorithm can be used for many relative error prediction with many independent variables.

1. Predicting Stock Price

Prediction of stock price is very important in finance industry not only because the accurate prediction of stock price could improve the financial portfolio and investment strategy, but also because the even small amount of gain could lead to the substantial financial increase. However, due to the volatility, complex financial market structure, and/or rapidly changing capital market, it is not easy to predict the stock prices efficiently. The prediction validity can be measured based on the prediction error, $Y - \tilde{Y}$, but in predicting stock price the relative prediction error, $(Y - \tilde{Y})/Y$, is much favorably considered than the prediction error itself because it is unit-free measurement (Hirose and Masuda, 2018).

Park and Stefanski (1998) predict the gasoline sales (Y) given population size (X) per county in Florida using relative error criterion. They presented

*Professor, Dept. of Statistics, Hankuk University of Foreign Studies, Yongin-si, Gyeonggi-do, South Korea. hspark@hufs.ac.kr.

THIS WORK WAS SUPPORTED BY HANKUK UNIVERSITY OF FOREIGN STUDIES RESEARCH FUND OF 2025.

the best relative error predictor

$$g_*(X) = \frac{\mathrm{E}\left(\frac{1}{Y}\middle| X\right)}{\mathrm{E}\left(\frac{1}{Y^2}\middle| X\right)} = \frac{\mathrm{E}\left(\frac{1}{Y}\middle| X\right)}{\mathrm{V}\left(\frac{1}{Y}\middle| X\right) + \left[\mathrm{E}\left(\frac{1}{Y^2}\middle| X\right)\right]^2} \tag{1}$$

with the relative error regression (Relative Least Squares: RLS),

$$\min_{\gamma_0,\gamma_1} \sum_{i=1}^{n} \left(\frac{Y_i - g_*(X_i)}{Y_i}\right)^2, \quad g_*(X_i) = \gamma_0 + \gamma_1 X_i \tag{2}$$

as Khoshgoftaar et. al. (1992) used.

Park and Stefanski (1998) presented the asymptotic properties for the best relative error predictors but they didn't suggest any variable selection algorithm which is essential when there are many covariates. In this article, Mallow's C_p-type algorithm is presented and the simulated data and results are illustrated.

2. Mallow's C_p-Type Algorithm

Mallow (1973) introduced his C_p statistic for variable selection in regression, and it has been widely used because it is a simple way to balance between the goodness of fit and the model complexity. In that article, Mallow (1973) suggested to use the measure quantity

$$C_p = \frac{RSS_p}{\hat{\sigma}^2} - (n - 2p) \qquad \text{or} \qquad C_p \propto RSS_p + 2p\,\hat{\sigma}^2 \tag{3}$$

where

$$\begin{aligned} RSS_p &= \sum_{i=1}^{n} (y_i - \boldsymbol{x}_{pi}^T \hat{\boldsymbol{\beta}}_p)^2 \\ X_p &= \text{the design matrix with the selected p-variables} \\ \hat{\sigma}^2 &= \text{Mean Squared Error from the full model} \end{aligned} \tag{4}$$

and, the classical heuristic is: among the all possible candidates to find out the small C_p and near to p. This C_p statistic is widely used in regression analysis and is adopted as one of the stopping criterion in stepwise regression in *SAS/STAT*® (SAS Institute, 2025). It is suggested that the best model should have the smallest C_p and closest to p as possible. When p increases, the complexity of the regression model increases. So, if we try to find the best model to have the smallest C_p, the p is to play a role of penalty for the model complexity.

As this C_p statistic is derived from the ordinary least squares, this can't be used for other complicated models such as generalized linear models, mixed models, and any models with high dimensional data. However, In practice, C_p remains popular in teaching and in applied regression when the focus is on straightforward linear models and the analyst wants a simple plot of C_p versus p.

In this paper, the new C_p-type statistic based on relative prediction error context is suggested such as

$$C_p^* = \sum_{i=1}^{n} \left(\frac{y_i - \boldsymbol{x}_{pi}^T \hat{\boldsymbol{\beta}}_p}{y_i} \right)^2 + \lambda\, p \tag{5}$$

where λ is the hyperparameter/regularization parameter to control the model complexity. Although we have not $E(C_p^*) \approx p$ as the OLS did, the relative prediction risk can be controlled by the corresponding penalty, $\lambda\, p$, for more complex models. As in almost every regularized model fitting, choice of the hyperparameter is critical. In practice, people tend to prespecify a finite set of values for the regularization parameter, then use validation dataset to find the regularization parameter (Li and Zhu, 2008; Jung and Hu, 2015). I used K-fold Cross-Validation criterion to decide the hyperparameter as Jung and Hu (2015) did.

Therefore, in this, the following algorithm strategy is suggested to find the best model based on Eq. (5):

(1) For the all possible subsets, consider the proper hyperparameter, λ, such as 0.0, 0.5, 1, 1.5, 2, 2.5, 3.0, 5.0.

(2) Given λ, find the best candidate model which minimizes the C_p-type relative prediction error in Eq. (5).

(3) Compare the K-fold cross validations of C_p^* for each λ, and find the optimal λ with the smallest K-fold CV.

(4) The corresponding model with the chosen λ is the best model.

3. Example: Simulated Data

For the better understanding for this variable selection method using relative error regression, we can simulate the following variable–selection scenario by generating six predictors x_1, x_2, x_3, x_4 letting only a subset enter the true model (e.g. x_1, x_2) with gaussian noises:

(1) Sample size $n = 300$

(2) Predictors : x_1, x_2, x_3, x_4 are from $N(0,1)$ mutually independent.

(3) The true model is $y_i = 15 + 3\,x_{1i} - 2\,x_{2i} + \epsilon_i$ where $\epsilon_i \sim N(0,1)$.

(4) Therefore, the relevant independent variables are x_1, x_2 while x_3, x_4 are the noise variables .

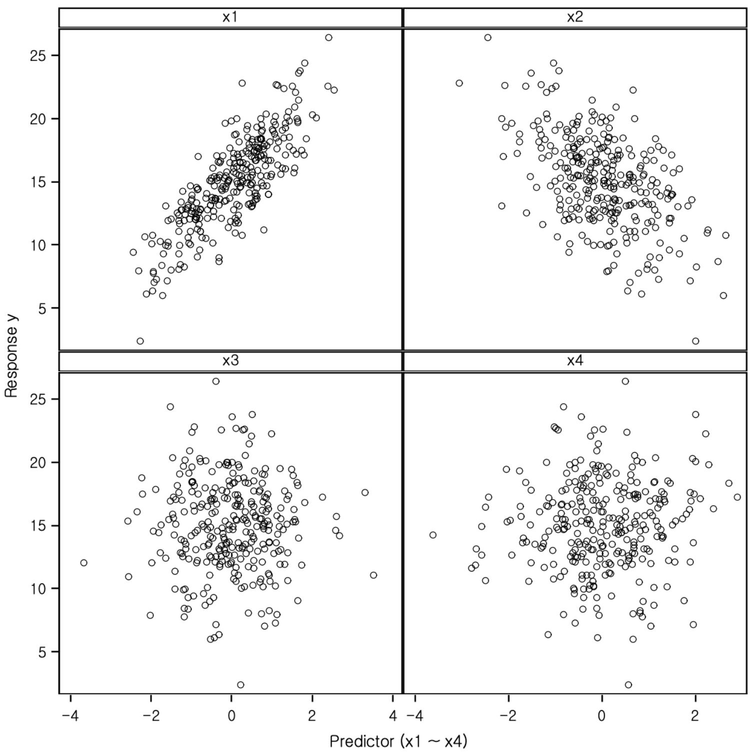

Figure 1. Simulated Data : Y vs. X1, X2, X3, X4

With 4 independent variables, I compared 15 model candidates with an intercept as shown in Table 1 out of the $2^4(=16)$ possible subsets.

Model_Name	$X1$	$X2$	$X3$	$X4$
model_001	o	x	x	x
model_002	x	o	x	x
model_003	x	o	o	x
model_004	x	x	x	o
model_012	o	o	x	x
model_013	o	x	o	x
model_014	o	x	x	o
model_023	x	o	o	x
model_024	x	o	x	o
model_034	x	x	o	o
model_234	x	o	o	o
model_134	o	x	o	o
model_124	o	o	x	o
model_123	o	o	o	x
model_000	o	o	o	o

Table 1. Possible subsets of independent variables

Table 2 shows the best model given λ and the corresponding C_p^* defined in Eq.(5), where the Relative Least Squares estimators are obtained from the train sets (240 obs.) and the validation is done for the validation data set (60 obs.). The sum_loss is the first part of C_p^* and cv_error is the K-fold (K=5) cross-validated mean relative squared residuals defined as

$$\text{cv\_error} := \frac{1}{5}\sum_{i=1}^{5}\frac{1}{60}\sum_{j=1}^{60}\left(\frac{y_{ij}-\boldsymbol{x}_{pij}^T\hat{\boldsymbol{\beta}}_{p(-i)}}{y_{ij}}\right)^2 \tag{6}$$

where y_{ij} is the jth observation of the ith fold and $\hat{\boldsymbol{\beta}}_{p(-i)}$ is the Relative Least Squares estimator with the ith fold omitted.

On Table 2 and Figure 2, the best model with the smallest cross-validation relative prediction error is model_012 with x_1, x_2 only, which is a reasonable result because the simulated y's were generated from x_1, x_2 not x_3, x_4.

In order to compare these results with those of OLS, I tried to fit the same data with OLS. Table 3 and Figure 3 illustrate the result of variable selection

λ	Model_Name	p	MCp	sum_loss	cv_error
0.0	model_000	4	1.9035	1.90348	0.00848
0.5	model_012	2	2.9060	1.90604	0.00816
1.0	model_012	2	3.9060	1.90604	0.00816
1.5	model_012	2	4.9060	1.90604	0.00816
2.0	model_012	2	5.9060	1.90604	0.00816
2.5	model_012	2	6.9060	1.90604	0.00816
3.0	model_012	2	7.9060	1.90604	0.00816
5.0	model_012	2	11.9060	1.90604	0.00816

TABLE 2. Cross-Validation error for different lambdas (Relative-error Least Squares: RLS)

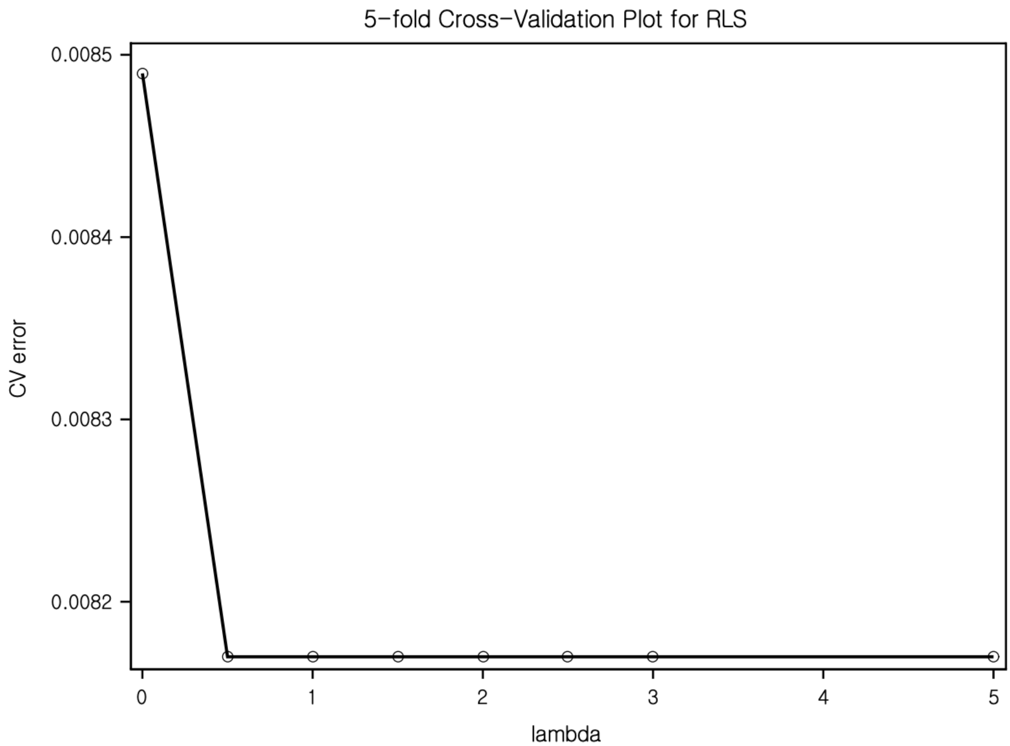

FIGURE 2. Cross-Validation error for different lambdas (Relative-error Least Squares: RLS)

based on cross-validation procedure. Interestingly, x_1, x_2 are selected even when we use OLS.

λ	Model_Name	p	MCp	sum_loss	cv_error
0.0	model_000	4	278.910	278.910	0.99907
0.5	model_123	3	280.417	278.917	0.95273
1.0	model_123	3	281.917	278.917	0.95273
1.5	model_012	2	293.035	280.035	0.95126
2.0	model_012	2	284.035	280.035	0.95126
2.5	model_012	2	285.035	280.035	0.95126
3.0	model_012	2	286.035	280.035	0.95126
5.0	model_012	2	290.035	280.035	0.95126

Table 3. Cross-Validation error for different lambdas (OLS)

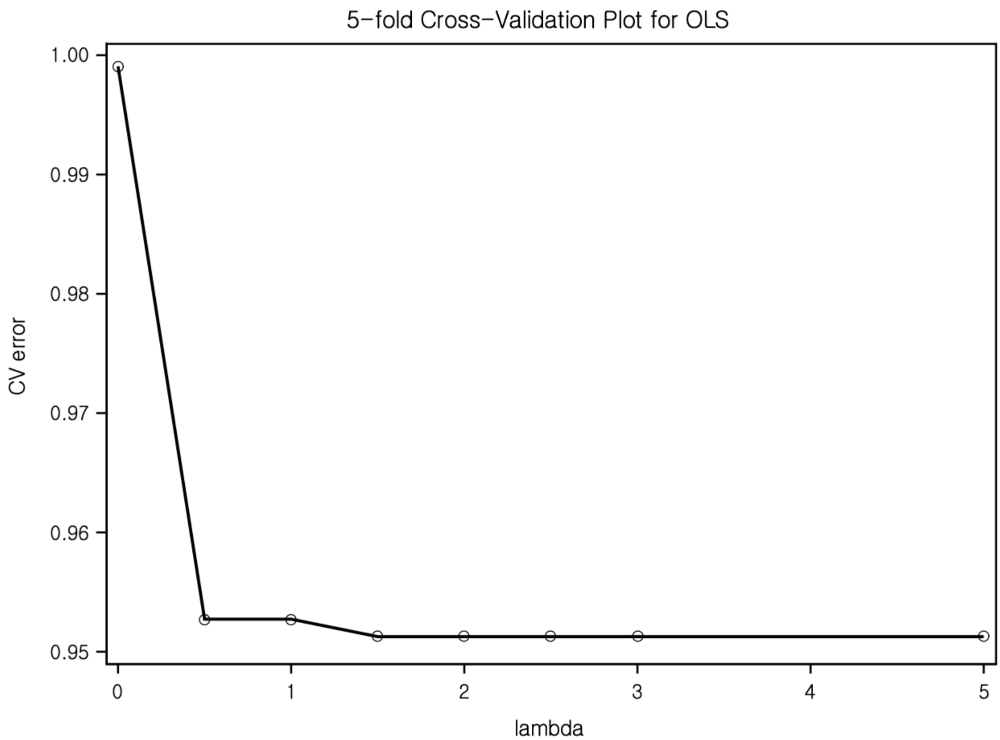

Figure 3. Cross-Validation error for different lambdas (OLS)

4. Concluding Remarks

Since C_p was introduced in 1973, it has been widely used in the basic regression course and in the practical areas. It is noted that the modern variable-selection methods such as AIC/BIC and LASSO arise within the same penalized-loss framework as Mallows's C_p, and many recent works compare them side by side (Zou *et. el.*, 2007)

Even though the more advanced variable selection methods are introduced as related to C_p statistics, C_p-type model selection algorithms are still popular not only because the average practitioners easily understand the concept, but also because they intuitively balance between reducing the prediction errors and penalizing the model complexity.

This article introduce a new variable selection algorithm based on C_p-type statistics considering the relative prediction error not the prediction error itself, and I think it could be a useful tool to anyone who wants to use Relative Least Squares (Park and Stefanski, 1998) in practice.

References

[1] K. Hirose and H. Masuda (2018) *Robust Relative Error Estimation*, Entropy, 20, 632; doi:10.3390/e20090632

[2] Heungsun Park and L.A. Stefanski (1998) *Relative error prediction*, Statistics & Probability Letters, Vol. 40, 227–236.

[3] C. L. Mallows (1973). *Some Comments on CP*, Technometrics. 15 (4): 661–675.

[4] SAS Institute (2025) *SAS/STAT® 15.3 User's Guide*, Cary, NC: SAS Institute Inc.

[5] Y. Li and J. Zhu (2008) *L_1 Norm Quantile Regression*, Journal of Computational and Graphical Statistics, Vol. 17, No. 1, Pages 1–23; doi: 10.1198/106186008X289155

[6] Y. Jung and J. Hu (2015) *A K-fold averaging cross-validation procedure*, Journal of Nonparametric Statistics, doi: 10.1080/10485252.2015.1010532

[7] H. Zou, T. Hastie and R. Tibshirani (2007) *On the degrees of freedom of the lasso*, Annals of Statistics 2007, Vol. 35, No. 5, 2173–2192.

5. Author Information

Heungsun Park (hspark@hufs.ac.kr)
Professor, Department of Statistics, Hankuk University of Foreign Studies, South Korea.

J. Basic Sci., HUFS, **62** (2026), pp. 140-146

Recovery of H-Beta Zeolite Activity for Plastic Pyrolysis via Thermal Dehydration[1]

YuJin Kwon,[2,†] Dain Yoon,[2,†] JungHwan Ahn,[2,†] Gyeongmo Park[2,†] and Doyun Kim[2,*]

Abstract

H-beta zeolite is an effective solid-acid catalyst for the catalytic pyrolysis and upcycling of polymeric waste; however, its apparent catalytic performance may gradually decrease during storage. In this study, we investigated whether adsorbed moisture and limited accessibility of the porous catalyst particles contributed to the observed loss of pyrolysis efficiency. Two pretreatment parameters, mechanical grinding and thermal drying, were evaluated individually and in combination. Four catalyst conditions were compared: untreated H-beta, ground H-beta, oven-dried H-beta, and H-beta subjected to grinding followed by oven drying. The combined pretreatment produced the highest pyrolysis efficiency among the tested conditions. These results support that both moisture removal and improved dispersion/exposure of the catalyst particles are important for restoring the effective catalytic activity of stored H-beta zeolite. The proposed pretreatment is operationally simple and may improve the reproducibility of small-scale plastic pyrolysis experiments.

1. Introduction

The accumulation of plastic waste has increased interest in thermochemical recycling methods capable of converting polymers into liquid fuels and chemical feedstocks. Pyrolysis is particularly attractive because it cleaves long polymer chains in the absence of oxygen and produces liquid, gaseous, and solid fractions. However, non-catalytic pyrolysis generally requires high temperatures and often generates a broad product distribution. The use of solid-acid catalysts can lower the effective cracking severity and promote the production of lighter hydrocarbon fractions.

H-beta zeolite is a promising catalyst for the pyrolysis of polyolefins because of its three-dimensional microporous framework and Brønsted acid sites. In the present system, H-beta showed superior catalytic performance compared with NH_3-beta and initially afforded a liquid oil yield of 95.17%. Nevertheless, the oil yield continuously decreased in subsequent

[1] This research was supported by the research fund 2026 of Hankuk University of Foreign Studies.
[2] Department of Chemistry, Hankuk University of Foreign Studies, Yongin 17035, Republic of Korea.
[†] These authors are contributed equally.
[*] Corresponding author. E-mail: doyunk@hufs.ac.kr

trials, falling to 85.44%, 49.75%, and finally 38.02% (**Figure 1**). This approximately 60% loss in yield raised a practical question regarding the origin of the rapid decline and the possibility of restoring catalyst performance by a simple pretreatment.

Zeolites can adsorb water from the surrounding atmosphere, and H-beta is sufficiently hydrophilic for moisture uptake. Adsorbed water may occupy pore space, interact with Brønsted acid sites, reducing the accessibility of hydrocarbon intermediates. In addition, moisture can promote particle aggregation, thereby burying internal active sites and reducing contact between the catalyst and the HDPE feed.

Based on these observations, we hypothesized that drying would recover the oil yield by removing adsorbed moisture. Initial drying experiments, however, showed only limited improvement, suggesting that moisture remained trapped inside aggregated particles. Mechanical grinding was therefore introduced to break the aggregates before drying. This study follows the sequential experimental development from liquid yield loss, to moisture-based hypothesis, to drying-only and grinding-only trials, and finally to a combined grinding-and-drying pretreatment.

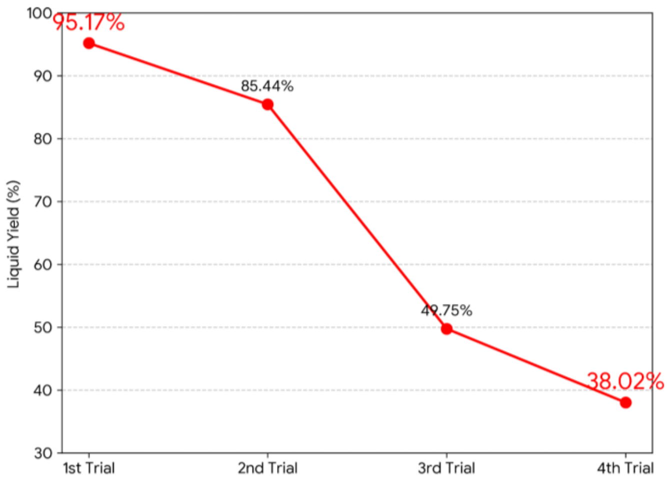

Figure 1. Progressive decline in liquid oil yield during catalytic pyrolysis of HDPE over H-beta zeolite. The recorded yields for the first through fourth trials were 95.17%, 85.44%, 49.75%, and 38.02%, respectively.

2. Experimental Section

2.1. Materials

High-density polyethylene (HDPE, LG Chemicals, South Korea) was used as the polymer feedstock, and H-beta zeolite (Zeolyst International, US) was used as the solid-acid catalyst. The catalyst was stored under ambient laboratory conditions.

2.2. Catalyst Pretreatment

The catalyst pretreatments were evaluated in the same order as the experimental development (**Table 1**). For vacuum drying, H-beta zeolite was dried for 1 h at room temperature under vacuum. For oven drying, the catalyst was heated at 80 °C for 24 h. For mechanical treatment, the catalyst was ground using a mortar and pestle. In the optimized sequential pretreatment, grinding was followed by oven drying at 80 °C for 24 h.

Table 1. The experimental conditions and purposes for the given pretreatment methods.

Pretreatment	Condition	Purpose
Vacuum drying	Room temperature, 1 h	Moisture removal
Oven drying only	80 °C, 24 h	Thermal moisture desorption
Grinding only	Mortar and pestle	Particle deagglomeration
Grinding + oven drying	Grinding, then 80 °C, 24 h	Deagglomeration followed by dehydration

2.3. Catalytic Pyrolysis and Oil-Yield Determination

Catalytic pyrolysis was carried out using HDPE and H-beta zeolite under the batch reactor systems and same reaction conditions (reaction for 350 °C for 6 h) for all pretreatment comparisons. The liquid product was collected after each experiment, and the oil yield was reported using the following equation:

$$\textit{Oil yield (\%)} = (\textit{mass of collected liquid product / initial mass of HDPE}) \times 100$$

3. Results and Discussions

3.1. Identification of the Problem

The first HDPE pyrolysis experiment over H-beta zeolite produced a liquid oil yield of 95.17%. The second trial remained high at 85.44%, but the third and fourth trials decreased sharply to 49.75% and 38.02%, respectively (**Figure 1**). Thus, the final measured yield was approximately 60% lower than the initial value. The continuous decrease indicated that the catalytic system was highly sensitive to catalyst storage conditions.

Because the catalyst had shown superior initial performance relative to NH_3-beta, the decline was not interpreted as evidence that H-beta was intrinsically unsuitable for HDPE pyrolysis. Instead, the change was attributed to a reversible loss of accessible catalytic function. The porous structure and hydrophilic character of H-beta suggested atmospheric moisture adsorption as the possible cause.

3.2. Moisture-Adsorption Hypothesis

The catalyst was not stored under inert condition (i.e., glove box), allowing ambient water vapor to adsorb on the zeolite. Moisture was proposed to contribute to deactivation in two ways. First, water could occupy the pores and interact with the Brønsted acid sites required for hydrocarbon cracking. Second, moisture could cause the fine zeolite particles to adhere to one another, forming aggregates that block pore entrances and reduce contact with HDPE.

The initial working hypothesis was therefore that drying alone would restore the oil yield. If water was the only relevant factor and remained readily accessible, vacuum or oven treatment should have recovered a substantial fraction of the original performance.

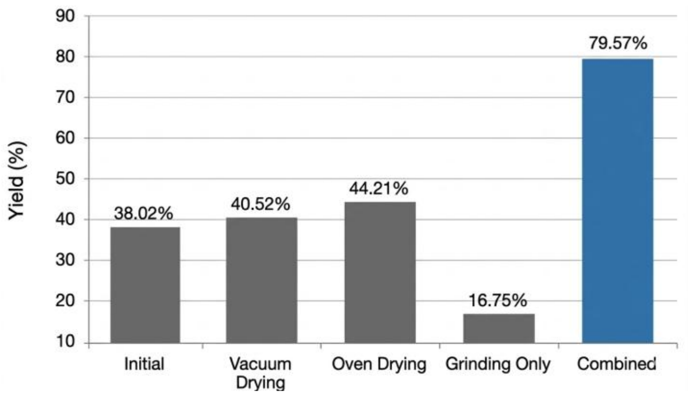

Figure 2. Comparison of liquid oil yields obtained after different H-beta pretreatments.

Include the untreated reference (38.02%), vacuum drying (40.52%), oven drying (44.21%), grinding only (16.75%), and sequential grinding followed by oven drying (79.57%).

3.3. Drying-Only Experiments

As can be seen in both **Table 1** and **Figure 2**, two drying protocols were evaluated. Vacuum drying for 1 h at room temperature slightly increased the oil yield from the 38.02% reference point to 40.52%. Oven drying at 80 °C for 24 h produced 44.21%.

These results showed that drying alone was insufficient. The modest difference between the reference state and the 24 h oven-dried catalyst suggested that a fraction of moisture may have been removed, but the active sites were not fully recovered. Moisture trapped within compact particle aggregates may have remained inaccessible to the drying environment.

3.4. Grinding-Only Experiment

To address particle aggregation, the H-beta zeolite was ground using a mortar and pestle. The purpose was to physically disrupt aggregates, re-expose buried acid sites, and increase contact between the catalyst and HDPE. Nevertheless, grinding alone reduced the oil yield to 16.75%, substantially below the 38.02% reference (**Figure 2**).

The failure of grinding alone can be interpreted within the moisture-based model. Although grinding may expose new surfaces and open previously blocked particle boundaries, it does not remove the water retained on or within the catalyst. It may even redistribute moisture across the newly exposed surfaces. Thus, mechanical deagglomeration without a subsequent dehydration step does not restore the effective acidity of the catalyst.

3.5. Sequential Grinding and Oven Drying

The optimized process combined the two treatments in a defined sequence: grinding followed by oven drying at 80 °C. Grinding was performed first to break particle aggregates and increase the accessibility of internal and interparticle moisture. The subsequent thermal treatment was then expected to remove water more efficiently from the newly exposed surfaces and pore entrances.

This sequential pretreatment increased the oil yield to 79.57% (**Figure 2**).

Compared with the untreated reference state of 38.02%, the oil yield increased by about 41.5 percentage points and reached approximately 2.09 times the reference value. The result was also far higher than the yields obtained after vacuum drying (40.52%), oven drying (44.21%), or grinding alone (16.75%).

The maximum observed oil yield of 79.57% remained below the first-trial value of 95.17%. The combined pretreatment achieved substantial recovery relative to the degraded 38.02% state, but additional factors such as catalyst aging, handling variation, irreversible deactivation, reactor variability, or differences in product recovery may account for the remaining gap.

4. Conclusion

The catalytic pyrolysis of HDPE over H-beta zeolite showed a pronounced decline in liquid oil yield from 95.17% in the first trial to 38.02% in the fourth trial. The degradation was attributed to atmospheric moisture uptake and moisture-assisted aggregation of the porous catalyst particles. Vacuum drying, oven drying, and grinding alone failed to restore the performance. In contrast, grinding followed by oven drying at 80 °C increased the oil yield to 79.57%. The result supports a sequential mechanism in which mechanical deagglomeration first exposes blocked surfaces and pore entrances, after which thermal dehydration removes retained moisture and restores access to Brønsted acid sites. Although the combined treatment did not fully recover the initial 95.17% yield, it provided the most effective restoration among the tested conditions and offers a simple pretreatment for improving H-beta performance in HDPE catalytic pyrolysis.

Acknowledgements

This research was supported by the research fund 2026 of Hankuk University of Foreign Studies.

References

[1] A. Corma; O. Marie; and F.J. Ortega; Interaction of water with the surface of a zeolite catalyst during catalytic cracking: a spectroscopy and kinetic study, *Journal of Catalysis,* **2004**, *222*, 338-347.

[2] A. Marcilla; A. Gómez-Siurana; F. Valdés; Catalytic pyrolysis of LDPE over H-beta and HZSM-5 zeolites in dynamic conditions: Study of the evolution of the process, *Journal of Analytical and Applied Pyrolysis*, **2007**, 79, 433-442.

저자정보

주저자 (공동):
권유진 / 화학과 / 학부연구생
윤다인 / 화학과 / 학부연구생
안정환 / 화학과 / 학부연구생
교신저자 :
김도윤 / 화학과 / 조교수

J. Basic Sci., HUFS, **62** (2026), pp. 147-152

Plasmonic Catalysis with Bimetallic Au@Pd Core-shell Nanoparticles[1]

Ahyeong Choi, Jeong-Wook Oh*[2]

ABSTRACT: Gold (Au) nanoparticles exhibit localized surface plasmon resonance (LSPR), which can enhance photocatalytic reactions through plasmonic effects; however, the intrinsic catalytic activity of Au is limited. In this study, Au@Pd core–shell nanoparticles with ultrathin Pd shells (nominal thickness 0.05–0.5 nm) were synthesized to combine the strong plasmonic properties of Au with the high catalytic activity of Pd. The nanoparticles were characterized by UV–Vis spectroscopy and transmission electron microscopy (TEM), and their plasmonic catalytic performance was evaluated by the photoreduction of methylene blue (MB) under simulated solar irradiation. The MB absorbance decreased with increasing irradiation time, indicating reduction of MB to leuco-methylene blue (LMB). Nanoparticles with thinner Pd shells exhibited higher reduction efficiency than those with thicker shells, indicating enhanced plasmonic catalytic performance. Although the absolute reduction efficiency was lower than that reported in our previous study, the same dependence on Pd shell thickness was observed. These results indicate that ultrathin Pd shells can enhance the plasmonic catalytic performance of Au@Pd nanoparticles and provide useful insights for the design of efficient plasmonic photocatalysts.

Introduction

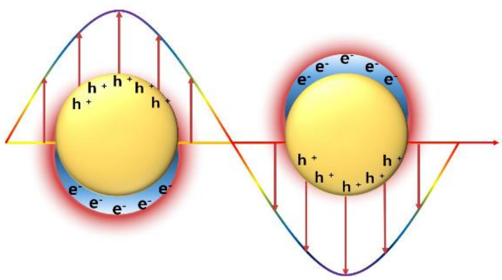

Figure 1. Schematic illustration of localized surface plasmon resonance (LSPR) induced by the coherent oscillation of conduction electrons under the oscillating electric field of light.

Gold (Au) nanoparticles exhibit strong plasmonic behavior known as localized surface plasmon resonance (LSPR). LSPR is the collective oscillation of conduction electrons in metallic nanostructures under light irradiation, and it can enhance photocatalytic reactions. In contrast, palladium (Pd) shows excellent catalytic performance but relatively weak plasmonic properties. Therefore, by combining Au and Pd in a core–shell structure, both the strong

---

[1] This research was supported by the research fund 2025 of Hankuk University of Foreign Studies.

[2] Department of Chemistry, Hankuk University of Foreign Studies, Yongin 17035, Republic of Korea. E-mail: jeongwoh@hufs.ac.kr

plasmonic effect of Au and the superior catalytic activity of Pd can be exploited. Based on this concept, Au@Pd core–shell nanoparticles were synthesized.

It has been reported that the photocatalytic performance of Au@Pd nanoparticles strongly depends on the Pd shell thickness and the Au core size: thinner Pd shells and smaller Au cores gave higher photocatalytic efficiency. This study focused on synthesizing Au@Pd nanoparticles with thinner Pd shells than those prepared previously. In this work, the nominal shell thickness was reduced to 0.05–0.5 nm, and the purpose of this study was to further verify that thinner Pd shells enhance plasmonic catalytic performance. Plasmonic catalysts of this type are of interest for applications such as photocatalysis, environmental remediation, degradation of organic pollutants, and energy conversion.

Experimental

Synthesis of Au@Pd Nanoparticles

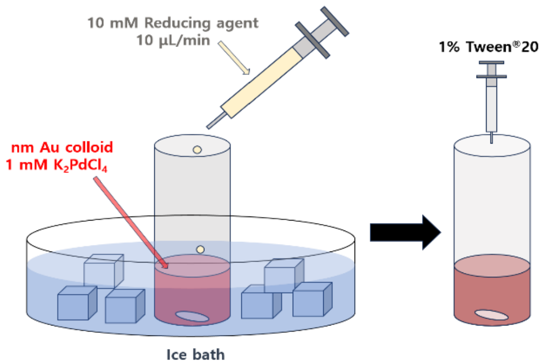

Figure 2. Schematic illustration of the synthesis of Au@Pd core–shell nanoparticles from Au colloid, K_2PdCl_4, L-ascorbic acid (L-AA), and Tween 20.

A 20 nm Au colloid was used as the core. In a vial, the 20 nm Au colloid was mixed with 1 mM K_2PdCl_4 (potassium tetrachloropalladate) solution; the amount of K_2PdCl_4 was adjusted according to the target Pd shell thickness. L-Ascorbic acid (L-AA) was used as the reducing agent. L-AA was injected slowly to control the reduction rate of Pd^{2+} and to promote uniform shell growth on the Au surface, because rapid reduction of Pd can produce separate Pd nuclei instead of a core–shell structure. Finally, 1% Tween 20 was added as a surfactant to stabilize the nanoparticles and prevent aggregation.

Centrifugation Process

After synthesis, the Au@Pd nanoparticles were transferred into microtubes and purified by a two-step centrifugation. The first centrifugation was carried out at 13,000 rpm for 15 min at 4 °C, followed by a second centrifugation at 10,000 rpm under the same conditions. A higher speed was used in the first step because polymeric species such as Tween 20 were still present, which hindered pellet formation. After the first washing step, most impurities were removed.

Because an excessively high speed can induce nanoparticle aggregation, a lower speed appropriate for 20 nm Au@Pd nanoparticles was used in the second step.

Photoreduction Test

The Au@Pd nanoparticles recovered after centrifugation were mixed with methylene blue (MB), L-AA, and deionized water (DIW). The mixture was irradiated with a solar simulator at 1000 W/m^2 (1 sun). UV–Vis spectra were recorded every 30 min to monitor the reduction of MB. As irradiation time increased, the blue color of the solution gradually faded, indicating reduction of MB to leuco-methylene blue (LMB).

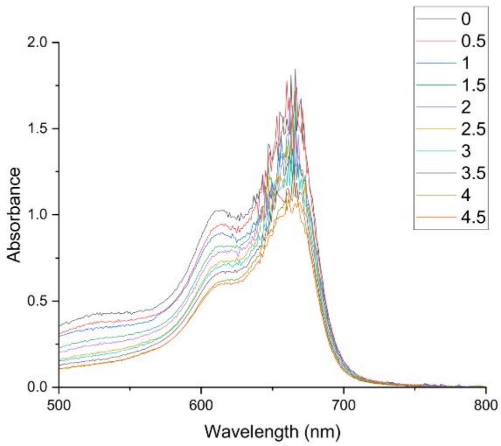

Figure 3. UV–Vis spectra of an MB solution containing Au@Pd nanoparticles, recorded every 30 min during photoreduction under light irradiation.

Results and Discussion

UV–Vis Spectra of Au@Pd with Different Shell Thicknesses

The UV–Vis spectra of Au@Pd nanoparticles with different Pd shell thicknesses were first measured (Figure 4). The absorbance of the Au LSPR band decreased as the Pd shell thickness increased. This trend is consistent with progressive Pd deposition on the Au surface: as the Pd shell becomes thicker, the plasmon of the Au core is increasingly damped by the Pd shell, lowering the absorbance.

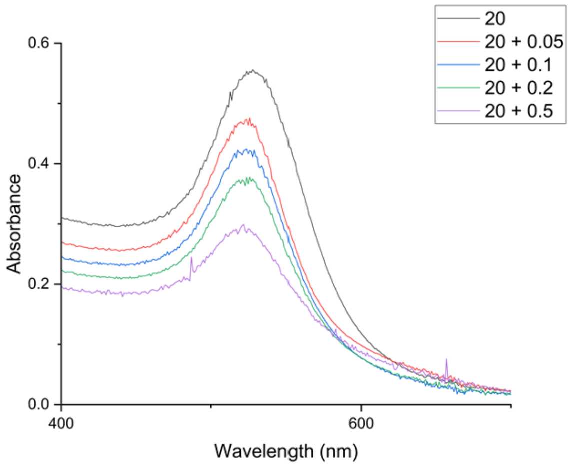

Figure 4. UV–Vis spectra of Au@Pd nanoparticles with different Pd shell thicknesses.

TEM Analysis

(a) (b)

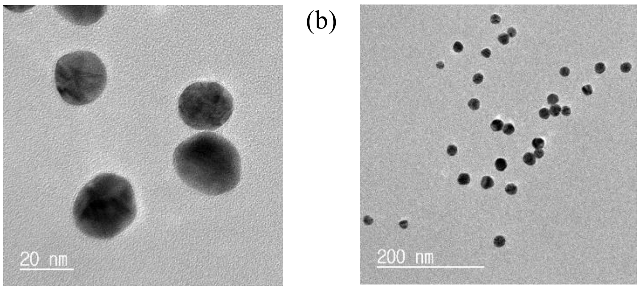

Figure 5. TEM images of Au@Pd nanoparticles with a Pd shell thickness of 0.2 nm: (a) 200k× magnification; (b) 40k× magnification.

TEM analysis was performed to observe the morphology and structure of the synthesized Au@Pd nanoparticles. Figure 5 shows Au@Pd nanoparticles with a nominal Pd shell thickness of 0.2 nm. Because such a thin Pd shell is difficult to resolve by conventional TEM, no distinct shell was observed. This is consistent with the formation of a very thin Pd layer that could not be directly imaged. For more detailed structural analysis, high-resolution TEM will be used in future work. In earlier work from our laboratory, reference samples with much thicker Pd shells showed clearly visible shells. In contrast, the thin-shell samples in this study showed no distinct shell boundary, supporting the interpretation that a Pd shell formed but was too thin to be resolved by conventional TEM.

Reduction Efficiency by Pd Shell Thickness

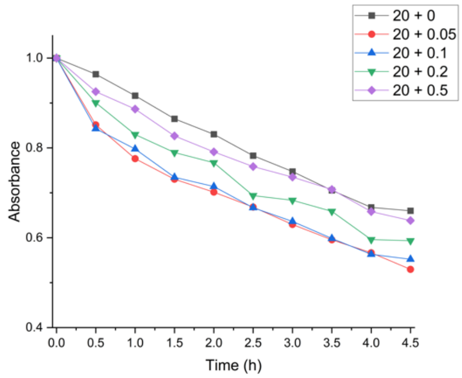

Figure 6. Change in MB absorbance over time for Au@Pd nanoparticles with different Pd shell thicknesses.

As irradiation time increased, the absorbance decreased continuously, indicating reduction of MB to LMB. Thinner Pd shells gave a larger decrease in absorbance, i.e., higher reduction efficiency. In addition, the Au@Pd nanoparticles showed higher reduction performance than bare Au nanoparticles. Although no distinct shell was observed by TEM for the thinnest-shell samples, the difference in reduction efficiency between bare Au and Au@Pd supports the formation of a thin Pd shell. Since the aim of this study was to examine how the Pd shell thickness affects catalytic performance in the sub-monolayer regime, the consistent "thinner-is-better" trend is the key result.

Conclusion

Au@Pd core–shell nanoparticles with ultrathin, sub-monolayer Pd shells were synthesized and evaluated for the plasmonic photoreduction of MB to LMB. Across the studied range of nominal Pd thickness (0.05–0.5 nm), thinner Pd shells consistently gave higher reduction efficiency, and all Au@Pd samples outperformed bare Au. This indicates that a minimal Pd coverage—one that preserves the Au LSPR while still providing catalytic sites—is favorable for plasmonic catalysis.

Because the performance improved monotonically down to the thinnest sample, the optimal Pd amount was not reached in this work. Future studies should therefore deposit even smaller amounts of Pd, below the current lower bound of 0.05 nm nominal thickness, to identify the optimal coverage at which plasmonic enhancement and catalytic activity are best balanced. In addition, the extremely thin Pd layer could not be resolved by conventional TEM; higher-resolution or aberration-corrected TEM, together with STEM–EDS elemental mapping, will be needed to directly confirm the presence and distribution of Pd and to correlate the nanostructure with the observed catalytic performance.

Acknowledgements

이 연구는 2025년 한국외국어대학교 학술연구비 지원에 의해 이루어진 것임.

References

[1] Niu, W.; Chua, Y. A. A.; Zhang, W.; Huang, H.; Lu, X. *J. Am. Chem. Soc.* **2015**, *137*, 10460–10463.

[2] Liu, W.; Zheng, G.; Wong, W.-L.; Wong, K.-Y. *Inorg. Chem. Commun.* **2019**, *107*, 107455.

[3] Yong, Z.; Shi, Q.; Fu, R.; Cheng, W. *Adv. Mater. Interfaces* **2021**, *8*, 2001686.

[4] Kang, E.; Seo, J.; Park, H.; Wrasman, C. J.; Shin, J. W.; Jo, M.-K.; Cargnello, M.; Park, J. Y.; Lee, H. *Adv. Mater. Interfaces* **2024**, *11*, 2301070.

[5] Park, H.; Chun, S.; Lee, J. H.; Son, J.; Kim, S.; Choi, J.; Ihee, H.; Lee, H.; Park, J. Y. *J. Am. Chem. Soc.* **2025**, *147*, 35913–35923.

[6] Cheng, Y.-C.; Deng, T.-S. *AIP Adv.* **2025**, *15*, 065008.

[7] Zheng, Z.; Tachikawa, T.; Majima, T. *J. Am. Chem. Soc.* **2015**, *137*, 948–957.

[8] Firmanti, M. I.; Ha, J. W. *ACS Appl. Mater. Interfaces* **2024**, *16*, 68601–68610.

저자정보

주저자: 최아영 / 한국외국어대학교 화학과 / 학부생

교신저자: 오정욱 / 한국외국어대학교 화학과 / 부교수

기초과학연구 제 62 집

인쇄 2026년 8월 6일
발행 2026년 8월 10일

발 행 인 소장 허성
운영위원 김해조, 신동화, 이기원, 이석주, 이태욱
인 쇄 처 외대문화사
발 행 소 한국외국어대학교 기초과학연구소
주 소 경기도 용인시 처인구 모현읍 외대로 81
17035

ISSN 2713-7465